

Contributions to Boundary Control of Distributed-Parameter Systems

DISSERTATION

zur Erlangung des Grades
des Doktors der Ingenieurwissenschaften
der Naturwissenschaftlich-Technischen Fakultät
der Universität des Saarlandes

VON

Abdurrahman Irscheid

Saarbrücken

2025

Tag des Kolloquiums: 27. Januar 2025

Dekan: Prof. Dr.-Ing. Dirk Bähre

Berichterstatter: Prof. Dr.-Ing. habil. Joachim Rudolph
Prof. Dr.-Ing. Dr. h.c. Oliver Sawodny
Prof. Dr.-Ing. habil. Thomas Meurer

Vorsitz: Prof. Dr. techn. Romanus Dyczij-Edlinger

Akad. Mitarbeiter: Dr. rer. nat. Michael Roland

Eidesstattliche Versicherung

Hiermit versichere ich an Eides statt, dass ich die vorliegende Arbeit selbstständig und ohne Benutzung anderer als der angegebenen Hilfsmittel angefertigt habe. Die aus anderen Quellen oder indirekt übernommenen Daten und Konzepte sind unter Angabe der Quelle gekennzeichnet. Die Arbeit wurde bisher weder im In- noch im Ausland in gleicher oder ähnlicher Form in einem Verfahren zur Erlangung eines akademischen Grades vorgelegt.

Saarbrücken, 31.1.2025

Ort, Datum

Abdurrahman Irscheid

Zusammenfassung

Eine neuartige Entwurfsmethodik wird für die Regelung von linearen hyperbolischen oder parabolischen partiellen Differentialgleichungen (PDEs) vorgestellt, welche an einem Rand aktuiert und am anderen Rand mit nichtlinearen gewöhnlichen Differentialgleichungen (ODEs) gekoppelt sind. In Anlehnung an die wohlbekanntete Backstepping-Methode für lineare Systeme wird eine nichtlineare Zustandstransformation herangezogen, um das System in eine für den Reglerentwurf besonders geeignete Form zu bringen. Das zentrale Ergebnis der vorliegenden Arbeit ist die Konstruktion dieser Zustandstransformation mithilfe der Lösung eines angemessen formulierten Cauchy-Problems. Die Verwendung einer flachheitsbasierten Parametrierung der entsprechenden PDE-Teilsysteme erleichtert diesen Entwurfsschritt. Zudem gestattet die Kombination von Backstepping und flachheitsbasierten Parametrierungen, auf bekannte Ergebnisse aus der bestehenden Literatur aufzubauen. Des Weiteren wird für den Spezialfall linearer Systeme gezeigt, dass der vorgestellte Ansatz sowohl für hyperbolische als auch für parabolische PDE-ODE-Systeme äquivalent zur Backstepping-Methode ist. Die in dieser Arbeit für den Reglerentwurf präsentierte Vorgehensweise bewältigt zuvor ungelöste Probleme und lässt sich aufgrund ihrer Systematik auf eine breitere Systemklasse erweitern. Allerdings sind im Rahmen dessen auch eine Vielzahl an Herausforderungen und interessanten Fragestellungen für weiterführende Untersuchungen entstanden.

Abstract

A novel framework is presented for the late-lumping boundary control of linear hyperbolic or parabolic partial differential equations (PDEs) that are interconnected with nonlinear ordinary differential equations (ODEs) at the unactuated boundary. Inspired by the well-established backstepping method for linear systems, a nonlinear state transformation is utilized to map the plant into a desired target system. The central result of this thesis is the construction of the state transformation through the solution of an appropriately formulated Cauchy problem. This is facilitated by the use of flatness-based parameterizations of the corresponding PDE subsystems. In fact, the combination of backstepping and flatness-based parameterizations allows this work to build upon a substantial body of existing literature. Furthermore, for the special case of linear systems, the approach is shown to be equivalent to the backstepping method for both hyperbolic and parabolic PDE-ODE systems. Although the presented control strategy overcomes previously unsolved problems and enables the systematic development of advanced designs for a broader system class, it has also given rise to numerous challenges and interesting problems for future research.

Contents

1	Introduction	1
1.1	State of the art	3
1.2	Contributions of this work	5
1.2.1	Contributions for hyperbolic systems	6
1.2.2	Contributions for parabolic systems	7
1.3	Organization	8
2	Hyperbolic systems	9
2.1	Problem formulation	10
2.1.1	System class	11
2.1.2	Assumptions	13
2.2	Solution-based control design	14
2.2.1	Preliminary backstepping transformation	14
2.2.2	Decoupling transformation	16
2.2.3	Control law	18
2.3	Solution of the inverse problem	18
2.3.1	State prediction at the unactuated boundary	19
2.3.2	Solvability of the nonlinear integro-differential equation	22
2.3.3	Interpretation of the state dependency	22
2.4	Stability analysis	24
2.4.1	The reference system in transformed coordinates	24
2.4.2	ODE state tracking error	25
2.4.3	PDE state tracking error	26
3	Parabolic systems	27
3.1	Linear reaction-diffusion equation	28
3.1.1	From open-loop control to state feedback	29
3.1.2	Analytical solution of the inverse problem	30
3.2	Linear parabolic PDE-ODE system	31
3.2.1	Control design	32
3.2.2	Analytical solution of the inverse problem	33

3.3	Nonlinear parabolic PDE-ODE system	34
3.3.1	Preliminary backstepping transformation	36
3.3.2	Nonlinear state transformation and state feedback	37
4	Conclusions and future work	43
4.1	Hyperbolic systems	43
4.2	Parabolic systems	44
4.3	Application to cooperative transportation with heavy ropes	45
5	Scientific publications	51
5.1	Output regulation for general heterodirectional linear hyperbolic PDEs coupled with nonlinear ODEs	52
5.2	Stabilizing nonlinear ODEs with diffusive actuator dynamics	67
A	Detailed calculations	75
A.1	Solving the Cauchy problem for a linear reaction-diffusion equation . .	75
A.1.1	Unactuated Neumann boundary	75
A.1.2	Unactuated Dirichlet boundary	77
A.2	Solving the Cauchy problem for a linear parabolic PDE-ODE system .	79
A.2.1	Unactuated Neumann boundary	79
A.2.2	Unactuated Dirichlet boundary	80
	References	83

Chapter 1

Introduction

Numerous technological processes, engineering problems and industrial applications can be modeled by distributed-parameter systems: for instance, torsional-axial drilling (Saldivar et al., 2014), communication networks (Espitia et al., 2017), stacker cranes (Staudacker et al., 2008), fire-rescue turntable ladders (Zimmert et al., 2011), evaporative cooling facades (Gschweng et al., 2024), plug-flow reactors (Bastin and Dochain, 1990, Ch. 1), canalized water-ways and irrigation networks (de Halleux et al., 2003), biomass separation settlers in wastewater treatment plants (Dochain and Vanrolleghem, 2005, Ch. 2), single-crystals production of compound semi-conductors (Rudolph et al., 2005), heavy-chain systems (Petit and Rouchon, 2002) and vehicular traffic flow (Lattanzio et al., 2011), to name but a few. In most cases, the corresponding mathematical descriptions are represented by partial differential equations (PDEs) that are directly deduced from laws of physics and first principles such as, e.g., energy and mass balance, conservation of momentum as well as heat transfer relations. Distributed-parameter systems offer higher accuracy than their largely simplified counterparts whenever the spatial distribution of physical quantities has a significant influence on a given process. Despite their potential complexity, it is of undeniable importance to understand the structure of these models for useful engineering applications that range from condition monitoring and fault diagnosis (see, e.g., Fischer and Deutscher (2022)) to controlled high-performance and high-precision tasks (see, e.g., Aoustin et al. (1997) and Meurer et al. (2008) for vibration control of flexible robot arms and piezoelectric cantilever beams, respectively). In view of these considerations, the design of controllers and observers for this class of systems has become a crucial aspect in various technological domains. However, from the perspective of control engineering, even simple systems can give rise to difficult challenges. One reason for that is the lack of a general (control) theory for PDEs. This is particularly evident in the context of linear PDEs compared to the well-understood theory for linear systems comprised of ordinary differential equations (ODEs). As such, there is considerable potential for further advancement in the field of control engineering for PDEs.



Figure 1.1: A triangle suspended by heavy ropes that are each actuated by a tricopter (Irscheid et al., 2019). Reproduced with permission from Springer Nature.

Of particular interest for this work are the challenges associated with boundary control for a subclass of distributed-parameter systems comprising linear PDEs, of either hyperbolic or parabolic type, that are defined on a finite, one-dimensional spatial domain. Its boundary is defined by two distinct spatial points, on which boundary conditions are imposed. For simplicity, the considered systems represent well-posed problems, i.e., both the existence of a unique solution of the associated PDEs as well as continuous dependence on initial data are guaranteed. Moreover, due to the restriction to boundary control, distributed in-domain actuation is disregarded¹. In fact, the control input is assumed to be located at one of the boundaries only. Furthermore, dynamical boundary conditions yield PDEs that are (in general bidirectionally) coupled with ODEs, i.e., so-called PDE-ODE systems. The objective of this work is to propose a strategy for the boundary control of linear (hyperbolic or parabolic) PDEs that are coupled with nonlinear ODEs at the unactuated boundary. Apart from the scarcity of results in this field, the system class in question is inspired by the previous work of the author on cooperative load transportation with heavy ropes (see Figure 1.1) in Irscheid et al. (2019). The experimental validations therein indicate that a flatness-based open-loop controller produces excellent results in the absence of external disturbances, but fails to meet performance requirements otherwise.

¹In the case of in-domain actuation, geometric and Lyapunov techniques can be found in, e.g., Christofides (2001) for nonlinear control of PDE systems.

1.1 State of the art

There exist two prominent and very distinct control strategies for boundary actuated PDEs. The first one is based on model reduction, i.e., obtaining a finite-dimensional approximation through a spatial discretization method. As noted in, e.g., Meurer (2013, Ch. 1), the employed discretization could vary from simple finite differences schemes on a predefined grid to more advanced schemes such as modal projections and balanced truncation. The resulting approximation is a system of ODEs, for which any standard control method can be designed. Such techniques are referred to as early lumping due to the fact that a finite-dimensional lumped-parameter model is used as a basis for the control design. In spite of that, the resulting closed loop is still an infinite-dimensional system, the stability of which has to be thoroughly investigated. In particular, the neglected dynamics of the system could be excited to the point of instability, which marks the main drawback of an early-lumping approach. This effect is also known as spillover (see, e.g., Balas (1978)). Contrary to that, late-lumping methods take into account the infinite-dimensional model description of the system dynamics. This oftentimes necessitates more involved mathematical concepts to derive the corresponding controllers. However, for practical reasons, the implementation still requires a finite-dimensional approximation of the resulting control law. With finer discretization of the latter, one obtains a more accurate approximation of the late-lumping controller, whereas the derivation of the control law itself is independent of the discretization scheme. This is not true for an early-lumping approach, where a more accurate finite-dimensional approximation of the system dynamics results in a different controller.

In contrast to the simplicity of an early-lumping design, the mathematical intricacies inherent to late lumping can be a deterrent for many engineers. That said, the benefits of late lumping have been demonstrated in numerous applications, thereby making it a valuable technique in control engineering. One such example is the undoubtedly successful backstepping method developed for linear distributed-parameter systems with boundary actuation (see, e.g., Krstic and Smyshlyaev (2008) for an introduction). In the last two decades, it allowed a new era to unfold for the boundary control of both hyperbolic and parabolic PDEs. It can also be generalized to encompass bidirectionally coupled PDE-ODE systems (see, e.g., Di Meglio et al. (2018); Deutscher et al. (2018); Wang and Krstic (2022) for hyperbolic systems and Wang and Krstic (2019); Deutscher and Gehring (2021) for parabolic systems). Numerous extensions were incorporated to account for, e.g., delay robustness in Auriol et al. (2018), underactuation of PDEs in Redaud et al. (2021), prescribed-time stability in Steeves et al. (2019), tracking control with flatness-based open-loop design in Meurer and Kugi (2009); Meurer (2013) and output regulation in Deutscher (2015), among other developments. However, backstepping mainly relies on (mostly linear) integral state transformations. As a consequence, an extension to linear PDEs that are coupled with nonlinear ODEs is not obvious.

For a wide class of hyperbolic systems, alternative methods have emerged to overcome the challenges associated with nonlinearities. For example, in Bekiaris-Liberis and Krstic (2013, Ch. 5) and Bekiaris-Liberis and Krstic (2014), prediction-based controllers are proposed for nonlinear ODEs interconnected with transport equations or wave actuator dynamics, respectively. The approach taken in Irscheid et al. (2021c) provides first insights into tracking control for heterodirectional 2×2 linear hyperbolic PDEs that are bidirectionally coupled with nonlinear ODEs, with the generalization to the $n \times n$ case presented in Irscheid et al. (2023). To deal with nonlinearities, Irscheid et al. (2021c) and Irscheid et al. (2023) use online predictions in the control and observer designs that follow from the solution of associated Cauchy problems. It is worth noting that Irscheid et al. (2022b) shows the equivalence with backstepping in the linear case, where online predictions are superfluous. This is in line with the findings in Strecker and Aamo (2017), which proposes a prediction-based output feedback method for 2×2 heterodirectional semilinear hyperbolic PDEs. Moreover, Strecker et al. (2022) and Irscheid et al. (2022a) demonstrate the validity of prediction-based methods when nonlinear terms are allowed in both the PDE and the ODE. Furthermore, the flatness-based feedback design for linear hyperbolic PDE-ODE systems in Woittennek (2013); Gehring and Woittennek (2022) has been successfully extended to the case of nonlinear boundary ODEs in Woittennek et al. (2022). Therein, flatness allows for a parameterization of system solutions by the trajectory of a flat output, upon which a state transformation into a hyperbolic controller form is constructed. This allows for a straightforward control design by assigning an appropriate closed-loop dynamics.

It should be noted that flatness-based parameterizations find use in numerous applications of open-loop control designs for both hyperbolic and parabolic systems (see, e.g., Rudolph (2003)). As stated before, Woittennek (2013); Woittennek et al. (2022) deduce feedback controllers from flatness-based parameterizations in the hyperbolic case. This raises the question, whether such parameterizations are the key to better understand the closed-loop control of parabolic systems as well and, thus, allow for an extension to the nonlinear case. For the latter system class, flatness-based open-loop controllers already exist and are derived by solving an associated nonlinear Cauchy problem (see, e.g., Lynch and Rudolph (2002); Schörkhuber et al. (2012, 2013)). However, up until most recently, flatness-based parameterizations had not been used for late-lumping closed-loop control designs, even for the linear examples considered in, e.g., Fliess et al. (1998); Laroche et al. (1998, 2000). To the best knowledge of the author, Irscheid et al. (2024) marks the first such use. Therein, a novel strategy is developed for controlling a linear reaction-diffusion equation that is cascaded with nonlinear ODEs at its unactuated boundary. Given the intricate nature of this problem, it had not been previously addressed in the existing literature. It is noteworthy that, for linear systems, the resulting control law coincides with the one obtained with backstepping (see, e.g., Smyshlyaev and Krstic (2004); Krstic (2009)).

In general, there is a scarcity of results on the control of nonlinear parabolic PDEs: Meurer and Zeitz (2005) proposes flatness-based open-loop control combined with an early-lumping feedback design and Bekiaris-Liberis and Vazquez (2019) suggests an output-feedback control for a class of Hamilton-Jacobi PDEs. For stabilizing semilinear parabolic plants comprising Volterra series nonlinearities, a nonlinear state transformation based on Volterra kernels is proposed in Vazquez and Krstic (2008a,b).

The main body of this thesis is based on the aforementioned publications of the author, especially Irscheid et al. (2023) and Irscheid et al. (2024). The following section presents a concise overview of the central results and methodological contributions.

1.2 Contributions of this work

This work presents new findings on the boundary control of linear hyperbolic or parabolic PDEs that are interconnected with nonlinear ODEs at the unactuated boundary. For both types of PDEs it offers a unifying perspective by establishing a control strategy based on the formulation of an appropriate Cauchy problem. Its solution is utilized to construct a nonlinear state transformation, which maps the plant into a desired target system. Interestingly, this state transformation reduces to a Volterra integral transformation for linear systems, which coincides with the well-known backstepping transformation (see, e.g., Krstic (2009) and Deutscher et al. (2017) for parabolic and hyperbolic PDE-ODE systems, respectively).

The results of this work exploit flatness-based parameterizations of the PDE subsystems in order to solve the corresponding Cauchy problems. Contrary to the ones used in the context of flatness-based open-loop control designs (see, e.g., Rudolph and Woittennek (2008)), the Cauchy problems considered here are defined for an auxiliary variable that is excited by the system state. This facilitates the introduction of a state transformation in the spirit of backstepping. As such, the methodology chosen in this work makes use of flatness-based parameterizations and concepts from backstepping. This differs from existing research combining the two, wherein flatness is typically used for an open-loop control design and a subsequent backstepping design stabilizes the tracking error (see, e.g., Meurer and Kugi (2009)). Other works using flatness-based parameterizations for a closed-loop control design are either restricted to the hyperbolic case (see, e.g., Woittennek (2013); Gehring et al. (2023)) or deploy an early-lumping approach (see, e.g., Meurer and Zeitz (2005)). In the latter, a finite-dimensional system approximation is obtained by truncating the flatness-based parameterization of the control input. In contrast, the design presented here yields a late-lumping controller.

Besides meeting the aforementioned control objective, this thesis lays down the groundwork to facilitate the development of new methods for a larger system class. For instance, the fundamental principles involved in the boundary control for hyperbolic

PDE-ODE systems are transferred in Irscheid et al. (2021b, 2023) to a corresponding observer design based on boundary measurements. Another example is the prescribed-time controller developed in Irscheid et al. (2022a) for a semilinear PDE-ODE system. It can be reasonably deduced that Irscheid et al. (2024) enables similar advancements in the parabolic case. These and numerous other interesting questions remain open, and new problems have emerged as an implication of this thesis.

The constructive approach pursued in this work has limitations with regards to the mathematical rigor such as a thorough investigation of stability, convergence of series and other mathematical details. Nevertheless, these limitations do not invalidate the overall significance of this work. Moreover, the primary findings focus on the new perspectives for boundary control and highlight the opportunities for further improvements. Yet, it is of utmost importance to pursue a careful investigation of the details that come short in this thesis within a suitable mathematical framework. In fact, a number of significant obstacles to the further development of the proposed approach have been identified.

1.2.1 Contributions for hyperbolic systems

The central findings on hyperbolic PDE-ODE systems have been published in

- (H1) Irscheid, A., Gehring, N., and Rudolph, J. (2021c). Trajectory tracking control for a class of 2×2 hyperbolic PDE-ODE systems. *IFAC-PapersOnLine*, 54(9):416–421,
- (H2) Irscheid, A., Gehring, N., Deutscher, J., and Rudolph, J. (2021b). Observer design for 2×2 linear hyperbolic PDEs that are bidirectionally coupled with nonlinear ODEs. In *2021 European Control Conference (ECC)*, pages 2506–2511,
- (H3) Irscheid, A., Gehring, N., Deutscher, J., and Rudolph, J. (2022b). Tracking control for 2×2 linear heterodirectional hyperbolic PDEs that are bidirectionally coupled with nonlinear ODEs. In Auriol, J., Deutscher, J., Mazanti, G., and Valmorbidia, G., editors, *Advances in Distributed Parameter Systems*, pages 117–142. Springer,
- (H4) Irscheid, A., Espitia, N., Perruquetti, W., and Rudolph, J. (2022a). Prescribed-time control for a class of semilinear hyperbolic PDE-ODE systems. *IFAC-PapersOnLine*, 55(26):47–52

and

- (H5) Irscheid, A., Deutscher, J., Gehring, N., and Rudolph, J. (2023). Output regulation for general heterodirectional linear hyperbolic PDEs coupled with nonlinear ODEs. *Automatica*, 148:110748.

In particular, (H1) introduced first results concerning tracking control for linear heterodirectional 2×2 hyperbolic PDEs with boundary actuation and bidirectional coupling with a nonlinear ODE at the unactuated boundary. Further developments in (H3) embedded the design in a systematic framework and characterized the control strategy by the solution of a Cauchy problem. Inspired by the latter, the proposed method is coined solution-based control. Moreover, (H3) also proved the equivalence to the backstepping controller from Deutscher et al. (2017) in the special case of linear systems. For the same system class with collocated measurement, the first solution-based observer design was established in (H2). A generalization of both control and observer designs to the case of $n \times n$ PDEs was proposed in (H5). Therein, an output regulation problem is solved in the presence of disturbances by taking advantage of solution-based methods. In fact, the results therein can be easily adjusted to design a trajectory tracking controller instead, as presented in Chapter 2 of this thesis. Furthermore, it is shown that a trivial modification of the design yields additional improvements of the results in (H5) (or equivalently Irscheid et al. (2023)).

It is worth noting that the solution-based method is not restricted to linear PDE subsystems: (H4) presented a prescribed-time controller for a semilinear PDE that is bidirectionally coupled with a nonlinear ODE. However, the system class considered in the present work comprises linear PDE subsystems for simplicity of presentation.

1.2.2 Contributions for parabolic systems

Transferring the solution-based control strategy developed for hyperbolic PDE-ODE systems onto the parabolic case resulted in the publication

- (P1) Irscheid, A., Gehring, N., Deutscher, J., and Rudolph, J. (2024). Stabilizing nonlinear ODEs with diffusive actuator dynamics. *IEEE Control Syst. Lett.*, 8:1259–1264.

It solves the stabilization problem for a (scalar) linear parabolic PDE with nonlinear boundary dynamics. To the best knowledge of the author, this problem had not been considered in the literature before. By that, the preliminary results in (P1) are of great significance for the boundary control of nonlinear parabolic PDE-ODE systems. Moreover, in the linear case, (P1) shows the equivalence to the backstepping method (see, e.g., Krstic (2009)). Chapter 3 revisits the contents of (P1) (or equivalently Irscheid et al. (2024)) to give an outline of solution-based control for parabolic PDE-ODE systems.

The central idea of the proposed design is inspired by the Cauchy problems that are well-known in the context of flatness-based open-loop control design (see, e.g., Fliess et al. (1998); Laroche et al. (1998)). Defining an appropriate (linear) Cauchy problem that depends on the system state makes it possible to deduce a nonlinear state transformation. It is meticulously designed to map the plant into a form that greatly

facilitates the design of a stabilizing state feedback. The latter only requires the existence of a suitable controller for the nonlinear ODE subsystem. In addition to this inherent assumption, only a set of technical requirements is imposed. Concerning the practicability of the design, (P1) proposes a numerical scheme for implementing the control law.

1.3 Organization

The main body of this thesis comprises Chapters 2 and 3 that are concerned with hyperbolic and parabolic PDE-ODE systems, respectively. Both chapters briefly present the respective outline of Irscheid et al. (2023) and Irscheid et al. (2024) in order to give an intuitive understanding of the developed methods.

Chapter 2 revisits the publication Irscheid et al. (2023) to introduce the central idea of the proposed control strategy. The methods therein allow for the derivation of tracking controllers for a general class of heterodirectional linear hyperbolic PDEs that are bidirectionally coupled with nonlinear ODEs at the unactuated boundary. Furthermore, slight modifications of the published results achieve a stabilization of the PDE subsystem in the theoretically minimal time. It is shown that this improvement of the result in Irscheid et al. (2023) stems from a straightforward modification of the design.

The insights gained for the control of hyperbolic systems are then adapted to the parabolic case. In particular, Chapter 3 encompasses the strategy proposed in Irscheid et al. (2024) for the control of parabolic PDE-ODE systems. The chapter starts with an introduction of a novel perspective for the control design in the linear case and shows its equivalence to existing backstepping controllers. This is followed by a discussion of the modifications necessary to account for a nonlinear ODE subsystem that is cascaded with a linear reaction-diffusion equation.

To conclude, Chapter 4 summarizes the findings and implications of this work, highlights open problems and offers directions for future research. Additionally, the effectiveness of the theory developed in this thesis is demonstrated in a numerical example on cooperative transportation with heavy ropes. Finally, the peer-reviewed and published journal papers Irscheid et al. (2023) and Irscheid et al. (2024) are attached in Chapter 5.

Chapter 2

Hyperbolic systems

The solution-based control design for hyperbolic systems was first introduced in Irscheid et al. (2021c) as a prediction-based control strategy that delivered preliminary results for a previously unsolved problem. In particular, it yields a tracking controller for linear heterodirectional 2×2 hyperbolic PDEs with boundary actuation and bidirectional coupling with a nonlinear ODE at the unactuated boundary. The method was further developed in Irscheid et al. (2022b) and, in the linear case, shown to be equivalent to the backstepping controller from Deutscher et al. (2017). As such, solution-based control is considered an extension of the latter. Furthermore, the first solution-based observer design was proposed in Irscheid et al. (2021b) for the same system class with collocated measurement. A generalization of both control and observer designs to the case of $n \times n$ PDEs was proposed in Irscheid et al. (2023) in the context of output regulation in the presence of disturbances. Moreover, the solution-based method is modular in the sense that it embeds a known control method for ODEs in a framework for PDE-ODE systems. For instance, Irscheid et al. (2022a) presented a prescribed-time controller for a semilinear PDE that is bidirectionally coupled with a nonlinear ODE by using a known prescribed-time controller for the ODE subsystem.

The foundation of solution-based control revolves around finding a particularly crafted Cauchy problem, the solution of which determines the control input. While the design of the Cauchy problem remains relatively simple, guaranteeing its well-posedness becomes more involved with increasing system complexity. This is the main disadvantage of the method. In general, solving the Cauchy problem for hyperbolic systems necessitates a state predictor. The emergence of such predictors is not surprising and can be traced back to the inherent nature of hyperbolic systems modeling time delays. In a linear setting, an analytical solution of the Cauchy problem can be obtained in terms of the system state and, thus, online prediction is avoided. However, for nonlinear systems, such expressions are hardly possible to find. To overcome this, the controller relies on a numerical scheme that has to be implemented online. Numerical predic-

tors have previously been proposed in Bekiaris-Liberis and Krstic (2013, Ch. 5) and Bekiaris-Liberis and Krstic (2014) for the stabilization of PDE-ODE cascades comprising nonlinear ODEs with actuator dynamics modeled as transport equations or wave equations, respectively. Additionally, they are also utilized in Strecker et al. (2022) to solve the output regulation problem for semilinear and quasilinear 2×2 hyperbolic PDE-ODE systems.

Beside the aforementioned relation to backstepping control for linear PDE-ODE systems (see, e.g., Di Meglio et al. (2018); Deutscher et al. (2019)), there exists a close relation to flatness-based control (see, e.g., Woittennek (2013)). Using differential parameterizations of system trajectories, the latter utilizes a controller canonical form that is well-suited for control design. For the nonlinear SISO system considered in Woittennek et al. (2022), obtaining the state of the canonical form requires the (online) solution of integral equations. In fact, they could be reformulated and interpreted as online predictors, which, however, is not necessary in the context of flatness-based parameterizations. It is worth noting that generalizing the controller canonical form to the MIMO case considered here represents one of the relevant research frontiers of flatness-based methods.

In what follows, the outline of solution-based control is introduced briefly for a nonlinear hyperbolic system. The main results are stated in Irscheid et al. (2023) and, thus, this chapter is intended to offer an intuitive presentation of the method. However, the contents of Irscheid et al. (2023) are slightly adjusted to solve a trajectory tracking problem instead of output regulation. In order to further demonstrate the modular nature of solution-based control, a trivial modification of the control design in Irscheid et al. (2023) is shown to yield improved performance in closed loop. In particular, the asymptotically stable closed-loop system is characterized by parallel transport equations (instead of a cascade) to impose minimal convergence time on the infinite-dimensional subsystem (similar to, e.g., Auriol and Di Meglio (2016) for linear PDEs).

2.1 Problem formulation

Instead of solving an output regulation problem in the presence of disturbances as done in Irscheid et al. (2023), a trajectory tracking problem is solved here for the undisturbed system. Additionally, in comparison with the system class considered in Irscheid et al. (2023), the nonlinearity that appears at the unactuated boundary condition depends not only on the ODE state but also on the PDE state. Note that these adjustments do not necessitate a significant modification of the design strategy.

2.1.1 System class

Consider a class of hyperbolic PDE-ODE systems of the form

$$\dot{\mathbf{w}}(t) = \mathbf{f}(\mathbf{w}(t), \mathbf{x}_-(0, t)) \quad (2.1a)$$

$$\mathbf{x}_+(0, t) = Q_0 \mathbf{x}_-(0, t) + \mathbf{c}(\mathbf{w}(t), \mathbf{x}_-(0, t)) \quad (2.1b)$$

$$\partial_t \mathbf{x}(z, t) = \Lambda(z) \partial_z \mathbf{x}(z, t) + A(z) \mathbf{x}(z, t) \quad (2.1c)$$

$$\mathbf{x}_-(1, t) = Q_1 \mathbf{x}_+(1, t) + \mathbf{u}(t) \quad (2.1d)$$

consisting of a nonlinear ODE subsystem (2.1a) with the lumped state $\mathbf{w}(t) \in \mathbb{R}^{n_w}$ and a linear heterodirectional hyperbolic PDE subsystem (2.1b)–(2.1d) with the distributed state $\mathbf{x}(z, t) \in \mathbb{R}^n$ defined for $z \in [0, 1]$ and $t \geq 0$. The subsystems are bidirectionally coupled by means of the vector field \mathbf{f} in (2.1a) and the function \mathbf{c} in (2.1b), that are both locally Lipschitz continuous w.r.t. the ODE state $\mathbf{w}(t)$ on any domain of interest. The function \mathbf{c} is also locally Lipschitz continuous w.r.t. its second argument $\mathbf{x}_-(0, t)$. Furthermore, let

$$\Lambda(z) = \text{diag}(\lambda_1^-(z), \dots, \lambda_{n_-}^-(z), \lambda_1^+(z), \dots, \lambda_{n_+}^+(z)) \quad (2.2a)$$

with strictly descending (and continuously differentiable) transport speeds

$$\lambda_1^-(z) > \dots > \lambda_{n_-}^-(z) > 0 > \lambda_1^+(z) > \dots > \lambda_{n_+}^+(z) \quad (2.2b)$$

for $z \in [0, 1]$ and define the corresponding state components¹ $\mathbf{x}_-(z, t) = E_-^T \mathbf{x}(z, t) \in \mathbb{R}^{n_-}$, $\mathbf{x}_+(z, t) = E_+^T \mathbf{x}(z, t) \in \mathbb{R}^{n_+}$ with $n = n_- + n_+$ as well as

$$E_- = \begin{bmatrix} I_{n_-} \\ 0 \end{bmatrix} \in \mathbb{R}^{n \times n_-}, \quad E_+ = \begin{bmatrix} 0 \\ I_{n_+} \end{bmatrix} \in \mathbb{R}^{n \times n_+}. \quad (2.3)$$

This implies that $\mathbf{x}_-(z, t)$ and $\mathbf{x}_+(z, t)$, coupled at the boundaries via $Q_0 \in \mathbb{R}^{n_+ \times n_-}$ and $Q_1 \in \mathbb{R}^{n_- \times n_+}$, describe the transport in the negative and positive z -direction, respectively. Moreover, define the functions

$$\phi_i^-(z) = \int_0^z \frac{1}{\lambda_i^-(\zeta)} d\zeta > 0, \quad z \in [0, 1] \quad (2.4a)$$

for $i \in \{1, \dots, n_-\}$ to obtain the time delay

$$\Delta_i^- = \phi_i^-(1) \quad (2.4b)$$

for the transport of the i -th component of $\mathbf{x}_-(z, t)$ between $z = 1$ and $z = 0$ as well as the functions

$$\phi_i^+(z) = \int_0^z \frac{-1}{\lambda_i^+(\zeta)} d\zeta > 0, \quad z \in [0, 1] \quad (2.4c)$$

¹In the following, for any vector $\mathbf{x} \in \mathbb{R}^n$, define $\mathbf{x}_- = E_-^T \mathbf{x} \in \mathbb{R}^{n_-}$ and $\mathbf{x}_+ = E_+^T \mathbf{x} \in \mathbb{R}^{n_+}$.

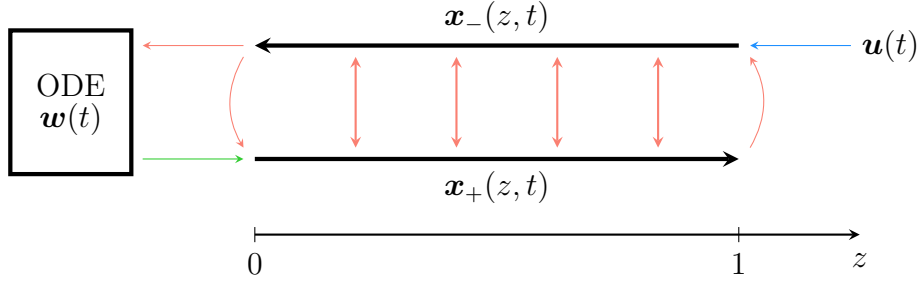


Figure 2.1: Schematic depiction of the PDE-ODE system (2.1).

for $i \in \{1, \dots, n_+\}$ to obtain the respective time delay

$$\Delta_i^+ = \phi_i^+(1) \quad (2.4d)$$

for the transport of the i -th component of $\mathbf{x}_+(z, t)$ between $z = 0$ and $z = 1$. Note that the inverse functions ψ_i^- with $\psi_i^-(\phi_i^-(z)) = z$ for $i \in \{1, \dots, n_-\}$ and ψ_i^+ with $\psi_i^+(\phi_i^+(z)) = z$ for $i \in \{1, \dots, n_+\}$ exist since both ϕ_i^- and ϕ_i^+ are strictly monotonically increasing. The in-domain coupling matrix $A(z) = [a_{ij}(z)]$ with $a_{ij} \in C^0([0, 1])$ is assumed to satisfy $a_{ii}(z) = 0$, $z \in [0, 1]$ for $i \in \{1, \dots, n\}$, which poses no restriction (see, e.g., Hu et al. (2016)). The PDE-ODE system (2.1) with the input $\mathbf{u}(t) \in \mathbb{R}^{n_-}$ is completed by initial conditions $\mathbf{w}(0) = \mathbf{w}_0 \in \mathbb{R}^{n_w}$ and piecewise continuous $\mathbf{x}(z, 0) = \mathbf{x}_0(z) \in \mathbb{R}^n$. The system structure and the interconnections between the PDE and ODE subsystems are illustrated in Figure 2.1.

Remark 2.1. System (2.1) describes the plant considered in Irscheid et al. (2023) in the undisturbed case with a more general nonlinear function \mathbf{c} in (2.1b). Here, \mathbf{c} depends not only on the ODE state $\mathbf{w}(t)$ but also on the boundary value $\mathbf{x}_-(0, t)$.

The objective is to design a state feedback that stabilizes a sufficiently smooth reference trajectory

$$t \mapsto (\mathbf{w}_r(t), \mathbf{x}_r(\cdot, t), \mathbf{u}_r(t)) \quad (2.5)$$

that satisfies the system dynamics (2.1), i.e.

$$\dot{\mathbf{w}}_r(t) = \mathbf{f}(\mathbf{w}_r(t), \mathbf{x}_{-,r}(0, t)) \quad (2.6a)$$

$$\mathbf{x}_{+,r}(0, t) = Q_0 \mathbf{x}_{-,r}(0, t) + \mathbf{c}(\mathbf{w}_r(t), \mathbf{x}_{-,r}(0, t)) \quad (2.6b)$$

$$\partial_t \mathbf{x}_r(z, t) = \Lambda(z) \partial_z \mathbf{x}_r(z, t) + A(z) \mathbf{x}_r(z, t) \quad (2.6c)$$

$$\mathbf{x}_{-,r}(1, t) = Q_1 \mathbf{x}_{+,r}(1, t) + \mathbf{u}_r(t). \quad (2.6d)$$

In order to guarantee trajectory tracking with the solution-based approach, a set of assumptions is imposed in the following.

2.1.2 Assumptions

The solution-based controller proposed in Section 2.2 makes use of a coordinate change that transforms the bidirectionally coupled PDE-ODE system (2.1) into a form suitable for control. The design is based on the fact that the \mathbf{x}_- -subsystem is fully boundary-actuated at $z = 1$ (cf. (2.1d)). This can be utilized to control not only the \mathbf{x}_- -subsystem but also the nonlinear ODE subsystem and the \mathbf{x}_+ -subsystem, that are both driven by the boundary value $\mathbf{x}_-(0, t)$ (see (2.1a) and (2.1b), respectively). In particular, the control design for the nonlinear ODE subsystem (2.1a) can be traced back to prediction-based methods for ODEs with delayed actuation. Hence, the following assumptions are made in order to facilitate the design and to ensure its feasibility.

Assumption 2.1. *The ODE subsystem (2.1a) is forward complete, i.e., there exists a unique solution $\mathbf{w}(t)$ on \mathbb{R}_0^+ for all initial conditions and every (measurable locally essentially) bounded $\mathbf{x}_-(0, t)$ (see, e.g., Angeli and Sontag (1999)).*

Note that forward completeness excludes finite escape time. Moreover, it is a typical assumption for the control of nonlinear ODEs with delays in the actuation channel (see, e.g., Bekiaris-Liberis and Krstic (2014)). The reason for this is the fact that a control action at the boundary $z = 1$ acts on the ODE subsystem (2.1a) at $z = 0$ only after a finite delay. In addition to that, Assumption 2.1 is essential for the control design in Section 2.2 since the latter requires a prediction of the ODE state $\mathbf{w}(t)$ on a (finite) time horizon.

Assumption 2.2. *For reference trajectories $\mathbf{w}_r(t)$ and $\mathbf{x}_{-,r}(0, t)$ satisfying (2.1a), there exists a tracking controller $\boldsymbol{\kappa}(t, \mathbf{w}(t))$ such that*

$$\dot{\mathbf{w}}(t) = \mathbf{f}(\mathbf{w}(t), \boldsymbol{\kappa}(t, \mathbf{w}(t))) \quad (2.7)$$

implies global asymptotic stability of $\mathbf{w}_r(t)$. Furthermore, let $\mathbf{x}_{-,r}(0, t) = \boldsymbol{\kappa}(t, \mathbf{w}_r(t))$ with

$$\lim_{\mathbf{w}(t) \rightarrow \mathbf{w}_r(t)} \|\boldsymbol{\kappa}(t, \mathbf{w}(t)) - \boldsymbol{\kappa}(t, \mathbf{w}_r(t))\| = 0. \quad (2.8)$$

Existence of a tracking controller $\boldsymbol{\kappa}(t, \mathbf{w}(t))$ for the nonlinear ODE subsystem (2.1a) in the case of immediate actuation is necessary for designing a solution-based controller for the PDE-ODE system (2.1). The explicit time dependence of $\boldsymbol{\kappa}(t, \mathbf{w}(t))$ represents its dependence on the reference trajectory $\mathbf{w}_r(t)$ and its derivatives. Furthermore, the second part of the assumption is required to show that convergence of the ODE state tracking error $\mathbf{w}(t) - \mathbf{w}_r(t)$ implies the same for the PDE state tracking error. For a Lipschitz continuous $\boldsymbol{\kappa}(t, \mathbf{w}(t))$, condition (2.8) is always true. Note that the stated property of global asymptotic convergence in Assumption 2.2 leads to global results for the controlled PDE-ODE system (2.1). A locally stabilizing $\boldsymbol{\kappa}(t, \mathbf{w}(t))$ is also possible in the context of the design in Section 2.2, however, the results would then be valid at least locally for initial conditions $\mathbf{w}(0)$ and $\mathbf{w}_r(0)$ in a subset of \mathbb{R}^{n_w} . In particular, the

region of attraction would depend on the initial profile $\mathbf{x}(z, 0)$ as well. For simplicity, only global results are pursued in the following, whereas for local results one may refer to the arguments made in Irscheid et al. (2022b).

Remark 2.2. *Assumptions 2.1 and 2.2 are always met in the case of stabilizable linear time-invariant ODE subsystems (2.1a).*

The remainder of this chapter is organized as follows. A solution-based tracking controller is derived in the next section. The resulting feedback law necessitates a prediction of the ODE state. Section 2.3 shows that the corresponding prediction problem can be formulated as a nonlinear integro-differential equation and investigates its solvability. An analysis of the tracking error in closed loop is given in Section 2.4, which concludes the chapter.

2.2 Solution-based control design

The control design relies on the solution of a Cauchy problem of hyperbolic character. More specifically, it is composed of PDEs that inherit the structure of the actuation channel, i.e., the subsystem describing the transport from the actuated boundary at $z = 1$ to the unactuated one at $z = 0$, however, the boundary condition is given at $z = 0$. In fact, PDEs for a transport in the negative z -direction with a boundary condition at $z = 0$ constitute a final value problem. Nevertheless, effectively, the Cauchy problem is solved backward in time, which is why it is also referred to as an inverse problem.

As depicted in Figure 2.1, the actuation channel, i.e., the \mathbf{x}_- -subsystem, and the \mathbf{x}_+ -subsystem are coupled due to the source term $A(z)\mathbf{x}(z, t)$ in (2.1c). Therefore, it is of great benefit to simplify the coupling in (2.1c) before commencing with the control design. For that, a preliminary coordinate transformation is introduced in Section 2.2.1. The main part of the solution-based approach is then carried out in Section 2.2.2 to decouple the PDE and ODE subsystems through yet another change of coordinates. The latter is formulated with the help of the aforementioned hyperbolic Cauchy problem. Afterwards, the control law is derived in Section 2.2.3 on the basis of the structure of the transformed PDE-ODE system.

2.2.1 Preliminary backstepping transformation

The solution-based control design is significantly simplified through the use of the invertible backstepping transformation²

$$\tilde{\mathbf{x}}(z, t) = \mathbf{x}(z, t) - \int_0^z K(z, \zeta)\mathbf{x}(\zeta, t) d\zeta =: \mathcal{T}_b[\mathbf{x}(t)](z) \quad (2.9)$$

²The square brackets in $\mathcal{T}_b[\mathbf{x}(t)](z)$ stand for a functional dependence on $\mathbf{x}(z, t)$ w.r.t. the spatial variable z .

(see, e.g., Krstic and Smyshlyaev (2008)) with the kernel $K(z, \zeta) \in \mathbb{R}^{n \times n}$ being the unique piecewise C^0 -solution of the kernel equations

$$\Lambda(z)\partial_z K(z, \zeta) + \partial_\zeta (K(z, \zeta)\Lambda(\zeta)) = K(z, \zeta)A(\zeta) \quad (2.10a)$$

$$K(z, z)\Lambda(z) - \Lambda(z)K(z, z) = A(z) \quad (2.10b)$$

$$K(z, 0)\Lambda(0)[E_- + E_+Q_0] = A_0(z), \quad (2.10c)$$

that are defined on the domain $0 \leq \zeta \leq z \leq 1$. Note that the matrix-valued equation (2.10c) is considered to be a boundary condition only for those rows i and columns j satisfying $1 \leq i \leq j \leq n_-$, allowing to freely assign the corresponding elements $a_{0,ij}$ of the matrix $A_0(z) \in \mathbb{R}^{n \times n_-}$, whereas the remainder of (2.10c) defines the remaining elements of $A_0(z)$. In fact, choosing $a_{0,ij}(z) = 0$ for $1 \leq i \leq j \leq n_-$ and $z \in [0, 1]$ results in $E_-^T A_0(z)$ being strictly lower triangular and, hence, yields a simpler structure of the PDE subsystem in transformed coordinates. This is a typical choice of boundary conditions for the kernel $K(z, \zeta)$ that is commonly used in the context of linear systems, where additional artificial conditions are imposed for uniqueness of the solution (see, e.g., Hu et al. (2019) for more details).

The transformation (2.9) maps (2.1) into the intermediate PDE-ODE system

$$\dot{\mathbf{w}}(t) = \mathbf{f}(\mathbf{w}(t), \tilde{\mathbf{x}}_-(0, t)) \quad (2.11a)$$

$$\tilde{\mathbf{x}}_+(0, t) = Q_0 \tilde{\mathbf{x}}_-(0, t) + \mathbf{c}(\mathbf{w}(t), \tilde{\mathbf{x}}_-(0, t)) \quad (2.11b)$$

$$\partial_t \tilde{\mathbf{x}}(z, t) = \Lambda(z)\partial_z \tilde{\mathbf{x}}(z, t) + A_0(z)\tilde{\mathbf{x}}_-(0, t) + H(z)\mathbf{c}(\mathbf{w}(t), \tilde{\mathbf{x}}_-(0, t)) \quad (2.11c)$$

$$\tilde{\mathbf{x}}_-(1, t) = \tilde{\mathbf{u}}(t), \quad (2.11d)$$

where

$$H(z) = K(z, 0)\Lambda(0)E_+ \quad (2.12)$$

and the state feedback

$$\tilde{\mathbf{u}}(t) = Q_1 \mathbf{x}_+(1, t) + \mathbf{u}(t) - \int_0^1 E_-^T K(1, z)\mathbf{x}(z, t) dz \quad (2.13)$$

introduces the new input $\tilde{\mathbf{u}}(t) \in \mathbb{R}^{n_-}$. The in-domain coupling term $A(z)\mathbf{x}(z, t)$, which is present in (2.1c) in original coordinates, is replaced with a distributed coupling of the boundary values $\tilde{\mathbf{x}}_-(0, t)$ and $\mathbf{w}(t)$ on the PDE subsystem (2.11c) in transformed coordinates by means of the terms $A_0(z)\tilde{\mathbf{x}}_-(0, t)$ and $H(z)\mathbf{c}(\mathbf{w}(t), \tilde{\mathbf{x}}_-(0, t))$. This coupling structure is illustrated in Figure 2.2.

Recalling that $E_-^T A_0(z)$ is strictly lower triangular, the PDE subsystem (2.11c) would be a cascade of transport equations if it were not for the term $H(z)\mathbf{c}(\mathbf{w}(t), \tilde{\mathbf{x}}_-(0, t))$. As a matter of fact, it is sufficient for control purposes to focus on the $\tilde{\mathbf{x}}_-$ -subsystem and, thus, the next transformation aims to decouple this subsystem from the ODE state $\mathbf{w}(t)$.

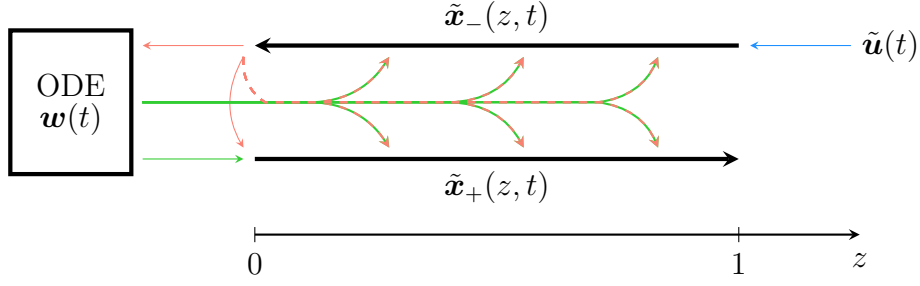


Figure 2.2: Schematic depiction of the intermediate PDE-ODE system (2.11).

2.2.2 Decoupling transformation

The central idea of the solution-based approach is the decoupling of the actuation channel through a change of coordinates that is derived from the solution of a suitable Cauchy problem. The latter comprises transport equations for a transport in the negative z -direction with boundary conditions given at $z = 0$. It is regarded as an inverse problem in the sense that the information at the boundary provides the solution backward in time. This will be further clarified in Section 2.3.

Introduce the Cauchy problem

$$\partial_t \tilde{\chi}_-(z, t) = \Lambda_-(z) \partial_z \tilde{\chi}_-(z, t) + E_-^T (A_0(z) \tilde{\chi}_-(0, t) + H(z) \mathbf{c}(\mathbf{w}(t), \tilde{\chi}_-(0, t))) \quad (2.14a)$$

$$\tilde{\chi}_-(0, t) = \boldsymbol{\kappa}(t, \mathbf{w}(t)) \quad (2.14b)$$

on the domain $(z, t) \in [0, 1] \times \mathbb{R}_0^+$, where the state feedback $\boldsymbol{\kappa}(t, \mathbf{w}(t)) \in \mathbb{R}^{n_-}$ is the one in Assumption 2.2 and $\Lambda_-(z) = E_-^T \Lambda(z) E_-$. Analogously, define the notation $\Lambda_+(z) = E_+^T \Lambda(z) E_+$. Then, the decoupling transformation

$$\check{\mathbf{x}}_-(z, t) = \tilde{\mathbf{x}}_-(z, t) - \tilde{\chi}_-(z, t) \quad (2.15a)$$

$$\check{\mathbf{x}}_+(z, t) = \tilde{\mathbf{x}}_+(z, t) \quad (2.15b)$$

maps the intermediate PDE-ODE system (2.11) into the cascaded system

$$\check{\mathbf{x}}_-(1, t) = \tilde{\mathbf{u}}(t) - \tilde{\chi}_-(1, t) \quad (2.16a)$$

$$\partial_t \check{\mathbf{x}}_-(z, t) = \Lambda_-(z) \partial_z \check{\mathbf{x}}_-(z, t) \quad (2.16b)$$

$$\dot{\mathbf{w}}(t) = \mathbf{f}(\mathbf{w}(t), \boldsymbol{\kappa}(t, \mathbf{w}(t)) + \check{\mathbf{x}}_-(0, t)) \quad (2.16c)$$

$$\check{\mathbf{x}}_+(0, t) = Q_0(\boldsymbol{\kappa}(t, \mathbf{w}(t)) + \check{\mathbf{x}}_-(0, t)) + \mathbf{c}(\mathbf{w}(t), \boldsymbol{\kappa}(t, \mathbf{w}(t)) + \check{\mathbf{x}}_-(0, t)) \quad (2.16d)$$

$$\begin{aligned} \partial_t \check{\mathbf{x}}_+(z, t) = \Lambda_+(z) \partial_z \check{\mathbf{x}}_+(z, t) + E_+^T A_0(z) (\boldsymbol{\kappa}(t, \mathbf{w}(t)) + \check{\mathbf{x}}_-(0, t)) \\ + E_+^T H(z) \mathbf{c}(\mathbf{w}(t), \boldsymbol{\kappa}(t, \mathbf{w}(t)) + \check{\mathbf{x}}_-(0, t)). \end{aligned} \quad (2.16e)$$

As depicted in Figure 2.3, the $\check{\mathbf{x}}_-$ -PDE (2.16b), which is fully boundary actuated through (2.16a), is cascaded with the ODE subsystem (2.16c) as well as the $\check{\mathbf{x}}_+$ -subsystem (2.16d)–(2.16e). In fact, to achieve tracking control, it is sufficient to stabilize the $\check{\mathbf{x}}_-$ -subsystem. This is a trivial task if $\tilde{\chi}_-(1, t)$ is known. For simplicity of

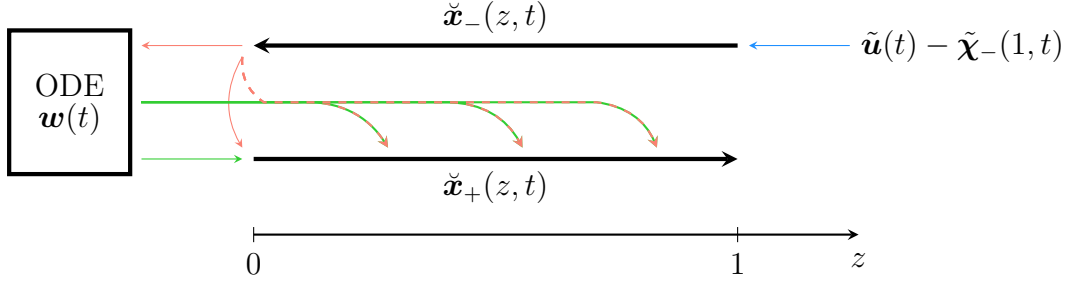


Figure 2.3: Schematic depiction of the system (2.16), where the $\check{\mathbf{x}}_-$ -subsystem is cascaded with the ODE as well as with the $\check{\mathbf{x}}_+$ -subsystem.

presentation, the subsequent design step assumes knowledge of the solution $\tilde{\chi}_-(z, t)$ of the inverse problem (2.14), which is discussed afterwards in Section 2.3.

Remark 2.3. *Disregarding the differences between the system class (2.1) and the one considered in Irscheid et al. (2023) (cf. Remark 2.1), the decoupling transformation used here is novel. It stems from a trivial modification of the Cauchy problem (2.14). As a consequence, the $\check{\mathbf{x}}_-$ -PDE (2.16b) describes a system of parallel transport equations (in the negative z -direction) that can be stabilized in the theoretically minimal time $\Delta_{n_-}^-$ (see the closed loop (2.22) in Section 2.2). This is a significant improvement of the result in Irscheid et al. (2023), where the corresponding transport equations are cascaded and, thus, the convergence time is the sum of all transport delays Δ_i^- , $i \in \{1, \dots, n_-\}$.*

Remark 2.4. *Although superfluous for the control design, one could try to eliminate the influence of the boundary values $\check{\mathbf{x}}_-(0, t)$ and $\mathbf{w}(t)$ on the $\check{\mathbf{x}}_+$ -subsystem (2.16d)–(2.16e) through an extension of the inverse problem (2.14). In particular, define the inverse problem*

$$\partial_t \tilde{\chi}(z, t) = \Lambda(z) \partial_z \tilde{\chi}(z, t) + A_0(z) \tilde{\mathbf{x}}_-(0, t) + H(z) \mathbf{c}(\mathbf{w}(t), \tilde{\mathbf{x}}_-(0, t)) \quad (2.17a)$$

$$\tilde{\chi}_-(0, t) = \boldsymbol{\kappa}(t, \mathbf{w}(t)) \quad (2.17b)$$

$$\tilde{\chi}_+(0, t) = Q_0 \tilde{\mathbf{x}}_-(0, t) + \mathbf{c}(\mathbf{w}(t), \tilde{\mathbf{x}}_-(0, t)) \quad (2.17c)$$

instead of (2.14), and replace (2.15b) with

$$\check{\mathbf{x}}_+(z, t) = \tilde{\mathbf{x}}_+(z, t) - \tilde{\chi}_+(z, t) \quad (2.18)$$

to obtain the transformed system

$$\dot{\mathbf{w}}(t) = \mathbf{f}(\mathbf{w}(t), \boldsymbol{\kappa}(t, \mathbf{w}(t)) + \check{\mathbf{x}}_-(0, t)) \quad (2.19a)$$

$$\check{\mathbf{x}}_+(0, t) = 0 \quad (2.19b)$$

$$\partial_t \check{\mathbf{x}}(z, t) = \Lambda(z) \partial_z \check{\mathbf{x}}(z, t) \quad (2.19c)$$

$$\check{\mathbf{x}}_-(1, t) = \tilde{\mathbf{u}}(t) - \tilde{\chi}_-(1, t) \quad (2.19d)$$

instead of (2.16). Despite the result (2.19) having a simpler structure in comparison with (2.16), the subsequent control design remains unaffected by the simplification of

the $\check{\mathbf{x}}_+$ -subsystem. As the benefit of this adjustment is questionable, using the extended inverse problem (2.17) instead of (2.14) will not be pursued further.

2.2.3 Control law

From the structure of the cascaded PDE-ODE system (2.16) it is obvious that the control law

$$\tilde{\mathbf{u}}(t) = \tilde{\chi}_-(1, t), \quad (2.20)$$

or equivalently

$$\mathbf{u}(t) = \tilde{\chi}_-(1, t) - Q_1 \mathbf{x}_+(1, t) + \int_0^1 E_-^T K(1, z) \mathbf{x}(z, t) dz \quad (2.21)$$

(cf. (2.13)), stabilizes the $\check{\mathbf{x}}_-$ -subsystem in finite time $\Delta_{n_-}^-$ (recall its definition in (2.4b)). In fact, the control law (2.20) yields the closed loop

$$\check{\mathbf{x}}_-(1, t) = \mathbf{0} \quad (2.22a)$$

$$\partial_t \check{\mathbf{x}}_-(z, t) = \Lambda_-(z) \partial_z \check{\mathbf{x}}_-(z, t) \quad (2.22b)$$

$$\dot{\mathbf{w}}(t) = \mathbf{f}(\mathbf{w}(t), \boldsymbol{\kappa}(t, \mathbf{w}(t))) + \check{\mathbf{x}}_-(0, t) \quad (2.22c)$$

$$\check{\mathbf{x}}_+(0, t) = Q_0(\boldsymbol{\kappa}(t, \mathbf{w}(t)) + \check{\mathbf{x}}_-(0, t)) + \mathbf{c}(\mathbf{w}(t), \boldsymbol{\kappa}(t, \mathbf{w}(t))) + \check{\mathbf{x}}_-(0, t) \quad (2.22d)$$

$$\begin{aligned} \partial_t \check{\mathbf{x}}_+(z, t) &= \Lambda_+(z) \partial_z \check{\mathbf{x}}_+(z, t) + E_+^T A_0(z) (\boldsymbol{\kappa}(t, \mathbf{w}(t)) + \check{\mathbf{x}}_-(0, t)) \\ &\quad + E_+^T H(z) \mathbf{c}(\mathbf{w}(t), \boldsymbol{\kappa}(t, \mathbf{w}(t))) + \check{\mathbf{x}}_-(0, t) \end{aligned} \quad (2.22e)$$

(see (2.16)). Special emphasis is given to the fact that

$$\check{x}_{-,i}(z, t) = 0, \quad t > \Delta_i^- \quad (2.23)$$

for $i \in \{1, \dots, n_-\}$, which implies

$$\check{\mathbf{x}}_-(z, t) = \mathbf{0}, \quad t > \Delta_{n_-}^- \quad (2.24)$$

for $z \in [0, 1]$. This differs from the results in Irscheid et al. (2023), where the finite-time convergence occurs only for $t > \sum_{i=1}^{n_-} \Delta_i^-$, as mentioned in Remark 2.3.

The next section is concerned with the solution of the inverse problem (2.14). More specifically, its solution will be shown to have a functional dependence on the PDE state $\mathbf{x}(z, t)$ and the ODE state $\mathbf{w}(t)$. Consequently, the control law (2.21) can be represented as a state feedback.

2.3 Solution of the inverse problem

For $i \in \{1, \dots, n_-\}$, let $\tilde{\chi}_i(z, t)$ and $\kappa_i(t, \mathbf{w}(t))$ as well as $\mathbf{a}_{0,i}^T(z)$ and $\mathbf{h}_i^T(z)$ be the i -th entry of $\tilde{\chi}_-(z, t)$ and $\boldsymbol{\kappa}(t, \mathbf{w}(t))$ as well as the i -th row of $A_0(z)$ and $H(z)$, respectively.

Then, the (formal) solution $\tilde{\chi}_-(z, t)$ of the inverse problem (2.14) is composed of the entries

$$\begin{aligned} \tilde{\chi}_i(z, t) = & \kappa_i(t + \phi_i^-(z), \mathbf{w}(t + \phi_i^-(z))) - \int_0^{\phi_i^-(z)} \mathbf{a}_{0,i}^T(\psi_i^-(\phi_i^-(z) - \sigma)) \tilde{\mathbf{x}}_-(0, t + \sigma) d\sigma \\ & - \int_0^{\phi_i^-(z)} \mathbf{h}_i^T(\psi_i^-(\phi_i^-(z) - \sigma)) \mathbf{c}(\mathbf{w}(t + \sigma), \tilde{\mathbf{x}}_-(0, t + \sigma)) d\sigma. \end{aligned} \quad (2.25)$$

This result follows from using the method of characteristics. In order to evaluate the formal solution (2.25) for $i \in \{1, \dots, n_-\}$ and $z \in [0, 1]$, the boundary values $\tilde{\mathbf{x}}_-(0, t + \tau)$ and $\mathbf{w}(t + \tau)$ at the boundary $z = 0$ have to be predicted for $\tau \in [0, \Delta_{n_-}^-]$. An explicit method is presented in Irscheid et al. (2023) for determining the required predictions on the basis of the PDE state $\tilde{\mathbf{x}}(z, t)$ and the ODE state $\mathbf{w}(t)$, both available at time t . The nature of the underlying prediction problem is discussed briefly in the following.

2.3.1 State prediction at the unactuated boundary

To refer to the predicted ODE state that is determined on the basis of the available system state at time t , introduce the notation

$$\mathbf{w}_p(\tau; t) = \mathbf{w}(t + \tau), \quad (2.26)$$

where t plays the role of a parameter and $\mathbf{w}(t + \tau)$ always exists by Assumption 2.1. A substitution of the ODE state $\mathbf{w}(t + \tau)$ with $\mathbf{w}_p(\tau; t)$ in (2.11a) yields the prediction problem

$$\frac{d\mathbf{w}_p}{d\tau}(\tau; t) = \mathbf{f}(\mathbf{w}_p(\tau; t), \tilde{\mathbf{x}}_-(0, t + \tau)) \quad (2.27)$$

with the initial value $\mathbf{w}_p(0; t) = \mathbf{w}(t)$. Hence, predicting the ODE state $\mathbf{w}(t + \tau)$ for $\tau \in \mathcal{I}_p = [0, \Delta_{n_-}^-]$ amounts to the solution of (2.27) on \mathcal{I}_p . In what follows, it is shown that the future values $\tilde{\mathbf{x}}_-(0, t + \tau)$, appearing in the prediction problem (2.27), can be written as a functional of $\mathbf{w}_p(\tau; t)$ and $\tilde{\mathbf{x}}_-(z, t)$ for fixed t .

Obtaining the future values $\tilde{\mathbf{x}}_-(0, t + \tau)$ is closely related to the solution (2.25) of the inverse problem (2.14). Applying the method of characteristics to solve (2.11c) component-wise yields the relation

$$\begin{aligned} \tilde{x}_{-,i}(0, t + \tau) = & \tilde{x}_{-,i}(\psi_i^-(\tau), t) + \int_0^\tau \mathbf{a}_{0,i}^T(\psi_i^-(\tau - \sigma)) \tilde{\mathbf{x}}_-(0, t + \sigma) d\sigma \\ & + \int_0^\tau \mathbf{h}_i^T(\psi_i^-(\tau - \sigma)) \mathbf{c}(\mathbf{w}(t + \sigma), \tilde{\mathbf{x}}_-(0, t + \sigma)) d\sigma \end{aligned} \quad (2.28)$$

for $\tau \in [0, \Delta_i^-]$ and $i \in \{1, \dots, n_-\}$. However, the corresponding solution branch for $\tau \in (\Delta_i^-, \Delta_{n_-}^-]$ is more involved and can be obtained on the basis of the following observation.

Determining the i -th entry $\tilde{u}_i(t)$ of $\tilde{\mathbf{u}}(t)$ in the control law (2.20) requires a prediction until $\tau = \Delta_i^-$ only (cf. (2.25) for $z = 1$). This infers that the solution branch (2.28) is sufficient to assign $\tilde{u}_i(t) = \tilde{\chi}_{-,i}(1, t)$ in (2.20). In fact, under the assumption that the latter holds for all future times, i.e., that the control law (2.20) is implemented for all $t \geq 0$, the closed-loop system (2.22) can be used to determine $\tilde{x}_{-,i}(0, t + \tau)$ for $\tau \in (\Delta_i^-, \Delta_{n_-}^-]$. This is clarified in the next step.

Evaluating the transformation (2.15a) at $z = 0$ and shifting time by τ results in

$$\tilde{\mathbf{x}}_-(0, t + \tau) = \tilde{\boldsymbol{\chi}}_-(0, t + \tau) + \tilde{\mathbf{x}}_-(0, t + \tau). \quad (2.29)$$

By using this together with (2.14b) and (2.23), it follows that

$$\tilde{x}_{-,i}(0, t + \tau) = \kappa_i(t + \tau, \mathbf{w}(t + \tau)) \quad (2.30)$$

for $\tau \in (\Delta_i^-, \Delta_{n_-}^-]$ and $i \in \{1, \dots, n_-\}$ in closed loop under the assumption that the control law (2.20) holds for all $t \geq 0$. Hence, in order to obtain the future values $\tilde{\mathbf{x}}_-(0, t + \tau)$ for $\tau \in \mathcal{I}_p$, the solution branches (2.28) and (2.30) are combined. Both branches are illustrated in Figure 2.4 for the cases $i = 1$, $i \in \{2, \dots, n_- - 1\}$ as well as $i = n_-$, wherein the variables $\tau_i^I \in [0, \Delta_i^-]$ and $\tau_i^{II} \in (\Delta_i^-, \Delta_{n_-}^-]$ are introduced to differentiate between boundary values that correspond to both solution branches. Note that the solution branch (2.28) is sufficient for the case $i = n_-$.

Remark 2.5. *The second solution branch (2.30) is obtained component-wise in closed loop on the basis of (2.23) at $z = 0$ after the time shift $t \mapsto t + \tau$ for $\tau \in (\Delta_i^-, \Delta_{n_-}^-]$ and $i \in \{1, \dots, n_-\}$. Although the prediction problem (2.27) necessitates knowledge of $\tilde{x}_{-,i}(0, t + \tau)$ only, it is possible to obtain $\tilde{x}_{-,i}$ on the entire region in Figure 2.4 that is highlighted in blue. This computation can be done using the method of characteristics. Consequently, one obtains trajectories $\tilde{u}_i(t + \tau)$, which denote the i -th entry of $\tilde{\mathbf{u}}(t + \tau)$ for $\tau \in (\Delta_i^-, \Delta_{n_-}^-]$, as illustrated in Figure 2.4. In other words, future input trajectories at $z = 1$ are determined by the desired closed-loop behavior at $z = 0$ in the future. This can be interpreted as quasi-static state feedback, tracing back the terminology to the context of flatness-based control of nonlinear ODEs (see, e.g., Rudolph (2021) for a detailed description). Note that an alternative approach could be a dynamic state feedback in the spirit of Knüppel et al. (2014), which necessitates state extensions.*

In summary, introducing the abbreviation

$$\tilde{c}_i(z, \mathbf{w}(t), \tilde{\mathbf{x}}_-(0, t)) = \mathbf{a}_{0,i}^T(z) \tilde{\mathbf{x}}_-(0, t) + \mathbf{h}_i^T(z) \mathbf{c}(\mathbf{w}(t), \tilde{\mathbf{x}}_-(0, t)) \quad (2.31)$$

yields

$$\tilde{x}_{-,i}(0, t + \tau) = \begin{cases} \tilde{x}_{-,i}(\psi_i^-(\tau), t) \\ \quad + \int_0^\tau \tilde{c}_i(\psi_i^-(\tau - \sigma), \mathbf{w}(t + \sigma), \tilde{\mathbf{x}}_-(0, t + \sigma)) \, d\sigma, & \tau \in [0, \Delta_i^-] \\ \kappa_i(t + \tau, \mathbf{w}(t + \tau)), & \tau \in (\Delta_i^-, \Delta_{n_-}^-] \end{cases} \quad (2.32)$$

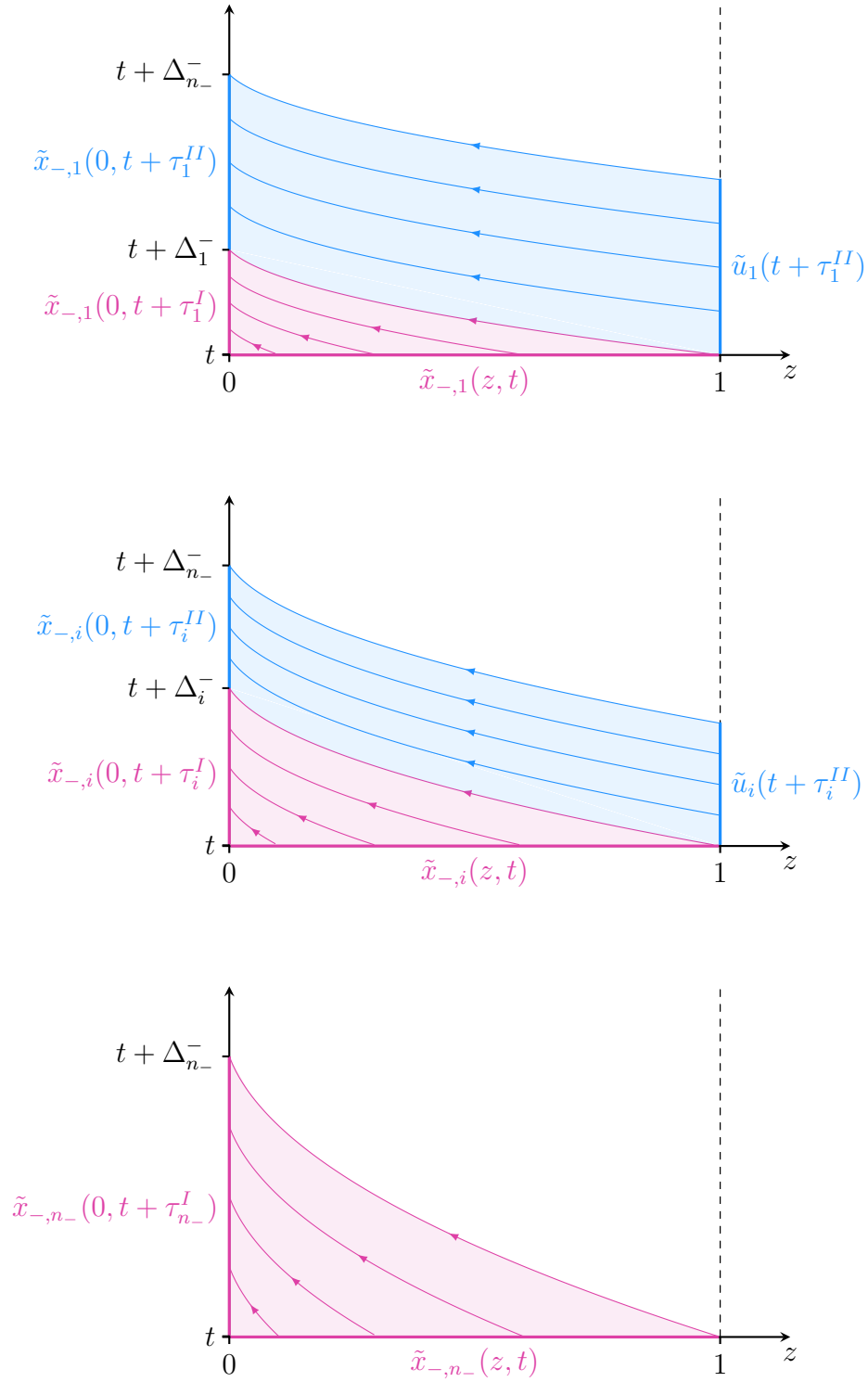


Figure 2.4: Composition of the solution branches (2.28), highlighted in red, and (2.30), highlighted in blue, for the cases $i = 1$, $i \in \{2, \dots, n-1\}$ and $i = n_-$. Therein, $\tilde{u}_i(t)$ denotes the i -th entry of $\tilde{\mathbf{u}}(t)$, $\tau_i^I \in [0, \Delta_i^-]$ and $\tau_i^{II} \in (\Delta_i^-, \Delta_{n-}^-]$.

for $\tau \in \mathcal{I}_p$ and $i \in \{1, \dots, n_-\}$. Inserting (2.32) into (2.27) and taking (2.26) into account results in the nonlinear integro-differential equation

$$\frac{d\mathbf{w}_p}{d\tau}(\tau; t) = \mathbf{f}(\mathbf{w}_p(\tau; t), \tilde{\mathbf{x}}_-(0, t + \tau)) \quad (2.33a)$$

$$\tilde{\mathbf{x}}_{-,i}(0, t + \tau) = \begin{cases} \tilde{x}_{-,i}(\psi_i^-(\tau), t) \\ \quad + \int_0^\tau \tilde{c}_i(\psi_i^-(\tau - \sigma), \mathbf{w}_p(\sigma; t), \tilde{\mathbf{x}}_-(0, t + \sigma)) \, d\sigma, & \tau \in [0, \Delta_i^-] \\ \kappa_i(t + \tau, \mathbf{w}_p(\tau; t)), & \tau \in (\Delta_i^-, \Delta_{n_-}^-] \end{cases} \quad (2.33b)$$

for $\mathbf{w}_p(\tau; t)$, the solvability of which is investigated in the following on \mathcal{I}_p for a given initial condition $\mathbf{w}_p(0; t) = \mathbf{w}(t)$.

2.3.2 Solvability of the nonlinear integro-differential equation

Note that the results in Irscheid et al. (2023) guarantee existence and uniqueness of the solution of (2.33) or equivalently (2.27) and (2.32). Nevertheless, the difference of the system classes under investigation (see Remark 2.1) necessitates a preceding analysis of (2.32).

For that, let $\tau \in [0, \Delta_1^-]$ and recall that $\Delta_1^- < \Delta_i^-$ for $i \in \{2, \dots, n_-\}$ (cf. (2.4a)–(2.4b)). Therefore, for all $i \in \{1, \dots, n_-\}$, the first solution branch in (2.32) can be used to obtain $\tilde{x}_{-,i}(0, t + \tau)$. Note that this requires the solution of a nonlinear Volterra integral equation of the second kind for $\tilde{x}_{-,i}(0, t + \tau)$. Moreover, due to the coupling between all entries of $\tilde{\mathbf{x}}_-(0, t)$ by means of $\tilde{c}_i(z, \mathbf{w}(t), \tilde{\mathbf{x}}_-(0, t))$, the resulting n_- equations have to be solved simultaneously. Hence, one obtains a vector-valued nonlinear Volterra integral equation of the second kind for $\tilde{\mathbf{x}}_-(0, t + \tau)$. However, this poses no restriction as the solvability of the integral equation is guaranteed by the Lipschitz continuity of $\tilde{c}_i(z, \mathbf{w}(t), \tilde{\mathbf{x}}_-(0, t))$ (defined in (2.31)) w.r.t. its third argument and the continuity w.r.t. its remaining arguments (see, e.g., Linz (1985, Ch. 4) for more details). A similar argument can be made for all $\tau \in \mathcal{I}_p$ after combining both solution branches in (2.32). Hence, the latter can be solved for $\tilde{\mathbf{x}}_-(0, t + \tau)$ for all $\tau \in \mathcal{I}_p$. Altogether, this makes it possible to obtain a general nonlinear Volterra integro-differential equation (GNVIDE) in the explicit form presented in Irscheid et al. (2023), for which existence of a unique solution is shown. Therefore, this will not be further pursued here.

2.3.3 Interpretation of the state dependency

Predicting the system state at $z = 0$ amounts to the solution of the GNVIDE (2.33). It can be shown, at least formally, that its solution $\mathbf{w}_p(\tau; t)$ and similarly $\tilde{\mathbf{x}}_-(0, t + \tau)$ both not only depend on the ODE state $\mathbf{w}(t)$ but also have a functional dependence on the PDE state $\tilde{\mathbf{x}}(z, t)$. Inserting this into (2.25), i.e., the entries $\tilde{\chi}_i(z, t)$ of the

solution $\tilde{\chi}_-(z, t)$ of the inverse problem (2.14), yields the same functional dependence for $\tilde{\chi}_-(z, t)$. This may be denoted as

$$\tilde{\chi}_-(z, t) = \tilde{\mathcal{X}}_-[\tilde{\mathbf{x}}(t), \mathbf{w}(t)](z). \quad (2.34)$$

Therefore, the decoupling transformation (2.15) can be written as a state transformation of the form

$$\check{\mathbf{x}}(z, t) = \tilde{\mathbf{x}}(z, t) - E_- \tilde{\mathcal{X}}_-[\tilde{\mathbf{x}}(t), \mathbf{w}(t)](z) =: \mathcal{T}_d[\tilde{\mathbf{x}}(t), \mathbf{w}(t)](z). \quad (2.35)$$

Note that a more explicit representation of this state dependency is omitted here.

Inverse transformation

The inverse of the decoupling transformation (2.15), i.e.,

$$\tilde{\mathbf{x}}_-(z, t) = \check{\mathbf{x}}_-(z, t) + \tilde{\chi}_-(z, t) \quad (2.36a)$$

$$\tilde{\mathbf{x}}_+(z, t) = \check{\mathbf{x}}_+(z, t) \quad (2.36b)$$

is investigated in what follows. Particular focus lies on its representation as an inverse state transformation $\tilde{\mathbf{x}}(z, t) = \mathcal{T}_d^{-1}[\check{\mathbf{x}}(t), \mathbf{w}(t)](z)$, mapping (2.16) into (2.11). For that, the Cauchy problem (2.14) has to be rewritten in terms of $\check{\mathbf{x}}(z, t)$. In particular, replace $\tilde{\mathbf{x}}_-(0, t)$ in (2.14) with $\boldsymbol{\kappa}(t, \mathbf{w}(t)) + \check{\mathbf{x}}_-(0, t)$ to obtain

$$\begin{aligned} \partial_t \tilde{\chi}_-(z, t) &= \Lambda_-(z) \partial_z \tilde{\chi}_-(z, t) + E_-^T A_0(z) (\boldsymbol{\kappa}(t, \mathbf{w}(t)) + \check{\mathbf{x}}_-(0, t)) \\ &\quad + E_-^T H(z) \mathbf{c}(\mathbf{w}(t), \boldsymbol{\kappa}(t, \mathbf{w}(t)) + \check{\mathbf{x}}_-(0, t)) \end{aligned} \quad (2.37a)$$

$$\tilde{\chi}_-(0, t) = \boldsymbol{\kappa}(t, \mathbf{w}(t)). \quad (2.37b)$$

Obviously, the latter can be solved component-wise with the method of characteristics (cf. (2.25)) since it has the same dependencies as (2.14). In fact, by the same reasoning as in Section 2.3.1, the corresponding prediction problem results in the GNVIDE

$$\frac{d\mathbf{w}_p}{d\tau}(\tau; t) = \mathbf{f}(\mathbf{w}_p(\tau; t), \boldsymbol{\kappa}(t, \mathbf{w}_p(\tau; t)) + \check{\mathbf{x}}_-(0, t + \tau)) \quad (2.38a)$$

$$\check{x}_{-,i}(0, t + \tau) = \begin{cases} \check{x}_{-,i}(\psi_i^-(\tau), t), & \tau \in [0, \Delta_i^-] \\ 0, & \tau \in (\Delta_i^-, \Delta_{n_-}^-] \end{cases} \quad (2.38b)$$

(cf. (2.33)) for $\mathbf{w}_p(\tau; t)$ with $\tau \in \mathcal{I}_p$ and $i \in \{1, \dots, n_-\}$. This result is an immediate consequence of (2.16c) with the application of the method of characteristics on (2.22a)–(2.22b) in closed loop. The solvability of (2.38) with the initial condition $\mathbf{w}_p(0; t) = \mathbf{w}(t)$ can be concluded analogously to Section 2.3.2. By that, the solution of (2.38) depends on the ODE state $\mathbf{w}(t)$ and has a functional dependence on the PDE state $\check{\mathbf{x}}(z, t)$. As such, the inverse transformation (2.36) is indeed a state transformation of the form $\tilde{\mathbf{x}}(z, t) = \mathcal{T}_d^{-1}[\check{\mathbf{x}}(t), \mathbf{w}(t)](z)$.

State feedback

In light of the expression (2.34) for the solution $\tilde{\chi}_-(z, t)$ of the inverse problem (2.14) and the preliminary backstepping transformation (2.9), the control law (2.21) is a feedback of the ODE state $\mathbf{w}(t)$ and the PDE state $\mathbf{x}(z, t)$ in original coordinates. In particular, (2.21) can be written as

$$\mathbf{u}(t) = \tilde{\mathcal{X}}_- [\mathcal{T}_b[\mathbf{x}(t)], \mathbf{w}(t)](1) - Q_1 \mathbf{x}_+(1, t) + \int_0^1 E_-^T K(1, z) \mathbf{x}(z, t) dz. \quad (2.39)$$

The closed-loop system follows from inserting the latter (or equivalently the state feedback (2.21)) into the PDE-ODE system (2.1). Next, the stability properties of the closed-loop system are discussed.

Remark 2.6. *Note that the kernel equations (2.10) can be solved offline using, e.g., the conl MATLAB library in Fischer et al. (2021). However, solving the GNVIDE (2.33) as suggested in Irscheid et al. (2023) yields a numerical scheme for online evaluation.*

2.4 Stability analysis

The stability analysis of the tracking error follows the proof in Irscheid et al. (2022b) with appropriate adjustments to account for differences in notation, system class and assumptions. In order to infer tracking in original coordinates, the tracking error dynamics is first investigated in transformed coordinates. For that, the transformations (2.9) and (2.15) are applied to the reference system (2.6).

2.4.1 The reference system in transformed coordinates

Applying the preliminary backstepping transformation (2.9) to the reference system (2.6), i.e., $\tilde{\mathbf{x}}_r(z, t) = \mathcal{T}_b[\mathbf{x}_r(t)](z)$, yields the intermediate reference system

$$\dot{\mathbf{w}}_r(t) = \mathbf{f}(\mathbf{w}_r(t), \tilde{\mathbf{x}}_{-,r}(0, t)) \quad (2.40a)$$

$$\tilde{\mathbf{x}}_{+,r}(0, t) = Q_0 \tilde{\mathbf{x}}_{-,r}(0, t) + \mathbf{c}(\mathbf{w}_r(t), \tilde{\mathbf{x}}_{-,r}(0, t)) \quad (2.40b)$$

$$\partial_t \tilde{\mathbf{x}}_r(z, t) = \Lambda(z) \partial_z \tilde{\mathbf{x}}_r(z, t) + A_0(z) \tilde{\mathbf{x}}_{-,r}(0, t) + H(z) \mathbf{c}(\mathbf{w}_r(t), \tilde{\mathbf{x}}_{-,r}(0, t)) \quad (2.40c)$$

$$\tilde{\mathbf{x}}_{-,r}(1, t) = \tilde{\mathbf{u}}_r(t) \quad (2.40d)$$

(cf. (2.11)) with the new reference input

$$\tilde{\mathbf{u}}_r(t) = Q_1 \mathbf{x}_{+,r}(1, t) + \mathbf{u}_r(t) - \int_0^1 E_-^T K(1, z) \mathbf{x}_r(z, t) dz \quad (2.41)$$

(cf. (2.13)). Next, define $\tilde{\chi}_{-,r}(z, t)$ to be the solution of

$$\begin{aligned} \partial_t \tilde{\chi}_{-,r}(z, t) &= \Lambda_-(z) \partial_z \tilde{\chi}_{-,r}(z, t) \\ &\quad + E_-^T (A_0(z) \tilde{\mathbf{x}}_{-,r}(0, t) + H(z) \mathbf{c}(\mathbf{w}_r(t), \tilde{\mathbf{x}}_{-,r}(0, t))) \end{aligned} \quad (2.42a)$$

$$\tilde{\chi}_{-,r}(0, t) = \boldsymbol{\kappa}(t, \mathbf{w}_r(t)), \quad (2.42b)$$

i.e., the Cauchy problem (2.14) after replacing $\mathbf{w}(t)$ and $\mathbf{x}(z, t)$ with $\mathbf{w}_r(t)$ and $\mathbf{x}_r(z, t)$, respectively. With that, the decoupling transformation $\check{\mathbf{x}}_r(z, t) = \mathcal{T}_d[\tilde{\mathbf{x}}_r(t), \mathbf{w}_r(t)](z)$, as defined in (2.35), maps (2.40) into

$$\check{\mathbf{x}}_{-,r}(1, t) = \tilde{\mathbf{u}}_r(t) - \tilde{\boldsymbol{\chi}}_{-,r}(1, t) \quad (2.43a)$$

$$\partial_t \check{\mathbf{x}}_{-,r}(z, t) = \Lambda_-(z) \partial_z \check{\mathbf{x}}_{-,r}(z, t) \quad (2.43b)$$

$$\dot{\mathbf{w}}_r(t) = \mathbf{f}(\mathbf{w}_r(t), \boldsymbol{\kappa}(t, \mathbf{w}_r(t))) \quad (2.43c)$$

$$\check{\mathbf{x}}_{+,r}(0, t) = Q_0 \boldsymbol{\kappa}(t, \mathbf{w}_r(t)) + \mathbf{c}(\mathbf{w}_r(t), \boldsymbol{\kappa}(t, \mathbf{w}_r(t))) \quad (2.43d)$$

$$\partial_t \check{\mathbf{x}}_{+,r}(z, t) = \Lambda_+(z) \partial_z \check{\mathbf{x}}_{+,r}(z, t) + E_+^T(A_0(z) \boldsymbol{\kappa}(t, \mathbf{w}_r(t)) + H(z) \mathbf{c}(\mathbf{w}_r(t), \boldsymbol{\kappa}(t, \mathbf{w}_r(t)))) \quad (2.43e)$$

(cf. (2.16)), after taking into account that

$$\check{\mathbf{x}}_{-,r}(0, t) = \tilde{\mathbf{x}}_{-,r}(z, t) - \tilde{\boldsymbol{\chi}}_{-,r}(z, t) = \mathbf{0}. \quad (2.44)$$

The latter holds in light of (2.42b), the evaluation of the backstepping transformation (2.9) at $z = 0$ and Assumption 2.2.

Note that (2.44) enables further simplification of (2.43). In fact, taking into account that $\check{\mathbf{x}}_{-,r}(z, t)$ satisfies the homogeneous transport equation (2.43b), it can be shown with the method of characteristics that (2.44) implies

$$\check{\mathbf{x}}_{-,r}(z, t) = \mathbf{0}. \quad (2.45)$$

Together with (2.43a), this yields

$$\tilde{\mathbf{u}}_r(t) = \tilde{\boldsymbol{\chi}}_{-,r}(1, t). \quad (2.46)$$

2.4.2 ODE state tracking error

Note that Assumption 2.1 in fact guarantees the existence of a unique solution $\mathbf{w}(t)$, especially for $t \in [0, \Delta_{n_-}^-]$, i.e., before the requirements of Assumption 2.2 hold. As a consequence of (2.24) in closed loop, the ODE subsystem (2.16c) takes the form (2.7) for $t > \Delta_{n_-}^-$. Therefore, by Assumption 2.2,

$$\lim_{t \rightarrow \infty} \|\mathbf{w}(t) - \mathbf{w}_r(t)\| = 0. \quad (2.47)$$

Another consequence of (2.24) is $\tilde{\mathbf{x}}_-(0, t) = \boldsymbol{\kappa}(t, \mathbf{w}(t))$ for $t > \Delta_{n_-}^-$, which follows from (2.14b) and the evaluation of (2.15a) at $z = 0$. In light of Assumption 2.2, particularly (2.8), this yields

$$\lim_{t \rightarrow \infty} \|\tilde{\mathbf{x}}_-(0, t) - \tilde{\mathbf{x}}_{-,r}(0, t)\| = 0. \quad (2.48)$$

2.4.3 PDE state tracking error

For $t > \Delta_{n_-}^-$, the PDE subsystems of the closed-loop system (2.22) and the corresponding reference system (2.43) read

$$\check{\mathbf{x}}_-(z, t) = \mathbf{0} \quad (2.49a)$$

$$\check{\mathbf{x}}_+(0, t) = Q_0 \boldsymbol{\kappa}(t, \mathbf{w}(t)) + \mathbf{c}(\mathbf{w}(t), \boldsymbol{\kappa}(t, \mathbf{w}(t))) \quad (2.49b)$$

$$\partial_t \check{\mathbf{x}}_+(z, t) = \Lambda_+(z) \partial_z \check{\mathbf{x}}_+(z, t) + E_+^T (A_0(z) \boldsymbol{\kappa}(t, \mathbf{w}(t)) + H(z) \mathbf{c}(\mathbf{w}(t), \boldsymbol{\kappa}(t, \mathbf{w}(t)))) \quad (2.49c)$$

and

$$\check{\mathbf{x}}_{-,r}(z, t) = \mathbf{0} \quad (2.50a)$$

$$\check{\mathbf{x}}_{+,r}(0, t) = Q_0 \boldsymbol{\kappa}(t, \mathbf{w}_r(t)) + \mathbf{c}(\mathbf{w}_r(t), \boldsymbol{\kappa}(t, \mathbf{w}_r(t))) \quad (2.50b)$$

$$\partial_t \check{\mathbf{x}}_{+,r}(z, t) = \Lambda_+(z) \partial_z \check{\mathbf{x}}_{+,r}(z, t) + E_+^T (A_0(z) \boldsymbol{\kappa}(t, \mathbf{w}_r(t)) + H(z) \mathbf{c}(\mathbf{w}_r(t), \boldsymbol{\kappa}(t, \mathbf{w}_r(t)))) \quad (2.50c)$$

in light of (2.24) and (2.45), respectively. Taking into account (2.8) as well as the Lipschitz continuity of \mathbf{c} yields³

$$\lim_{t \rightarrow \infty} \|\check{\mathbf{x}}(t) - \check{\mathbf{x}}_r(t)\|_\infty = 0 \quad (2.51)$$

(refer to the proof in Irscheid et al. (2022b)). The same argument can be made to show that

$$\lim_{t \rightarrow \infty} \|\tilde{\boldsymbol{\chi}}_-(t) - \tilde{\boldsymbol{\chi}}_{-,r}(t)\|_\infty = 0 \quad (2.52)$$

as a consequence of (2.14), (2.42) and (2.48). Taking into account the definition of the decoupling transformation (2.15), (2.51) and (2.52) imply

$$\lim_{t \rightarrow \infty} \|\tilde{\mathbf{x}}(t) - \tilde{\mathbf{x}}_r(t)\|_\infty = 0. \quad (2.53)$$

Hence, by the invertibility of the preliminary backstepping transformation (2.9), tracking is achieved in original coordinates, i.e.,

$$\lim_{t \rightarrow \infty} \|\mathbf{x}(t) - \mathbf{x}_r(t)\|_\infty = 0. \quad (2.54)$$

In summary, (2.47) and (2.54) infer tracking of the reference trajectory (2.5) in the closed-loop system that results from inserting the control law (2.21) into the PDE-ODE system (2.1).

³For any distributed variable $\mathbf{x}(z, t) \in \mathbb{R}^n$, $(z, t) \in [0, 1] \times \mathbb{R}_0^+$, denote by $\|\mathbf{x}(t)\|_\infty$ the supremum norm $\sup_{z \in [0, 1]} \|\mathbf{x}(z, t)\|$.

Chapter 3

Parabolic systems

In the previous chapter, the control strategy proposed for hyperbolic systems revolves around the solution of an appropriately chosen Cauchy problem w.r.t. the spatial variable. This is closely linked to a flatness-based parameterization of solutions, which exist for parabolic systems as well (see, e.g., Rudolph and Woittennek (2008)). This motivates an investigation of a solution-based control strategy for parabolic PDE-ODE systems. As a matter of fact, the ideas explored in this chapter are used in Irscheid et al. (2024) to design a stabilizing controller for a (scalar) linear parabolic PDE with nonlinear boundary dynamics. This recent result marks an important advancement because the latter control problem had not been resolved with existing methods in the literature.

Although the control of linear parabolic systems is well-understood through the lens of backstepping (see, e.g., Smyshlyaev and Krstic (2004); Krstic and Smyshlyaev (2008); Deutscher and Gehring (2021)), the main idea of solution-based control for parabolic systems is introduced in the following for two linear examples before presenting the nonlinear case. In fact, the strategies employed for each of the linear examples are utilized in the control design for the nonlinear problem. It should be noted that the resulting controller is expressed implicitly in terms of the system state, in contrast to the explicit state feedback that is obtained in the linear setting.

First, revisiting a reaction-diffusion equation, the explicit solution of the corresponding parabolic Cauchy problem is derived as a functional of the system state in Section 3.1. Despite the calculations being tedious, an interesting equivalence is established with the well-known backstepping transformations. Similarly, a linear PDE-ODE system is studied afterwards in Section 3.2 to better understand the impact of the ODE subsystem on the solution of the Cauchy problem. Finally, the main results of Irscheid et al. (2024) are presented in Section 3.3 for the case of nonlinear boundary ODEs.

Notation

This chapter uses the same notation as in Irscheid et al. (2024), which is briefly recalled in the following. The k -th derivative $h^{(k)}$, $k \in \mathbb{N}_0$ of a smooth function $t \mapsto h(t)$ is written as $h^{(k)} = \left(\frac{d}{dt}\right)^k h$, indicating that the operator $\frac{d}{dt}$ is applied k times to the function h . The class of analytic functions is denoted as \mathcal{C}^ω . A function h is called Gevrey of order $\alpha > 0$, in short $h \in \mathcal{G}_\alpha$, if $\exists M, R > 0$ such that $\sup_{t \geq 0} |h^{(k)}(t)| \leq M \frac{(k!)^\alpha}{R^k}$ for all $k \in \mathbb{N}_0$ (see, e.g., Rodino (1993, Def. 1.4.1)). Note that analytic functions are Gevrey of order $\alpha = 1$, i.e., $\mathcal{C}^\omega = \mathcal{G}_1$, and that $h \in \mathcal{G}_{\alpha_1}$ implies $h \in \mathcal{G}_{\alpha_2}$ for all $\alpha_1 \leq \alpha_2$. Furthermore, introduce the class $\mathcal{C}^\omega \mathcal{G}_2$ of functions $(z, t) \mapsto x(z, t)$ that are analytic in z and of Gevrey class two w.r.t. t , i.e., $x \in \mathcal{C}^\omega \mathcal{G}_2$.

3.1 Linear reaction-diffusion equation

Consider the boundary-actuated parabolic system

$$\partial_z x(0, t) = 0 \tag{3.1a}$$

$$\partial_t x(z, t) = \partial_z^2 x(z, t) + rx(z, t) \tag{3.1b}$$

$$x(1, t) = u(t) \tag{3.1c}$$

for $r \in \mathbb{R}$ and $(z, t) \in [0, 1] \times \mathbb{R}_0^+$ with state $x(z, t) \in \mathbb{R}$, input $u(t)$ and initial condition $x(z, 0) = x_0(z) \in \mathbb{R}$. This linear reaction-diffusion equation with Neumann boundary at $z = 0$ and Dirichlet actuation¹ at $z = 1$ is known to admit a so-called flat output $y(t) = x(0, t)$, which allows for a differential parameterization of not only the boundary values but also the entire distributed state (see, e.g., Fliess et al. (1998); Laroche et al. (1998) for details). In Laroche et al. (2000), this flatness-based parameterization is represented by the solution of the Cauchy problem

$$\partial_z^2 x(z, t) = \partial_t x(z, t) - rx(z, t) \tag{3.2a}$$

$$x(0, t) = y(t) \tag{3.2b}$$

$$\partial_z x(0, t) = 0 \tag{3.2c}$$

w.r.t. z , where the control input $u(t) = x(1, t)$ takes the role of an output. Note that (3.2) is an inverse² problem because $y(t)$ is prescribed and $u(t)$ is sought, conversely to the original problem (3.1). Solving (3.2) formally with a power-series ansatz yields

$$x(z, t) = \sum_{k=0}^{\infty} \frac{z^{2k}}{(2k)!} \left(\frac{d}{dt} - r\right)^k y(t), \tag{3.3}$$

¹Other types of boundary conditions can be treated similarly, as detailed in Appendix A.1.2 for a Dirichlet boundary at $z = 0$ and sketched in Remark 3.2 for Neumann actuation at $z = 1$.

²This terminology is used in Chapter 2 to refer to Cauchy problems that are solved backward in time, without mentioning the role of input and output.

i.e., infinitely many time derivatives of the flat output $y(t)$ appear in the parameterization of the PDE state $x(z, t)$. In fact, inserting a suitable³ reference y_r for y in (3.3), an open-loop controller is obtained by evaluating the resulting expression at $z = 1$. Hence, a flatness-based parameterization is very useful for the open-loop control design (see, e.g., Rudolph (2003) for applications of flatness-based open-loop control designs).

3.1.1 From open-loop control to state feedback

In the context of open-loop control, it is beneficial to plan the reference y_r without introducing an initial error. Therefore, y_r should be chosen to match the (infinitely many) initial conditions $y^{(k)}(0)$, $k \in \mathbb{N}_0$, of the flat output $y(t)$, which are implied by the initial profile $x_0(z)$, $z \in [0, 1]$, of the PDE state $x(z, t)$ via (3.3) evaluated at $t = 0$. In order to examine the influence of a differently chosen reference, consider the inverse problem

$$\partial_z^2 \chi(z, t) = \partial_t \chi(z, t) - r \chi(z, t) \quad (3.4a)$$

$$\chi(0, t) = y_r(t) \quad (3.4b)$$

$$\partial_z \chi(0, t) = 0 \quad (3.4c)$$

for $\chi(z, t) \in \mathbb{R}$, $(z, t) \in [0, 1] \times \mathbb{R}_0^+$, with output $u_r(t) = \chi(1, t)$ and arbitrary initial conditions for y_r . Furthermore, define the error

$$\tilde{x}(z, t) = x(z, t) - \chi(z, t), \quad (3.5)$$

for which

$$\partial_z \tilde{x}(0, t) = 0 \quad (3.6a)$$

$$\partial_t \tilde{x}(z, t) = \partial_z^2 \tilde{x}(z, t) + r \tilde{x}(z, t) \quad (3.6b)$$

$$\tilde{x}(1, t) = u(t) - u_r(t) \quad (3.6c)$$

can be deduced from the plant (3.1) and the Cauchy problem (3.4). In the case of open-loop control, i.e., $u(t) = u_r(t)$, the error system (3.6) is easily shown to be exponentially stable in $\mathcal{L}_2([0, 1])$ and in the supremum norm if and only if $r < \pi^2/4$ (see, e.g., Meurer and Kugi (2009, Lem. 6 and 7)). This provokes the question whether it is possible to modify the inverse problem (3.4) such that the error system is exponentially stable for arbitrary reaction coefficients $r \in \mathbb{R}$.

The (possibly destabilizing) reaction term $r\tilde{x}(z, t)$ in (3.6b) can be eliminated by replacing (3.4) with the Cauchy problem

$$\partial_z^2 \chi(z, t) = \partial_t \chi(z, t) - r x(z, t) \quad (3.7a)$$

$$\chi(0, t) = y_r(t) \quad (3.7b)$$

$$\partial_z \chi(0, t) = 0, \quad (3.7c)$$

³The series in (3.3) converges for any y of Gevrey class two (see, e.g., Fliess et al. (1998); Laroche et al. (1998)). Thus, a reference $y_r \in \mathcal{G}_2$ is chosen.

which is excited by both the PDE state $x(z, t)$ and the reference $y_r(t)$ in (3.7a) and (3.7b), respectively. As a result, the error system reads

$$\partial_z \tilde{x}(0, t) = 0 \quad (3.8a)$$

$$\partial_t \tilde{x}(z, t) = \partial_z^2 \tilde{x}(z, t) \quad (3.8b)$$

$$\tilde{x}(1, t) = u(t) - \chi(1, t) \quad (3.8c)$$

instead of (3.6). Note that (3.8) can be made exponentially stable by the controller

$$u(t) = \chi(1, t), \quad (3.9)$$

which will be shown to be a state feedback due to the dependence of the inverse problem (3.7) on $x(z, t)$. As this type of feedback requires solving an inverse problem, similar to the method proposed in Chapter 2, it will be referred to as solution-based controller.

3.1.2 Analytical solution of the inverse problem

The linearity of the inverse problem (3.7) allows to obtain its solution by superposing the solutions of two simpler problems: the case $y_r(t) = 0$ and the case $x(z, t) = 0$. The latter is solved in, e.g., Laroche et al. (1998) and is, thus, omitted here. Hence, for simplicity, consider the special case of stabilization, i.e., $y_r(t) = 0$.

By using a power-series ansatz for $\chi(z, t)$ in (3.7) and inserting the solution (3.3) for $x(z, t)$ as well as $y_r(t) = 0$, one obtains

$$\chi(z, t) = \sum_{k=0}^{\infty} \frac{z^{2k}}{(2k)!} \left(\left(\frac{d}{dt} - r \right)^k - \left(\frac{d}{dt} \right)^k \right) y(t). \quad (3.10)$$

It is shown in Appendix A.1.1 that this solution can equivalently be expressed as

$$\chi(z, t) = \int_0^z k(z, \zeta) x(\zeta, t) d\zeta \quad (3.11a)$$

with the integral kernel

$$k(z, \zeta) = -rz \frac{I_1(\sqrt{r(z^2 - \zeta^2)})}{\sqrt{r(z^2 - \zeta^2)}}, \quad (3.11b)$$

where I_1 is the modified Bessel function of first kind and first order. With that, the solution $\chi(z, t)$ given in (3.11) takes the form of a Volterra integral and, thus,

$$\tilde{x}(z, t) = x(z, t) - \int_0^z k(z, \zeta) x(\zeta, t) d\zeta \quad (3.12)$$

(cf. (3.5)) is as a Volterra integral transformation of the PDE state $x(z, t)$.

Note that (3.12) is the (invertible) backstepping transformation that is employed in, e.g., Smyshlyaev and Krstic (2004) to map the plant (3.1) into the so-called target system (3.8). Furthermore, the resulting backstepping controller coincides with the one found here after inserting the solution (3.11) for $z = 1$ into the control law (3.9). This yields a static feedback of the state $x(z, t)$. At last, stability of the error system (3.8) infers the same in original coordinates by the bounded invertibility of the backstepping transformation (3.12). As the inverse can be obtained in a similar fashion, its explicit determination is omitted here.

Remark 3.1. *Instead of the power-series ansatz (3.10), one could use a Volterra integral (3.11a) with an unknown kernel $k(z, \zeta)$ for the solution of (3.7). By inserting this ansatz in (3.7), it can be shown that the kernel has to satisfy*

$$\partial_z^2 k(z, \zeta) - \partial_\zeta^2 k(z, \zeta) = rk(z, \zeta) \quad (3.13a)$$

$$2k(z, z) = -rz \quad (3.13b)$$

$$\partial_\zeta k(z, 0) = 0 \quad (3.13c)$$

for $0 \leq \zeta \leq z \leq 1$. As detailed in, e.g., Smyshlyaev and Krstic (2004), solving these kernel equations yields (3.11b).

Remark 3.2. *The flatness-based parameterization (3.3) of the PDE state $x(z, t)$ is preserved when the Dirichlet actuation in (3.1c) is replaced with Neumann actuation. As a consequence, both the Cauchy problem (3.7) and its solution (3.11) remain unaltered. However, the resulting control law differs from (3.9) as it has to be chosen in such a way that the corresponding error system*

$$\partial_z \tilde{x}(0, t) = 0 \quad (3.14a)$$

$$\partial_t \tilde{x}(z, t) = \partial_z^2 \tilde{x}(z, t) \quad (3.14b)$$

$$\partial_z \tilde{x}(1, t) = u(t) - \partial_z \chi(1, t) \quad (3.14c)$$

(cf. (3.8)) is made asymptotically stable. For instance, using Meurer and Kugi (2009, Lem. 6), exponential stability can be proven with the controller

$$u(t) = \partial_z \chi(1, t) - \gamma(x(1, t) - \chi(1, t)) \quad (3.15)$$

for $\gamma > 0$. In contrast, changing the type of boundary condition at $z = 0$ does not preserve the flatness-based parameterization of $x(z, t)$ nor the solution of the Cauchy problem (3.7). This is detailed in Appendix A.1.2 for the sake of completeness.

3.2 Linear parabolic PDE-ODE system

Thus far, the Cauchy problem (3.7) for the linear reaction-diffusion equation has been shown to admit a solution that has a functional dependence on the PDE state $x(z, t)$

as can be seen from the Volterra integral in (3.11a). Moreover, this makes the change of coordinates (3.5) a Volterra integral state transformation (cf. (3.12)), usually referred to as a backstepping transformation (see, e.g., Krstic and Smyshlyaev (2008)). Furthermore, Krstic (2009) extends the backstepping method to linear parabolic PDE-ODE cascades. This motivates an investigation of solution-based control for this class of systems in order to better understand the impact of an ODE subsystem on the solution of the corresponding Cauchy problem.

For that, consider the linear parabolic PDE-ODE cascade

$$\dot{\mathbf{w}}(t) = F\mathbf{w}(t) + \mathbf{b}x(0, t) \quad (3.16a)$$

$$\partial_z x(0, t) = 0 \quad (3.16b)$$

$$\partial_t x(z, t) = \partial_z^2 x(z, t) \quad (3.16c)$$

$$x(1, t) = u(t) \quad (3.16d)$$

with the ODE state $\mathbf{w}(t) \in \mathbb{R}^n$, the PDE state $x(z, t) \in \mathbb{R}$ and a stabilizable pair (F, \mathbf{b}) , i.e., there exists a $\mathbf{k} \in \mathbb{R}^n$ such that $F + \mathbf{b}\mathbf{k}^T$ is Hurwitz. The initial conditions $\mathbf{w}(0) = \mathbf{w}_0 \in \mathbb{R}^n$ and $x(0, t) = x_0(z) \in \mathbb{R}$ complete the system.

3.2.1 Control design

In order to stabilize (3.16) in the spirit of solution-based control, introduce the Cauchy problem

$$\partial_z^2 \chi(z, t) = \partial_t \chi(z, t) \quad (3.17a)$$

$$\chi(0, t) = \mathbf{k}^T \mathbf{w}(t) \quad (3.17b)$$

$$\partial_z \chi(0, t) = 0 \quad (3.17c)$$

for $\chi(z, t) \in \mathbb{R}$, $(z, t) \in [0, 1] \times \mathbb{R}_0^+$, which is excited by the ODE state $\mathbf{w}(t)$. Then, the change of coordinates

$$\tilde{x}(z, t) = x(z, t) - \chi(z, t), \quad (3.18)$$

together with the control law

$$u(t) = \chi(1, t), \quad (3.19)$$

maps (3.16) into the asymptotically stable error system

$$\dot{\mathbf{w}}(t) = \tilde{F}\mathbf{w}(t) + \mathbf{b}\tilde{x}(0, t) \quad (3.20a)$$

$$\partial_z \tilde{x}(0, t) = 0 \quad (3.20b)$$

$$\partial_t \tilde{x}(z, t) = \partial_z^2 \tilde{x}(z, t) \quad (3.20c)$$

$$\tilde{x}(1, t) = 0, \quad (3.20d)$$

wherein $\tilde{F} = F + \mathbf{b}\mathbf{k}^T$ is Hurwitz. It is straightforward to show the exponential stability of (3.20), especially due to its cascaded structure (see, e.g., Krstic (2009) for the proof of exponential stability in an appropriate norm). Next, it is shown that the control law (3.19) can be expressed as a state feedback by solving (3.17) analytically.

3.2.2 Analytical solution of the inverse problem

Note that the PDE subsystem (3.16b)–(3.16d) is identical to (3.1) with $r = 0$. Consequently, the PDE subsystem admits the flat output $y(t) = x(0, t)$ and it follows that

$$x(z, t) = \sum_{k=0}^{\infty} \frac{z^{2k}}{(2k)!} \left(\frac{d}{dt}\right)^k y(t) \quad (3.21)$$

(cf. (3.3)) is a parameterization of the PDE state $x(z, t)$. Similarly, inserting a power-series ansatz for the solution $\chi(z, t)$ of the inverse problem (3.17) yields

$$\chi(z, t) = \sum_{k=0}^{\infty} \frac{z^{2k}}{(2k)!} \left(\frac{d}{dt}\right)^k \mathbf{k}^T \mathbf{w}(t). \quad (3.22)$$

The goal is to find an expression of the latter in terms of the ODE state $\mathbf{w}(t)$ and the PDE state $x(z, t)$. For that, motivated by the parameterization (3.21) of $x(z, t)$, it is useful to first rewrite (3.22) in terms of $\mathbf{w}(t)$ and derivatives of the flat output $y(t)$ as an intermediate step. In particular, the k -th derivative of $\mathbf{k}^T \mathbf{w}(t)$ in (3.22) can be expressed as

$$\left(\frac{d}{dt}\right)^k \mathbf{k}^T \mathbf{w}(t) = \mathbf{k}^T F^k \mathbf{w}(t) + \mathbf{k}^T \sum_{l=0}^{k-1} F^{k-1-l} \mathbf{b} y^{(l)}(t) \quad (3.23)$$

by successively inserting the ODE (3.16a) in light of $y(t) = x(0, t)$. Taking into account (3.23), the manipulations in Appendix A.2.1 reveal that (3.22) can equivalently be expressed as

$$\chi(z, t) = \mathbf{n}^T(z) \mathbf{w}(t) + \int_0^z \mathbf{m}^T(z - \zeta) \mathbf{b} x(\zeta, t) d\zeta, \quad (3.24)$$

where $\mathbf{n}^T(z)$ is the unique solution of the initial value problem

$$\frac{d^2 \mathbf{n}^T}{dz^2}(z) = \mathbf{n}^T(z) F \quad (3.25a)$$

$$\mathbf{n}^T(0) = \mathbf{k}^T \quad (3.25b)$$

$$\frac{d \mathbf{n}^T}{dz}(0) = \mathbf{0}^T \quad (3.25c)$$

on $z \in [0, 1]$ and

$$\mathbf{m}^T(z) = \int_0^z \mathbf{n}^T(\zeta) d\zeta. \quad (3.26)$$

As a consequence, by inserting the solution (3.24), evaluated at $z = 1$, into (3.19), one obtains a feedback of the states $\mathbf{w}(t)$ and $x(z, t)$. Furthermore, (3.24) allows to express the change of coordinates (3.18) as

$$\tilde{x}(z, t) = x(z, t) - \int_0^z \mathbf{m}^T(z - \zeta) \mathbf{b} x(\zeta, t) d\zeta - \mathbf{n}^T(z) \mathbf{w}(t), \quad (3.27)$$

which is a Volterra integral state transformation. In fact, it is easy to verify that the inverse transformation reads

$$x(z, t) = \tilde{x}(z, t) + \int_0^z \tilde{\mathbf{m}}^T(z - \zeta) \mathbf{b} \tilde{x}(\zeta, t) d\zeta + \tilde{\mathbf{n}}^T(z) \mathbf{w}(t), \quad (3.28)$$

where $\tilde{\mathbf{n}}^T(z)$ is the unique solution of the initial value problem

$$\frac{d^2 \tilde{\mathbf{n}}^T}{dz^2}(z) = \tilde{\mathbf{n}}^T(z) \tilde{F} \quad (3.29a)$$

$$\tilde{\mathbf{n}}^T(0) = \mathbf{k}^T \quad (3.29b)$$

$$\frac{d \tilde{\mathbf{n}}^T}{dz}(0) = \mathbf{0}^T \quad (3.29c)$$

(cf. (3.25)) on $z \in [0, 1]$ and

$$\tilde{\mathbf{m}}^T(z) = \int_0^z \tilde{\mathbf{n}}^T(\zeta) d\zeta \quad (3.30)$$

(cf. (3.26)). It can be derived as follows. Taking the control law (3.19) as well as (3.18) into account, the inverse transformation $x(z, t) = \tilde{x}(z, t) + \chi(z, t)$ maps (3.20) into (3.16). Similar to (3.23), the time derivatives of $\mathbf{k}^T \mathbf{w}(t)$ in (3.22) can be expressed by successively inserting the ODE (3.20a). As a result, the subsequent calculations are identical to the ones in Appendix A.2.1 after replacing F and $y(t)$ with \tilde{F} and $\tilde{y}(t) = \tilde{x}(0, t)$, respectively, where $\tilde{y}(t)$ denotes the flat output of the PDE subsystem (3.20b)–(3.20d).

Remark 3.3. *The state transformation (3.27) and its inverse (3.28) coincide with the ones in Krstic (2009) that are derived from the perspective of backstepping for the PDE-ODE system (3.16).*

Remark 3.4. *The control design for the PDE-ODE system (3.16) can easily be adapted to the case of unactuated Dirichlet boundary. Such a system is considered as an example in Irscheid et al. (2024). However, the required calculations are only briefly discussed therein, which is why they are presented in more detail in Appendix A.2.2.*

3.3 Nonlinear parabolic PDE-ODE system

The ideas presented for the previous elementary examples are combined in the following to control a more complex and, in particular, nonlinear PDE-ODE system. The main results are stated in Irscheid et al. (2024) and, thus, this section is intended to offer a brief presentation of the challenges associated with nonlinearities. In particular, it is shown that the solution-based control of a PDE-ODE cascade with nonlinear ODE differs from its linear counterpart only in the time derivatives of the (presumed to be

known) controller for the ODE subsystem (cf. (3.23)). It is worth noting that Irscheid et al. (2024) considers a PDE-ODE cascade with Dirichlet boundary at $z = 0$, whereas the case with Neumann boundary is considered in what follows.

The boundary-actuated PDE-ODE cascade

$$\dot{\mathbf{w}}(t) = \mathbf{f}(\mathbf{w}(t), x(0, t)) \quad (3.31a)$$

$$\partial_z x(0, t) = 0 \quad (3.31b)$$

$$\partial_t x(z, t) = \partial_z^2 x(z, t) + rx(z, t) \quad (3.31c)$$

$$x(1, t) = u(t) \quad (3.31d)$$

consists of the nonlinear ODE subsystem (3.31a) with the lumped state $\mathbf{w}(t) \in \mathbb{R}^n$ and the parabolic PDE subsystem (3.31b)–(3.31d) with the distributed state $x(z, t) \in \mathbb{R}$ defined for $(z, t) \in [0, 1] \times \mathbb{R}_0^+$. The subsystems are cascaded in the sense that the boundary value $x(0, t)$ acts on the ODE (3.31a) through the second argument of the Lipschitz continuous vector field \mathbf{f} . Moreover, the PDE (3.31c) is a linear reaction-diffusion equation with reaction coefficient $r \in \mathbb{R}$. System (3.31) is completed with initial conditions $\mathbf{w}(0) = \mathbf{w}_0 \in \mathbb{R}^n$ and $x(z, 0) = x_0(z) \in \mathbb{R}$.

Remark 3.5. *Note that the PDE subsystem (3.31b)–(3.31d) has previously been considered in Section 3.1. Furthermore, the linear ODE dynamics (3.16a) considered in Section 3.2 is a special case of (3.31a).*

This section aims to derive a controller that asymptotically stabilizes the origin of the PDE-ODE cascade (3.31). In the spirit of Irscheid et al. (2024), the control design for (3.31) is based on a stabilizing controller for the ODE subsystem (3.31a), wherein $x(0, t)$ takes the role of an input. This is guaranteed by the following assumption.

Assumption 3.1 (cf. Irscheid et al. (2024)). *There exists an analytic function $\kappa(\mathbf{w}(t))$ such that*

$$\dot{\mathbf{w}}(t) = \mathbf{f}(\mathbf{w}(t), \kappa(\mathbf{w}(t)) + \varpi(t)) \quad (3.32)$$

implies input-to-state stability of the origin w.r.t. $\varpi(t) \in \mathbb{R}$.

Assuming existence of a controller $\kappa(\mathbf{w}(t))$ is analogous to Assumption 2.2 for the hyperbolic system in Chapter 2. Moreover, input-to-state stability is sufficient for the control design presented in the sequel, and it is a typical prerequisite for similar classes of cascaded systems (see, e.g., Krstic et al. (1995); Irscheid et al. (2023)).

Remark 3.6. *Assumption 3.1 is automatically satisfied for the linear PDE-ODE system (3.16) considered in Section 3.2 with $\kappa(\mathbf{w}(t)) = \mathbf{k}^\top \mathbf{w}(t)$. This is due to the fact that the pair (F, \mathbf{b}) in (3.16a) is stabilizable.*

For the well-posedness of the Cauchy problem considered in the sequel, the following technical assumption is imposed.

Assumption 3.2 (cf. Irscheid et al. (2024)). *The ODE subsystem (3.31a) is forward complete, the nonlinear function \mathbf{f} is analytic, and the initial condition x_0 is analytic on $[0, 1]$.*

Forward completeness of the ODE subsystem (3.31a) ensures existence of a unique solution $\mathbf{w}(t)$ for all initial conditions and every (measurable locally essentially) bounded $x(0, t)$ (recall Assumption 2.1 in Chapter 2 and see, e.g., Angeli and Sontag (1999) for details). Hence, the ODE subsystem cannot exhibit a finite escape time.

As a matter of fact, Assumptions 3.1 and 3.2 ensure that the theoretical results in Irscheid et al. (2024) are applicable in the following. This is especially important for the well-posedness of the Cauchy problem and convergence of the formal power-series representation of its solution. Hence, the subsequent design steps will only give an outline of the control strategy as all details can be found in the latter reference. Moreover, the control design for the nonlinear PDE-ODE system (3.31) is inspired by the ideas presented for the linear reaction-diffusion equation (3.1) and the linear parabolic PDE-ODE system (3.16) in Sections 3.1 and 3.2, respectively (recall Remark 3.5). In particular, the control design is split into two steps: a preliminary backstepping transformation and a subsequent nonlinear state transformation in order to facilitate the stabilization of the PDE and ODE subsystems, respectively.

3.3.1 Preliminary backstepping transformation

Analogously to Section 3.1, the possibly destabilizing reaction term $rx(z, t)$ in (3.31c) can be eliminated by utilizing the backstepping transformation (3.12). It can be verified that it maps the PDE-ODE system (3.31) into the intermediate system

$$\dot{\mathbf{w}}(t) = \mathbf{f}(\mathbf{w}(t), \tilde{x}(0, t)) \quad (3.33a)$$

$$\partial_z \tilde{x}(0, t) = 0 \quad (3.33b)$$

$$\partial_t \tilde{x}(z, t) = \partial_z^2 \tilde{x}(z, t) \quad (3.33c)$$

$$\tilde{x}(1, t) = \tilde{u}(t) \quad (3.33d)$$

with the new input

$$\tilde{u}(t) = u(t) - \int_0^1 k(1, \zeta) x(\zeta, t) \, d\zeta \quad (3.34)$$

(cf. (3.8), (3.9) and (3.11)). Setting aside the nonlinearity of the vector field \mathbf{f} , note that (3.33) admits the same structure as the linear PDE-ODE system (3.16) considered in Section 3.2. This motivates the next transformation.

3.3.2 Nonlinear state transformation and state feedback

Inspired by the control design in Section 3.2.1, introduce the Cauchy problem

$$\partial_z^2 \tilde{\chi}(z, t) = \partial_t \tilde{\chi}(z, t) \quad (3.35a)$$

$$\tilde{\chi}(0, t) = \kappa(\mathbf{w}(t)) \quad (3.35b)$$

$$\partial_z \tilde{\chi}(0, t) = 0 \quad (3.35c)$$

(cf. (3.17)) for $\tilde{\chi}(z, t) \in \mathbb{R}$ and $(z, t) \in [0, 1] \times \mathbb{R}_0^+$. With that, the change of coordinates

$$\check{x}(z, t) = \tilde{x}(z, t) - \tilde{\chi}(z, t) \quad (3.36)$$

and the control law

$$\tilde{u}(t) = \tilde{\chi}(1, t), \quad (3.37)$$

map the intermediate PDE-ODE system (3.33) into the target system

$$\dot{\mathbf{w}}(t) = \mathbf{f}(\mathbf{w}(t), \kappa(\mathbf{w}(t)) + \check{x}(0, t)) \quad (3.38a)$$

$$\partial_z \check{x}(0, t) = 0 \quad (3.38b)$$

$$\partial_t \check{x}(z, t) = \partial_z^2 \check{x}(z, t) \quad (3.38c)$$

$$\check{x}(1, t) = 0. \quad (3.38d)$$

Note the structural similarity to the asymptotically stable error system (3.20). In fact, by the arguments made in Irscheid et al. (2024), it can be verified that the origin of the nonlinear target system (3.38) is asymptotically stable. This is a consequence of the exponential stability of the linear PDE subsystem (3.38b)–(3.38d) in the \mathcal{H}^1 -norm as well as the supremum norm (see, e.g., Meurer and Kugi (2009, Lem. 7)) and, by Assumption 3.1, the presumed input-to-state stability of the ODE subsystem (3.38a) w.r.t. $\check{x}(0, t)$.

For the special case of a linear system, it is possible to express the solution $\tilde{\chi}(z, t)$ of (3.35) explicitly in terms of $\mathbf{w}(t)$ and $\tilde{x}(z, t)$ (cf. (3.24)). However, due to the nonlinearity of the vector field \mathbf{f} and the ODE controller κ , only an implicit expression can be derived in the following. It is based on the formal solution

$$\tilde{\chi}(z, t) = \sum_{k=0}^{\infty} \frac{z^{2k}}{(2k)!} \left(\frac{d}{dt}\right)^k \kappa(\mathbf{w}(t)), \quad (3.39)$$

which is obtained by inserting a power-series ansatz for the solution $\tilde{\chi}(z, t)$ of (3.35), similar to (3.22).

Implicit solution of the inverse problem

The intermediate PDE subsystem (3.33b)–(3.33d) admits the flat output $\tilde{y}(t) = \tilde{x}(0, t)$, by which the parameterization

$$\tilde{x}(z, t) = \sum_{k=0}^{\infty} \frac{z^{2k}}{(2k)!} \left(\frac{d}{dt}\right)^k \tilde{y}(t) \quad (3.40)$$

of the PDE state $\tilde{x}(z, t)$ can be inferred analogously to (3.21). This motivates the definition of the following equivalent state representation of the intermediate system (3.33). For that, introduce the flat coordinates

$$\tilde{y}_k(t) = \left(\frac{d}{dt}\right)^k \tilde{y}(t), \quad k \in \mathbb{N}_0 \quad (3.41)$$

and insert the power series (3.40) into the intermediate system (3.33) to obtain

$$\underbrace{\frac{d}{dt} \begin{bmatrix} \mathbf{w}(t) \\ \tilde{y}_0(t) \\ \tilde{y}_1(t) \\ \vdots \end{bmatrix}}_{\tilde{\mathbf{w}}(t)} = \underbrace{\begin{bmatrix} \mathbf{f}(\mathbf{w}(t), \tilde{y}_0(t)) \\ \tilde{y}_1(t) \\ \tilde{y}_2(t) \\ \vdots \end{bmatrix}}_{\tilde{\mathbf{g}}(\tilde{\mathbf{w}}(t))} \quad (3.42a)$$

$$\sum_{k=0}^{\infty} \frac{1}{(2k)!} \tilde{y}_k(t) = \tilde{u}(t) \quad (3.42b)$$

with the (infinite-dimensional) state $\tilde{\mathbf{w}}(t)$. The series representation (3.40) may also be expressed in terms of the flat coordinates $\tilde{y}_k(t)$, which yields

$$\tilde{x}(z, t) = \sum_{k=0}^{\infty} \frac{z^{2k}}{(2k)!} \tilde{y}_k(t). \quad (3.43)$$

Note that the set of monomials z^{2k} of even degree is linearly independent and dense in $\mathcal{L}_2([0, 1])$. Therefore, (3.43) can be viewed as a transformation between the PDE state $\tilde{x}(z, t)$ of (3.33) and the flat coordinates $\tilde{y}_k(t)$ that constitute the infinite-dimensional subsystem of (3.42).

Remark 3.7. *The equivalence between the system representations (3.33) and (3.42) is to be understood for $\tilde{x} \in \mathcal{C}^\omega \mathcal{G}_2$, i.e., when the power series (3.40) and (3.43) converge on $[0, 1]$. Then, $\tilde{y}_k(t) = \partial_z^{2k} \tilde{x}(0, t)$ for $k \in \mathbb{N}_0$.*

Using the auxiliary variable $\tilde{\mathbf{y}}^{[k]} = (\tilde{y}_0, \dots, \tilde{y}_k)$ for $k \in \mathbb{N}_0$, the k -th derivative of $\kappa(\mathbf{w}(t))$ in (3.39) can be written in terms of the infinite-dimensional state $\tilde{\mathbf{w}}(t)$ as

$$\left(\frac{d}{dt}\right)^k \kappa(\mathbf{w}(t)) = \tilde{\phi}_k(\mathbf{w}(t), \tilde{\mathbf{y}}^{[k-1]}(t)), \quad (3.44)$$

where $\tilde{\phi}_k = L_{\tilde{\mathbf{g}}}^k \tilde{\eta}$ denotes the k -th Lie-derivative of $\tilde{\eta}(\tilde{\mathbf{w}}) := \kappa(\mathbf{w})$ along $\tilde{\mathbf{g}}$ and $\tilde{\mathbf{y}}^{[-1]}$ is defined to be empty. Inserting the Lie derivatives (3.44) into the formal solution (3.39) allows to express $\tilde{\chi}(z, t)$ in terms of $\tilde{\mathbf{w}}(t)$, i.e.,

$$\tilde{\chi}(z, t) = \sum_{k=0}^{\infty} \frac{z^{2k}}{(2k)!} \tilde{\phi}_k(\mathbf{w}(t), \tilde{\mathbf{y}}^{[k-1]}(t)). \quad (3.45)$$

Remark 3.8. *For the linear PDE-ODE cascade (3.16), (3.44) can be expressed explicitly in the form (3.23). Therein, y has to be replaced with \tilde{y} to maintain a consistent notation. The linear counterpart of (3.45) can be rearranged (see the manipulations in Appendix A.2.1) in such a way that $\tilde{\chi}(z, t)$ is expressed in terms of the ODE state $\mathbf{w}(t)$ and the PDE state $\tilde{x}(z, t)$ (cf. (3.24)).*

Interpretation of the state dependency

Inserting the representations (3.43) and (3.45) of $\tilde{x}(z, t)$ and $\tilde{\chi}(z, t)$, respectively, into the coordinate change (3.36) gives

$$\check{x}(z, t) = \sum_{k=0}^{\infty} \frac{z^{2k}}{(2k)!} \left(\tilde{y}_k(t) - \tilde{\phi}_k(\mathbf{w}(t), \tilde{\mathbf{y}}^{[k-1]}(t)) \right). \quad (3.46)$$

This makes the latter a nonlinear state transformation that maps (3.42) into (3.38). Due to the equivalence between the flat coordinates $\tilde{y}_k(t)$ and the PDE state $\tilde{x}(z, t)$ in the sense of (3.43), $\check{x}(z, t)$ can be expressed implicitly in terms of the ODE state $\mathbf{w}(t)$ and the PDE state $\tilde{x}(z, t)$ of the intermediate system (3.33). This state transformation is, thus, a generalization of the classical backstepping transformation of Volterra type (cf. (3.24)) to nonlinear settings. Furthermore, with the same reasoning, the control law (3.37) is a state feedback of $\mathbf{w}(t)$ and $\tilde{x}(z, t)$. In light of the input transformation (3.34) and the preliminary backstepping transformation (3.12), it can be verified that

$$u(t) = \tilde{\chi}(1, t) + \int_0^1 k(1, \zeta) x(\zeta, t) d\zeta \quad (3.47)$$

is a state feedback of $\mathbf{w}(t)$ and $x(z, t)$, i.e., the state of the nonlinear PDE-ODE system (3.31) in original coordinates.

Remark 3.9. *In order to implement the controller (3.47), $\tilde{\chi}(1, t)$ can be approximated with the numerical scheme presented in Irscheid et al. (2024) after replacing the odd powers $z^{2k+1}/(2k+1)!$ with their even counterparts $z^{2k}/(2k)!$ as a consequence of interchanging the Dirichlet boundary condition therein with the Neumann boundary condition (3.31b) considered here.*

Next, the inverse transformation is investigated in detail on the basis of the method sketched in Irscheid et al. (2024, Rem. 3).

Inverse transformation

Taking into account the control law (3.37), the inverse transformation $\tilde{x}(z, t) = \check{x}(z, t) + \tilde{\chi}(z, t)$ maps (3.38) into the intermediate PDE-ODE system (3.33). In order to express this change of coordinates as a state transformation (at least implicitly) in terms of the ODE state $\mathbf{w}(t)$ and the PDE state $\check{x}(z, t)$, introduce the flat coordinates

$$\check{y}_k(t) = \left(\frac{d}{dt} \right)^k \check{y}(t), \quad k \in \mathbb{N}_0 \quad (3.48)$$

(cf. (3.41)), where $\check{y}(t) = \check{x}(0, t)$ denotes the flat output of the PDE subsystem (3.31b)–(3.31d). Then, similar to (3.43), one obtains the parameterization

$$\check{x}(z, t) = \sum_{k=0}^{\infty} \frac{z^{2k}}{(2k)!} \check{y}_k(t) \quad (3.49)$$

of the PDE state $\check{x}(z, t)$. Inserting this parameterization into the error system (3.38) yields the equivalent representation

$$\underbrace{\frac{d}{dt} \begin{bmatrix} \mathbf{w}(t) \\ \check{y}_0(t) \\ \check{y}_1(t) \\ \vdots \end{bmatrix}}_{\check{\mathbf{w}}(t)} = \underbrace{\begin{bmatrix} \mathbf{f}(\mathbf{w}(t), \kappa(\mathbf{w}(t)) + \check{y}_0(t)) \\ \check{y}_1(t) \\ \check{y}_2(t) \\ \vdots \end{bmatrix}}_{\check{\mathbf{g}}(\check{\mathbf{w}}(t))} \quad (3.50a)$$

$$\sum_{k=0}^{\infty} \frac{1}{(2k)!} \check{y}_k(t) = 0 \quad (3.50b)$$

(cf. (3.42)) with the (infinite-dimensional) state $\check{\mathbf{w}}(t)$. With that it is possible to express the time derivatives in (3.39) in terms of the infinite-dimensional state $\check{\mathbf{w}}(t)$, as follows. Defining $\check{\mathbf{y}}^{[k]} = (\check{y}_0, \dots, \check{y}_k)$ for $k \in \mathbb{N}_0$ and in analogy to (3.44), the k -th derivative of $\kappa(\mathbf{w}(t))$ in (3.39) can be written as

$$\left(\frac{d}{dt}\right)^k \kappa(\mathbf{w}(t)) = \check{\phi}_k(\mathbf{w}(t), \check{\mathbf{y}}^{[k-1]}(t)), \quad (3.51)$$

where $\check{\phi}_k = L_{\check{\mathbf{g}}}^k \check{\eta}$ denotes the k -th Lie-derivative of $\check{\eta}(\check{\mathbf{w}}) := \kappa(\mathbf{w})$ along $\check{\mathbf{g}}$ and $\check{\mathbf{y}}^{[-1]}$ is defined to be empty. Finally, $\check{\chi}(z, t)$ can be expressed in terms of $\check{\mathbf{w}}(t)$ by inserting (3.51) into (3.39). This results in

$$\check{\chi}(z, t) = \sum_{k=0}^{\infty} \frac{z^{2k}}{(2k)!} \check{\phi}_k(\mathbf{w}(t), \check{\mathbf{y}}^{[k-1]}(t)) \quad (3.52)$$

(cf. (3.45)). In light of (3.49) and (3.52), the inverse of the coordinate change (3.36) (or equivalently (3.46)) reads

$$\tilde{x}(z, t) = \sum_{k=0}^{\infty} \frac{z^{2k}}{(2k)!} \left(\check{y}_k(t) + \check{\phi}_k(\mathbf{w}(t), \check{\mathbf{y}}^{[k-1]}(t)) \right). \quad (3.53)$$

As such, recalling (3.49), the latter can be expressed implicitly in terms of the ODE state $\mathbf{w}(t)$ and the PDE state $\check{x}(z, t)$ of the error system (3.38).

Remark 3.10. *The implicit nature of the transformation between the PDE state $\tilde{x}(z, t)$ of the intermediate system (3.33) and the PDE state $\check{x}(z, t)$ of the target system (3.38) obstructs a thorough examination of the stability properties of the closed loop in original coordinates. This is the subject of future research. Interestingly, dispensing with the notion of the PDE states $\tilde{x}(z, t)$ and $\check{x}(z, t)$, one could instead examine the mapping between the system description (3.42) and its counterpart (3.50) for the target system. In particular, this amounts to an investigation of the relations*

$$\check{y}_k(t) = \tilde{y}_k(t) - \check{\phi}_k(\mathbf{w}(t), \tilde{\mathbf{y}}^{[k-1]}(t)) \quad (3.54a)$$

$$\tilde{y}_k(t) = \check{y}_k(t) + \check{\phi}_k(\mathbf{w}(t), \check{\mathbf{y}}^{[k-1]}(t)) \quad (3.54b)$$

between the corresponding flat coordinates $\tilde{y}_k(t)$ and $\check{y}_k(t)$ for $k \in \mathbb{N}_0$. Note that the transformation (3.54a) and its inverse (3.54b) are implied by (3.49) and (3.46) as well as (3.43) and (3.53), respectively.

Chapter 4

Conclusions and future work

The solution-based control strategy presented in this thesis offers a promising perspective for the boundary control of nonlinear PDE-ODE systems of both hyperbolic or parabolic type. It extends backstepping designs for linear PDE-ODE systems in the sense that both are equivalent in the linear case. Furthermore, the proposed approach builds upon established control strategies, thus yielding a new tool with the potential to solve challenging, open problems.

The following sections recapitulate the main results for hyperbolic and parabolic systems that are stated in Chapters 2 and 3 as well as in the papers incorporated into this thesis. Additionally, recommendations for future research as well as a selection of open problems are given for each system class separately. The chapter concludes with preliminary results on cooperative transportation with heavy ropes as an application of the theory developed in this thesis.

4.1 Hyperbolic systems

The solution-based approach allows to derive tracking controllers for a general class of heterodirectional linear hyperbolic PDEs that are bidirectionally coupled with nonlinear ODEs. The findings of Chapter 2 can be easily generalized for larger system classes. For instance, the preliminary backstepping transformation (2.9) can be formulated with the help of a corresponding Cauchy problem, which can be extended to account for certain PDE nonlinearities. However, the drawback is a higher complexity for solving the prediction problem. Related methods in, e.g., Strecker et al. (2022) address such problems in the case of semilinear and quasilinear 2×2 PDE-ODE systems. It is also possible to use the results of this chapter to achieve tracking in finite time by choosing $\kappa(t, \mathbf{w}(t))$ to be a prescribed finite-time tracking controller. Such controllers are systematically derived in Irscheid et al. (2021a) for flat ODEs on the basis of a time-scale transformation (different from the perspective presented in the

original work Song et al. (2017)). In fact, Irscheid et al. (2022a) incorporates such a control method into the framework of semilinear hyperbolic PDE-ODE systems by constructing an appropriate Cauchy problem in the same way as proposed here. This demonstrates that solution-based control is not restricted to linear hyperbolic PDEs.

As a matter of fact, solution-based observer designs are also possible on the basis of analogous ideas. For a system class similar to (2.1) with collocated boundary measurement, Irscheid et al. (2023) presents an observer that comprises the same steps: a preliminary backstepping transformation, a change of coordinates that is inferred from the solution of a Cauchy problem as well as a prediction of the nonlinear boundary dynamics. In particular, the backstepping transformation is used to derive an observer for the PDE subsystem. The second state transformation aims to decouple the PDE observer error dynamics from the ODE subsystem. Then, the solution of a prediction problem yields the estimates of the ODE state based on the ones obtained from a retarded observer for the nonlinear boundary dynamics. For that, existence of an ODE observer is presumed (in analogy to Assumption 2.2 for control design). The overall design is modular in the sense that the ODE observer can be interchanged easily. An introduction to solution-based observer designs is given in Irscheid et al. (2021b) for a 2×2 PDE subsystem, whereas more details can be found in Irscheid et al. (2023) for general heterodirectional PDE subsystems.

In spite of these achievements, there are many open problems that have not yet been addressed for both controller and observer designs. One of the more interesting problems is the control of not fully boundary-actuated systems. An application of solution-based methods seems promising, however, no thorough investigation has taken place yet. Another open problem is to address the class of so-called ODE-PDE-ODE systems, which arise when a finite-dimensional actuator model is considered. These (and many more) open issues shape the frontier of current research.

4.2 Parabolic systems

Chapter 3 gives an outline on the boundary control of parabolic PDE-ODE systems. As shown for the linear examples in Sections 3.1 and 3.2, the resulting control law is equivalent to the one obtained through backstepping. In fact, the approach can be interpreted as an extension of the latter in the sense that the nonlinear state transformation (3.46) in Section 3.3 generalizes the well-known Volterra integral state transformation. This is an important result for further extensions. However, it is not obvious whether asymptotic stability of the origin of the target system (3.38) implies the same in original coordinates or only the weaker property of attractivity. Therefore, it remains to study the continuity of the map (3.46) and its inverse (3.53). In particular, Remark 3.10 suggests that the transformation (3.54) should be examined first. As such, this is but one of the many interesting questions that arise from this work.

After resolving the aforementioned stability issue, it is essentially straightforward to generalize the findings of this work to stabilize a reference trajectory, to account for bidirectional coupling between the ODE and PDE subsystems as well as to consider semilinear parabolic PDEs. Investigating the latter, it is reasonable to expect a relation to Vazquez and Krstic (2008a,b), wherein a nonlinear state transformation based on Volterra kernels is proposed for stabilizing semilinear parabolic plants comprising Volterra series nonlinearities. Moreover, it is of interest to explore observer designs for nonlinear parabolic systems with the tools introduced here, especially since the solution-based approach is used for observer designs in the hyperbolic case (see, e.g., Irscheid et al. (2021b, 2023)). Naturally, these problems represent only a sample of the next steps for future research.

4.3 Application to cooperative transportation with heavy ropes

Investigating the particular class of distributed-parameter systems considered in this thesis is originally inspired by the author's previous work on cooperative load transportation with heavy ropes (see Figure 1.1). Modeling the load as a rigid body in space results in nonlinear equations of motion. These nonlinear ODEs are bidirectionally coupled with linear hyperbolic PDEs describing the horizontal deflection of the ropes, yielding a nonlinear hyperbolic PDE-ODE system with bidirectional coupling at the unactuated boundary (see Irscheid et al. (2019) for a detailed model description).

The flatness-based open-loop controller in Irscheid et al. (2019) is designed for a rest-to-rest motion between equilibrium configurations in finite time. The control objective is to transition the load to a desired position with a desired orientation. The experimental results in Irscheid et al. (2019) show excellent open-loop performance, thus indirectly demonstrating the validity of the chosen PDE-ODE model that describes the system. However, open-loop control fails in the presence of external disturbances or initial errors. This necessitates the use of a stabilizing state feedback to improve the tracking performance. By using the solution-based methods proposed in Chapter 2, it is possible to obtain an asymptotically stable closed loop. Nevertheless, the number of ropes and the position of their load-side suspension points must yield an at least fully-actuated ODE subsystem in order to satisfy Assumption 2.2. For instance, if the load is, e.g., a point mass, attaching one rope is sufficient, whereas for a rigid rod it is necessary to attach two ropes at two distinct points. Similarly, transporting a membrane in the horizontal plane requires three attachment points that determine the plane, i.e., they cannot lie on a straight line.

Note that the design of a solution-based state feedback for the planar transportation problem is particularly facilitated by the fact that the only coupling between the ropes

occurs at the load-side end, i.e., through the load dynamics. As a consequence of this system structure, the PDE subsystems can be controlled independently for each rope in parallel. In contrast, the ODE subsystem describing the load is affected by all rope subsystems, which implies that both the ODE controller in Assumption 2.2 as well as the prediction problem (see Section 2.3.1) require a coordination between all ropes. In light of these considerations, the solution-based methods developed in Chapter 2 can be directly applied to the cooperative load transportation with heavy ropes. This is the subject of future research.

For the time being, preliminary simulation results for a rigid rod carried by two heavy ropes serve as a proof of concept. As depicted in Figure 4.1, the reference configuration of the load is planned in such a way that its center of mass transitions in finite time between two equilibrium positions in the horizontal plane, while the rod completes a quarter turn. Figures 4.2 and 4.3 illustrate the closed-loop behavior for nonzero initial tracking errors of both the ODE and PDE subsystems. The coordinates $x_m(t)$ and $y_m(t)$ of the rod's center of mass in the horizontal x - y -plane as well as the angle $\theta(t)$ between the rod and the positive x -direction converge to their respective references $x_{m,r}(t)$, $y_{m,r}(t)$ and $\theta_r(t)$, as depicted in Figure 4.4.

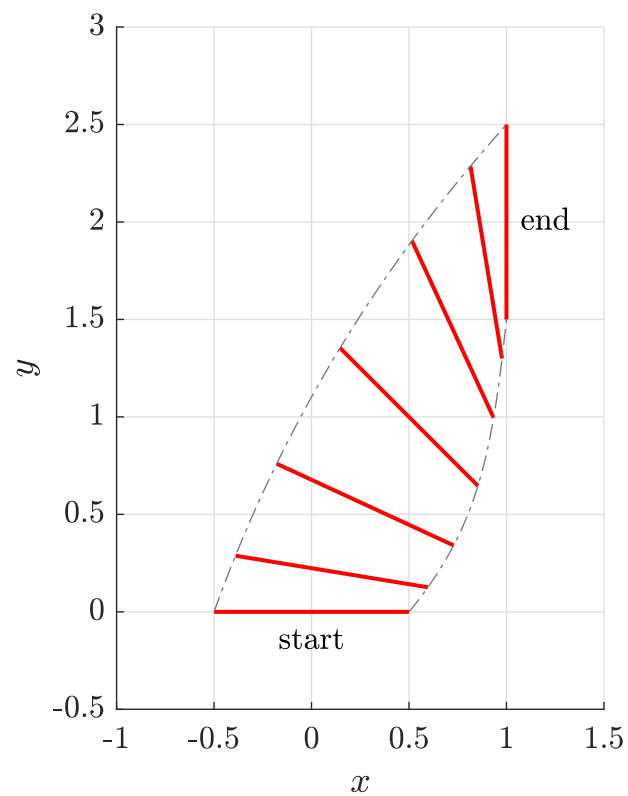


Figure 4.1: Snapshots of the desired planar transition of the rod configuration are depicted with a solid line, whereas the path of each of its end points is depicted with a dash-dotted line. The center of mass transitions from the origin to the coordinates $(1, 2)$ in the x - y -plane, while the rod makes a clock-wise quarter turn.

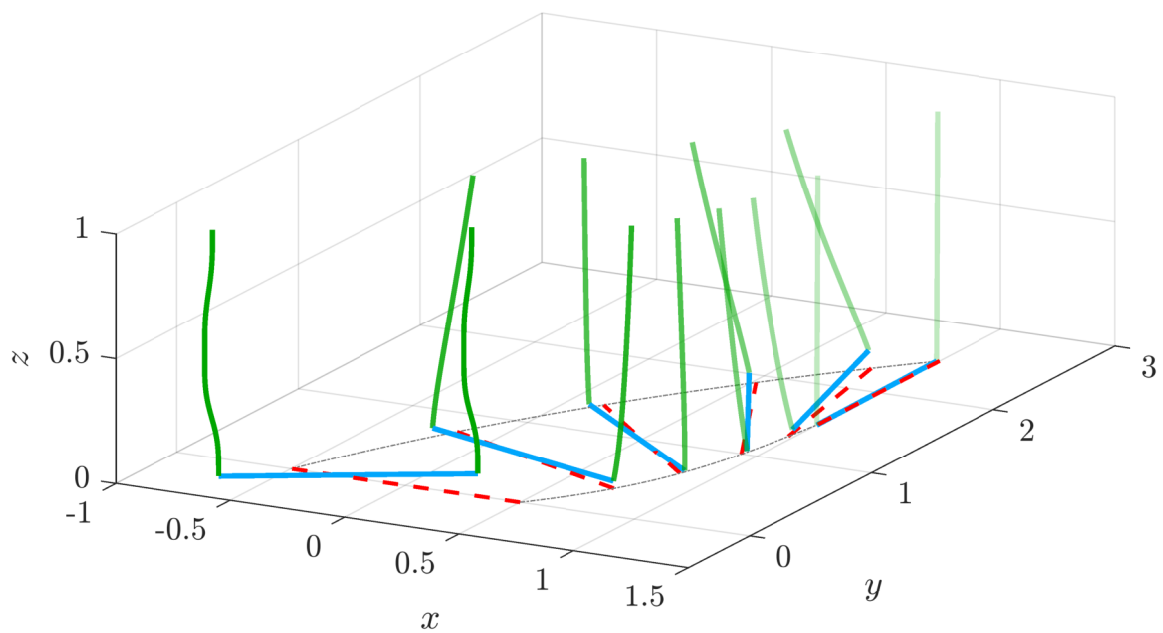


Figure 4.2: Snapshots during the cooperative load transportation with two heavy ropes in closed loop. For better contrast, the opacity of the ropes decreases with increasing time. The reference configuration of the rod is depicted with the dashed lines, whereas the solid horizontal line depicts its actual configuration, which starts with an initial position and orientation error. Moreover, the initial rope deflection introduces an initial PDE state tracking error.

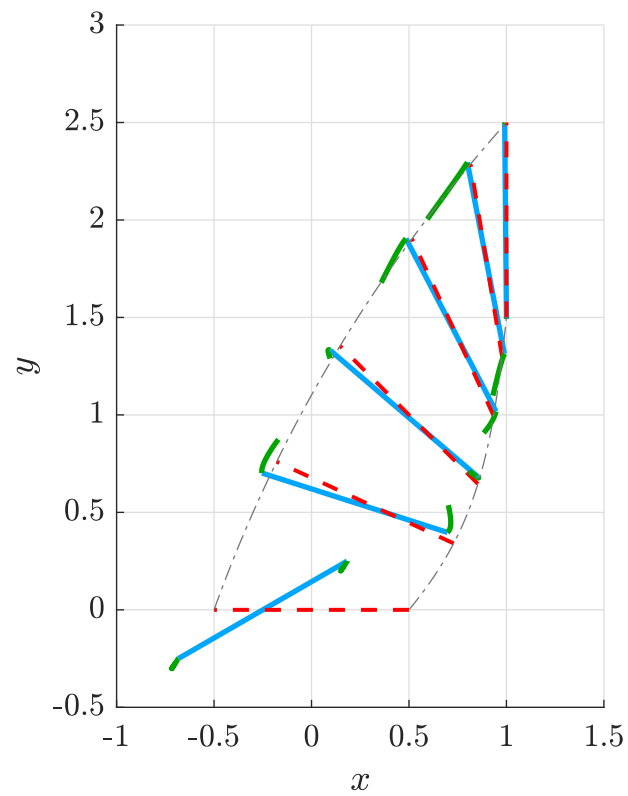


Figure 4.3: The projection of the snapshots from Figure 4.2 onto the horizontal plane illustrates the convergence in closed loop.

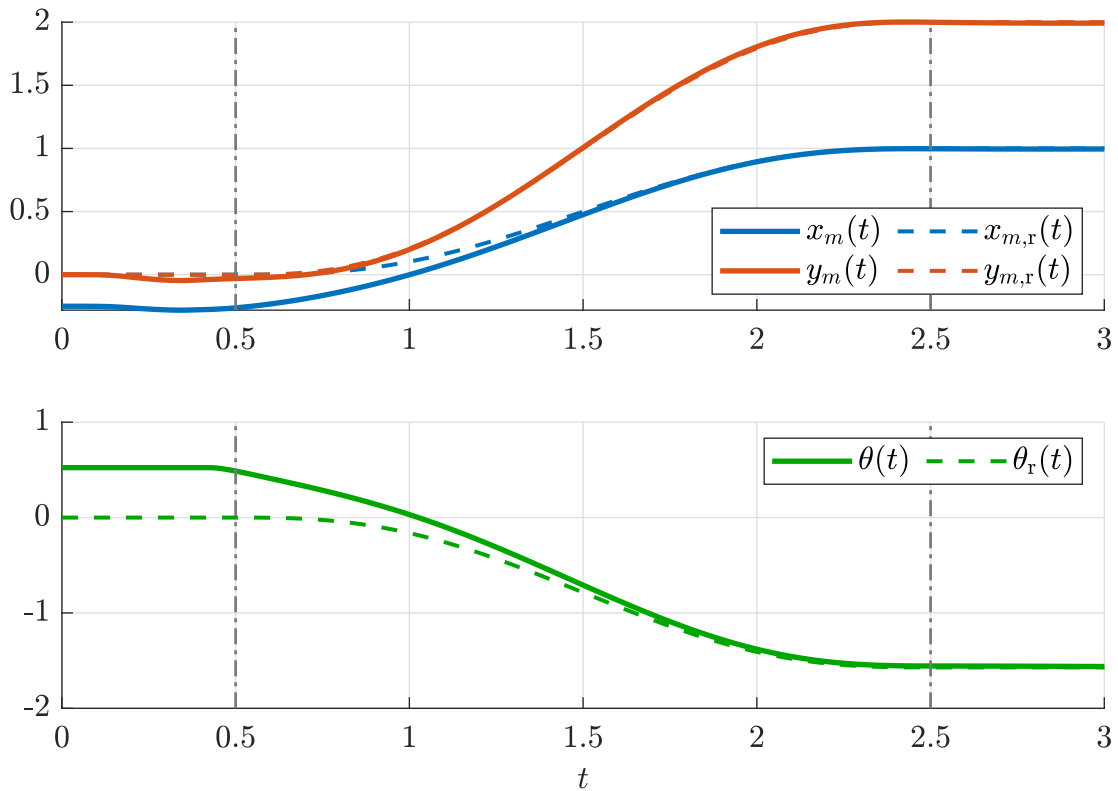


Figure 4.4: The vertical lines depict the start and end times for the planned transition between the two equilibrium configurations of the reference rod. The configuration of the rod converges to its reference although the initial conditions $x_m(0) = -0.25$, $y_m(0) = 0$ and $\theta(0) = \pi/6$ lead to initial position and orientation tracking errors.

Chapter 5

Scientific publications

The peer-reviewed and published journal papers

Irscheid, A., Deutscher, J., Gehring, N., and Rudolph, J. (2023). Output regulation for general heterodirectional linear hyperbolic PDEs coupled with nonlinear ODEs. *Automatica*, 148:110748

and

Irscheid, A., Gehring, N., Deutscher, J., and Rudolph, J. (2024). Stabilizing nonlinear ODEs with diffusive actuator dynamics. *IEEE Control Syst. Lett.*, 8:1259–1264

are attached below. For each paper, the following terminology suggested in Allen et al. (2019) is used to indicate the authors' contribution.

- **Conceptualization**
Ideas; formulation of overarching research goals and aims
- **Methodology**
Development or design of methodology; creation of models
- **Software**
Programming, software development; designing computer programs; implementation of the computer code and supporting algorithms; testing of existing code components
- **Validation**
Verification, whether as a part of the activity or separate, of the overall replication/reproducibility of results/experiments and other research outputs

- **Writing of Original Draft**
Preparation, creation and/or presentation of the published work, specifically writing the initial draft (including substantive translation)
- **Review & Editing**
Preparation, creation and/or presentation of the published work by those from the original research group, specifically critical review, commentary or revision – including pre- or postpublication stages
- **Visualization**
Preparation, creation and/or presentation of the published work, specifically visualization/ data presentation
- **Supervision**
Oversight and leadership responsibility for the research activity planning and execution, including mentorship external to the core team

5.1 Output regulation for general heterodirectional linear hyperbolic PDEs coupled with nonlinear ODEs

The contributions of each author are listed in what follows.

Abdurrahman Irscheid (40 %)

Conceptualization, Methodology, Validation, Writing of Original Draft, Review & Editing, Software

Joachim Deutscher (30 %)

Conceptualization, Methodology, Writing of Original Draft, Review & Editing

Nicole Gehring (25 %)

Methodology, Validation, Review & Editing, Visualization

Joachim Rudolph (5 %)



Review & Editing, Supervision


Automatica 148 (2023) 110748

Contents lists available at [ScienceDirect](https://www.sciencedirect.com)

Automatica

journal homepage: www.elsevier.com/locate/automatica



Output regulation for general heterodirectional linear hyperbolic PDEs coupled with nonlinear ODEs[☆]

Abdurrahman Irscheid^{a,*}, Joachim Deutscher^b, Nicole Gehring^c, Joachim Rudolph^a

^a Chair of Systems Theory and Control Engineering, Saarland University, Saarbrücken, Germany
^b Institute of Measurement, Control and Microtechnology, Ulm University, Ulm, Germany
^c Institute of Automatic Control and Control Systems Technology, Johannes Kepler University Linz, Linz, Austria

ARTICLE INFO

Article history:
 Received 18 February 2022
 Received in revised form 23 September 2022
 Accepted 28 September 2022
 Available online xxxx

Keywords:
 Distributed-parameter systems
 Hyperbolic systems
 Nonlinear PDE–ODE systems
 Output regulation
 Prediction
 Observer design
 Output feedback
 Backstepping

ABSTRACT

This paper considers general heterodirectional linear hyperbolic PDEs with boundary actuation and collocated measurement, that are bidirectionally coupled with nonlinear ODEs at the unactuated boundary. An output feedback regulator is designed to have the control output track a reference in the presence of disturbances, with a nonlinear signal model generating the reference and the disturbances. This leads to new challenges for both the observer and controller design. The regulator design makes use of results from output regulation theory for nonlinear lumped-parameter and distributed-parameter systems. The derivation of the state feedback regulator requires solving a new type of regulator equations, which consist of a Cauchy problem for linear and semilinear hyperbolic PDEs. A key component of the novel observer design is a nonlinear retarded observer for a finite-dimensional subsystem. Both the controller and the observer design are systematic in nature and derived in several successive steps, that include backstepping transformations and, most notably, predictions of PDE and ODE states. The latter are shown to be the unique solution of general nonlinear Volterra integro-differential equations. Combining the observer with the state feedback regulator is proven to achieve output regulation for the closed-loop system. A numerical example illustrates and confirms the theoretical results.

© 2022 Elsevier Ltd. All rights reserved.

1. Introduction

1.1. Background and motivation

In recent years, there has been considerable research activity concerning the output regulation of boundary controlled distributed-parameter systems (DPSs) to ensure reference tracking in the presence of disturbances. As the reference and disturbance signals are assumed to be generated by a known finite-dimensional exogenous model, there exist systematic methods for the regulator design (see, e.g., [Aulisa and Gilliam \(2016\)](#) for an overview and [Natarajan, Gilliam, and Weiss \(2014\)](#), [Paunonen and Pohjolainen \(2014\)](#) for general abstract systems). In this setup, the so-called regulator equations have to be solved to determine the regulator. If the state of the DPS and the signal model is

known, the regulator can be interpreted as a state feedback with a feedforward part that ensures tracking and disturbance rejection w.r.t. the output to be controlled. Otherwise, based on a measurement (that does not have to coincide with the control output), an observer is required for both the DPS and the signal model.

A very constructive and general regulator design makes use of the backstepping approach in, e.g., [Krstic and Smyshlyaev \(2008\)](#). First results proposing backstepping-based output regulation of 2×2 hyperbolic partial differential equations (PDEs) can be found in [Aamo \(2013\)](#). This result is extended to general heterodirectional hyperbolic PDEs in [Anfinsen and Aamo \(2017\)](#) and [Deutscher \(2017\)](#). Backstepping is also used in, e.g., [Deutscher, Gehring, and Kern \(2018\)](#) and [Di Meglio, Argomedeo, Hu, and Krstic \(2018\)](#) for the control of hyperbolic PDEs that are coupled with ordinary differential equations (ODEs), which arise from dynamic boundary conditions (BCs) or from the coupling of lumped-parameter systems at the boundary. Therefore, it is natural to extend backstepping-based output regulation to this class of so-called PDE–ODE systems. Output regulators for linear wave-ODE systems are presented in [Deutscher and Gabriel \(2021\)](#), [Gu, Wang, and Guo \(2018\)](#), [Liu and Wang \(2017\)](#) and [Zhou, Guo, and Wu \(2016\)](#), where the former are restricted to PDE–ODE cascades. In

[☆] The material in this paper was not presented at any conference. This paper was recommended for publication in revised form by Associate Editor Rafael Vazquez under the direction of Editor Miroslav Krstic.

* Corresponding author.
 E-mail addresses: a.irscheid@lsr.uni-saarland.de (A. Irscheid), joachim.deutscher@uni-ulm.de (J. Deutscher), nicole.gehring@jku.at (N. Gehring), j.rudolph@lsr.uni-saarland.de (J. Rudolph).

<https://doi.org/10.1016/j.automatica.2022.110748>
 0005-1098/© 2022 Elsevier Ltd. All rights reserved.

A. Irscheid, J. Deutscher, N. Gehring et al.

Automatica 148 (2023) 110748

the present paper, the output regulation problem is solved for the significantly more challenging case of general heterodirectional linear hyperbolic PDEs bidirectionally coupled with nonlinear ODEs. This general class of hyperbolic PDE–ODE systems, where the ODEs are nonlinear, covers a variety of models for technical applications, most famously oil well drilling (Bekiaris-Liberis & Krstic, 2014; Sagert, Di Meglio, Krstic, & Rouchon, 2013; Saldivar et al., 2014). However, even disregarding output regulation, most control designs found in the literature only apply to linear PDE–ODE systems, which is why Sagert et al. (2013) makes use of a linearized model. The leading standard for the control of these linear DPSs is the backstepping method (see Di Meglio et al., 2018 for stabilization, Auriol, Bribiesca-Argomedo, Bou Saba, Di Loreto, and Di Meglio (2018) for delay-robust stabilization, Deutscher et al. (2018), Deutscher, Gehring, and Kern (2019) for output feedback control and Auriol, Bribiesca-Argomedo, Niculescu, & Redaud, 2021; Redaud, Auriol, & Niculescu, 2021 for networked systems that are not-fully boundary actuated). In the case of nonlinear boundary ODEs, the results are scarce. To the best of the authors' knowledge, it is only cascades of linear PDEs and nonlinear ODEs, for which backstepping designs exist (see Cai and Diagne (2021)).

Control strategies for PDEs interconnected with nonlinear ODEs are not restricted to backstepping. Regarding the flatness-based designs in Gehring and Woittennek (2022), Knüppel, Woittennek, Boussaada, Mounier, and Niculescu (2014) and Woittennek (2013), it seems tangible to extend their underlying ideas to the general setup considered in this paper. Moreover, recently, prediction-based methods emerged for the control and observer design for PDE–ODE systems. For instance, prediction-based controllers are proposed for nonlinear ODEs interconnected with transport equations or a wave PDE in Bekiaris-Liberis and Krstic (2013) and Bekiaris-Liberis and Krstic (2014, Ch. 5), respectively. The strategy pursued in Irscheid, Gehring and Rudolph (2021) yields first results on the tracking control of general 2×2 linear hyperbolic PDEs that are bidirectionally coupled with nonlinear ODEs. An observer design for the same class of PDE–ODE systems can be found in Irscheid, Gehring, Deutscher and Rudolph (2021). In fact, prediction-based methods and backstepping are closely related, with their equivalence proven in Irscheid, Gehring, Deutscher, and Rudolph (2022) for a class of linear PDE–ODE systems. This matches the observation made in Strecker and Aamo (2017), in which a prediction-based output feedback is designed for 2×2 heterodirectional semilinear hyperbolic PDEs.

1.2. Contributions

This paper solves the output regulation problem for boundary-controlled general heterodirectional linear hyperbolic PDEs that are bidirectionally coupled with nonlinear ODEs at the unactuated boundary. A very general setup is obtained by allowing for disturbances to act at the unactuated PDE boundary, the nonlinear ODEs and the output to be controlled. Both the disturbances and the reference for the control output are generated by a nonlinear signal model. This leads to new challenges in the regulator design. In particular, one has to combine ideas from output regulation theory for nonlinear lumped-parameter systems (see, e.g., Huang (2004) and Isidori (1995, Ch. 8)) with results for DPS (see, e.g. Deutscher et al. (2019) and in particular Irscheid et al., 2022; Irscheid, Gehring, Rudolph, 2021). This yields a new type of regulator equations, which consist of a Cauchy problem for linear and semilinear hyperbolic PDEs. Its solvability is verified and a systematic design procedure for the state feedback regulator is obtained. Another challenge concerns the observer design on the basis of a collocated measurement. In fact, this paper generalizes the ideas from Irscheid, Gehring,

Deutscher et al. (2021) developed for 2×2 PDEs to the general heterodirectional case considered here. The proposed observer is combined with the state feedback regulator to achieve output regulation for the closed-loop system.

Note that the output regulation problem has previously not even been solved for those general heterodirectional hyperbolic PDE–ODE systems, where the ODEs and the signal model are linear. This contribution directly presents the results for the nonlinear case by basing the regulator and observer design on predictions of the PDE and ODE states.

1.3. Organization

The paper is structured as follows. The output regulation problem is stated in Section 2. By three consecutive state transformations, a state feedback regulator is designed in Section 3. The observer, constructively derived in Section 4, estimates the state of the plant and the signal model. Combining the results from Sections 3 and 4, the output feedback regulator is obtained, which is shown in Section 5 to achieve both output tracking and disturbance rejection. Finally, the numerical example in Section 6 illustrates the closed-loop behavior and the overall performance.

1.4. Notation

The i th component of a vector $h \in \mathbb{R}^n$ is denoted by h_i for $i = 1, \dots, n$, i.e., $h = \text{col}_1^n(h_i) = \text{col}(h_1, \dots, h_n)$. As usual, $e_i \in \mathbb{R}^n$, $i = 1, \dots, n$, is a unit vector, I_n the identity matrix in $\mathbb{R}^{n \times n}$. Furthermore, introduce the matrices

$$E_- = \begin{bmatrix} I_{n_-} \\ 0 \end{bmatrix} \in \mathbb{R}^{n \times n_-} \quad \text{and} \quad E_+ = \begin{bmatrix} 0 \\ I_{n_+} \end{bmatrix} \in \mathbb{R}^{n \times n_+}. \quad (1)$$

Then, define ${}_M = E_-^T M$, $M_- = ME_-$, ${}_+M = E_+^T M$ and $M_+ = ME_+$ for matrices M of suitable dimensions. For $v \in \mathbb{R}^n$ with $\|v\| = \|v\|_{\mathbb{R}^n}$, define $v_- = E_-^T v \in \mathbb{R}^{n_-}$ and $v_+ = E_+^T v \in \mathbb{R}^{n_+}$. Where convenient, the time argument is omitted (for example $x(z, t) \equiv x(z)$).

2. Problem formulation

Consider the coupled hyperbolic PDE–ODE system

$$\partial_t x(z, t) = A(z)\partial_z x(z, t) + A(z)x(z, t) \quad (2a)$$

$$x_+(0, t) = Q_0 x_-(0, t) + c(w(t), d(t)), \quad t > 0 \quad (2b)$$

$$x_-(1, t) = Q_1 x_+(1, t) + u(t), \quad t > 0 \quad (2c)$$

$$\dot{w}(t) = f(w(t), x_-(0, t), d(t)), \quad t > 0 \quad (2d)$$

$$y(t) = Gx_-(0, t) + g(w(t), d(t)), \quad t \geq 0 \quad (2e)$$

$$\eta(t) = x_+(1, t), \quad t \geq 0. \quad (2f)$$

Therein, the PDE (2a) is defined on $(0, 1) \times \mathbb{R}^+$ and

$$A(z) = \text{diag}(\lambda_1^-(z), \dots, \lambda_{n_-}^-(z), \lambda_1^+(z), \dots, \lambda_{n_+}^+(z)) \quad (3)$$

with C^1 -functions $\lambda_1^-(z) > \dots > \lambda_{n_-}^-(z) > 0 > \lambda_1^+(z) > \dots > \lambda_{n_+}^+(z)$, $z \in [0, 1]$, $n_- + n_+ = n$, is assumed, giving rise to a heterodirectional PDE subsystem with the state $x(z, t) = \text{col}(x_-(z, t), x_+(z, t)) \in \mathbb{R}^n$, where $x_-(z, t) \in \mathbb{R}^{n_-}$ propagates in the negative z -direction and $x_+(z, t) \in \mathbb{R}^{n_+}$ in the opposite direction. For $i = 1, \dots, n_-$ define $\phi_i^-(z) = \int_0^z (d\xi / \lambda_i^-(\xi)) > 0$, $z \in [0, 1]$, the inverse $\psi_i^- = (\phi_i^-)^{-1}$ and $\Delta_i^- = \phi_i^-(1)$. Similarly, $\phi_i^+(z) = -\int_0^z (d\xi / \lambda_i^+(\xi)) > 0$, $\psi_i^+ = (\phi_i^+)^{-1}$ and $\Delta_i^+ = \phi_i^+(1)$ for $i = 1, \dots, n_+$. Note that ψ_i^- and ψ_i^+ exist, because ϕ_i^- and ϕ_i^+ are strictly monotonically increasing. The entries of $A(z) = [A_{ij}(z)]$ are C^1 -functions and satisfy $A_{ij}(z) = 0$, $z \in [0, 1]$, $i = 1, \dots, n$, without loss of generality (see, e.g., Hu, Di Meglio, Vazquez, and

2

Krstic (2016)). The state of the ODE (2d) is $w(t) \in \mathbb{R}^{n_w}$ with (2b) and (2d) stemming from a dynamic boundary condition at the unactuated boundary $z = 0$. It is assumed that the functions c, f and g are known and sufficiently smooth w.r.t. their arguments, with $c(0, 0) = 0, f(0, 0, 0) = 0$ and $g(0, 0) = 0$. The control input of the system is $u(t) \in \mathbb{R}^n$ and the unmeasurable disturbance input is $d(t) \in \mathbb{R}^p$. The output to be controlled is $y(t) \in \mathbb{R}^{n_y}$ and the measurement is the collocated output $\eta(t) \in \mathbb{R}^{n_\eta}$. The initial condition (IC) of (2) comprises $x(z, 0) = x_0(z) \in \mathbb{R}^n$, assumed piecewise continuous, and $w(0) = w_0 \in \mathbb{R}^{n_w}$.

The reference $r(t) = q_r(v_r(t)) \in \mathbb{R}^{n_r}$ is the output of a known reference model $\dot{v}_r(t) = s_r(v_r(t)), v_r(0) = v_{r,0} \in \mathbb{R}^{n_r}$. Similarly, the disturbance $d(t) = p_d(v_d(t))$ is the output of a known disturbance model $\dot{v}_d(t) = s_d(v_d(t)), v_d(0) = v_{d,0} \in \mathbb{R}^{n_d}$. With $v = \text{col}(v_r, v_d)$ and $n_r + n_d = n_v$ this gives rise to the joint nonlinear signal model

$$\dot{v}(t) = s(v(t)), \quad t > 0, \quad v(0) = v_0 \in \mathbb{R}^{n_v} \quad (4a)$$

$$d(t) = p(v(t)), \quad t \geq 0 \quad (4b)$$

$$r(t) = q(v(t)), \quad t \geq 0 \quad (4c)$$

with sufficiently smooth functions s, p and q satisfying $s(0) = 0, p(0) = 0$ and $q(0) = 0$. It is assumed that only $r(t)$ is available to the regulator. This situation occurs, for example, if a human operator or superimposed central system solely supplies $r(t)$.

For the solution of the output regulation problem, the following assumptions are imposed on (2d) and (4a), with $\det G \neq 0$ for simplicity in (2e) (see also Remark 7).

Assumption 1. The ODE subsystem (2d) is forward complete (see Krstic (2010)) and $\dot{w} = f(w, k(w) + \varpi_1, \varpi_2)$ is input-to-state stable w.r.t. $\varpi = \text{col}(\varpi_1, \varpi_2)$ for a continuously differentiable function $k : \mathbb{R}^{n_w} \rightarrow \mathbb{R}^{n_w}$ with $k(0) = 0$. Furthermore, the linear approximation of $\dot{w} = f(w, k(w), 0)$ about its equilibrium $w = 0$ is asymptotically stable. \triangleleft

Forward completeness means that the solution of (2d) exists for all ICs and locally bounded input signals $x_-(0, t)$ and $d(t)$ for $t \geq 0$. In particular, the system does not exhibit a finite escape time. This is a fundamental requirement, because a stabilizing feedback acts on the ODE subsystem only after a finite delay, due to the hyperbolic character of the PDE subsystem. Note that input-to-state stability implies that $k(w)$ is a globally asymptotically stabilizing state feedback. Various system classes with these properties are discussed in Krstic (2010). Finally, a prerequisite for the required asymptotic stability of the linearized approximation is the stabilizability of the pair $(\partial_w f(0, 0, 0), \partial_{x_-(0, \cdot)} f(0, 0, 0))$.

Assumption 2. The system (4a) is neutrally stable, i.e., its origin is Lyapunov stable and every point in an open neighborhood is Poisson stable (see, e.g., Huang (2004, Rem. 3.2) for a definition). \triangleleft

Note that Poisson stability of (4) implies that the signals generated by (4) are persistent and bounded. This is a standard assumption in nonlinear output regulation theory (see Huang (2004, Ch. 3)) and together with Assumption 1, these two requirements are imposed for the design of the state feedback regulator (in Section 3). The next two assumptions concern the existence of ODE observers. Introduce the combined state $w_o = \text{col}(v_d, w)$ such that $c_o(w_o) = c(w, p_d(v_d))$ and $f_o(w_o, x_-(0)) = \text{col}(s_d(v_d), f(w, x_-(0), p_d(v_d)))$ can be used.

Assumption 3. There exists a (forward-complete) observer

$$\dot{\hat{v}}_r(t) = \bar{s}_r(\hat{v}_r(t), r(t)) \quad (5)$$

for $\hat{v}_r(t) = s_r(v_r(t))$ such that the origin of the dynamics in error coordinates $v_r - \hat{v}_r$ is globally attractive. \triangleleft

Assumption 4. There exists a (forward-complete) observer

$$\dot{\hat{w}}_o = \bar{f}_o(\hat{w}_o, x_-(0) + \varpi_1, c_o(w_o) + \varpi_2) \quad (6)$$

for $\dot{w}_o = f_o(w_o, x_-(0))$ such that the dynamics of the error $w_o - \hat{w}_o$ is input-to-state stable w.r.t. $\varpi = \text{col}(\varpi_1, \varpi_2)$. Furthermore, for $\varpi = 0$, the origin of the corresponding error dynamics is globally attractive. \triangleleft

The observer (6) is basically a standard nonlinear observer designed with inputs $x_-(0)$ and $c_o(w_o)$, where the former is interpreted as the input of the w_o -dynamics and the latter as its output. As $x_-(0)$ and $c_o(w_o)$ are unknown, the observer (6) is introduced with a respective error ϖ (see Section 4.3 for details). Moreover, the forward completeness of (5) and (6) ensures the absence of a finite escape time. Standard methods for the design of such observers can be found in Bernard (2019), whereas Birk and Zeitz (1988) and Röbenack and Lynch (2007) present systematic methods to determine observers and give conditions for global convergence.

Remark 5. The existence of an observer for the PDE-ODE system (2) and the signal model (4) requires that the observers (5) and (6) for the nonlinear subsystems (2d) and (4a) exist. The global convergence of the estimates \hat{v}_r and \hat{w}_o to their respective system states v_r and w_o , stated in Assumptions 3 and 4, is imposed for convenience and is irrelevant for the proposed method. If, instead, only a locally convergent observer is available, the design proposed in the paper can be extended to this setup. In particular, the overall observer error inherits its stability properties from those assumed for the observers of the nonlinear subsystems (2d) and (4a).

In this paper, the (local) nonlinear output regulation problem is solved for (2) by output feedback control. This amounts to designing a compensator ensuring local closed-loop stability such that

$$\lim_{t \rightarrow \infty} e_y(t) = \lim_{t \rightarrow \infty} (y(t) - r(t)) = 0 \quad (7)$$

for all ICs of the plant (2) and the compensator located in open neighborhoods of their respective origins.

3. State feedback regulator

The design of the state feedback regulator is split into multiple, successive steps, each of which pursues a specific goal. Fig. 1 offers an overview of the design with its three consecutive transformations as well as a prediction step. First, a backstepping transformation maps the PDE subsystem into a simpler structure. Based on that, another PDE state transformation allows to decouple the PDE from the ODE subsystem, resulting in a cascaded system representation. In the absence of a signal model (4), this second step is sufficient to determine a stabilizing controller. In order to achieve output regulation (7), a third state transformation is invoked. It leads to a set of new regulator equations, the solvability of which is shown in Section 3.3. As the resulting regulator requires future values of both the ODE and the PDE states, a prediction problem is solved in the forth and final design step. In the end, the state feedback regulator in Section 3.5 is shown to guarantee reference tracking for the control output in the presence of disturbances.

3.1. Stabilization of the PDE subsystem

In order to stabilize the PDE subsystem in (2) as well as to simplify the structure of the decoupling and regulator equations, the invertible backstepping transformation

$$\tilde{x}(z, t) = x(z, t) - \int_0^z K(z, \zeta)x(\zeta, t) d\zeta = \mathcal{T}[x(t)](z) \quad (8)$$

A. Irscheid, J. Deutscher, N. Gehring et al.

Automatica 148 (2023) 110748

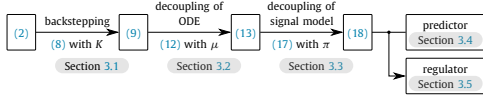


Fig. 1. Overview of the state feedback regulator design, highlighting the transformations and predictor.

(cf., e.g., Krstic and Smyshlyayev (2008)) with the kernel $K(z, \zeta) \in \mathbb{R}^{n \times n}$ is utilized to map (2a)–(2e) into the intermediate target system

$$\partial_t \tilde{x}(z, t) = \Lambda(z) \partial_z \tilde{x}(z, t) + A_0(z) \tilde{x}_-(0, t) + H(z) c(w(t), d(t)) \quad (9a)$$

$$\tilde{x}_+(0, t) = Q_0 \tilde{x}_-(0, t) + c(w(t), d(t)) \quad (9b)$$

$$\tilde{x}_-(1, t) = \tilde{u}(t) \quad (9c)$$

$$\dot{w}(t) = f(w(t), \tilde{x}_-(0, t), d(t)) \quad (9d)$$

$$y(t) = G \tilde{x}_-(0, t) + g(w(t), d(t)) \quad (9e)$$

with $H(z) = K(z, 0) \Lambda_+(0)$ and a matrix $A_0(z)$, where ${}_+A_0(z) = [a_{ij}^+(z)] \in \mathbb{R}^{n_+ \times n_+}$ is strictly lower triangular and ${}_+A_0(z) = [a_{ij}^+(z)] \in \mathbb{R}^{n_+ \times n_+}$ has no specific form. Hence, disregarding the impact of the ODE states $w(t)$ and $d(t)$, (9a) is a cascade of transport PDEs. Based on that, following the subsequent design steps, the PDE subsystem becomes finite-time stable in the final target system. In order to obtain (9c), the new input

$$\tilde{u}(t) = Q_1 x_+(1, t) + u(t) - \int_0^1 -K(1, \zeta) x(\zeta, t) d\zeta \quad (10)$$

is introduced. Furthermore, Hu, Vazquez, Di Meglio, and Krstic (2019) shows that $K(z, \zeta)$ is the unique piecewise C^1 -solution of the kernel equations

$$\Lambda(z) \partial_z K(z, \zeta) + \partial_\zeta (K(z, \zeta) \Lambda(\zeta)) = K(z, \zeta) A(\zeta) \quad (11a)$$

$$K(z, 0) (\Lambda_-(0) + \Lambda_+(0) Q_0) = A_0(z) \quad (11b)$$

$$K(z, z) \Lambda(z) - \Lambda(z) K(z, z) = A(z), \quad (11c)$$

that are defined on the domain $0 \leq \zeta \leq z \leq 1$. Note that (11) is only a BC for $a_{ij}^+(z)$, $i \leq j$, with the remaining equations defining the elements of $A_0(z)$. Additionally, artificial BCs have to be imposed for uniqueness of solution (see Hu et al. (2019)). Therefore, (11) is a simplified way of stating the kernel equations and the definition of $A_0(z)$.

3.2. Decoupling of the PDE subsystem

In order to map (9) into a PDE-ODE cascade, the decoupling transformation

$$\varepsilon(z, t) = \tilde{x}(z, t) - \mu(z, t) \quad (12)$$

is introduced. Therein, $\mu(z, t) \in \mathbb{R}^n$ is determined such that (9) takes the form

$$\partial_t \varepsilon(z, t) = \Lambda(z) \partial_z \varepsilon(z, t) + A_0(z) \varepsilon_-(0, t) \quad (13a)$$

$$\varepsilon_+(0, t) = Q_0 \varepsilon_-(0, t) \quad (13b)$$

$$\varepsilon_-(1, t) = \tilde{u}(t) - \mu_-(1, t) \quad (13c)$$

$$\dot{w}(t) = f(w(t), k(w(t)) + \varepsilon_-(0, t), d(t)) \quad (13d)$$

$$y(t) = G \varepsilon_-(0, t) + k(w(t)) + g(w(t), d(t)), \quad (13e)$$

where the state feedback $k(w(t)) \in \mathbb{R}^{n_-}$ is known by Assumption 1. In order to obtain (13), differentiate (12) w.r.t. time and

make use of (9) to show that $\mu(z, t)$ has to satisfy the decoupling equations

$$\partial_t \mu(z, t) = \Lambda(z) \partial_z \mu(z, t) + A_0(z) k(w(t)) + H(z) c(w(t), p(v(t))) \quad (14a)$$

$$\mu_+(0, t) = Q_0 k(w(t)) + c(w(t), p(v(t))) \quad (14b)$$

$$\mu_-(0, t) = k(w(t)) \quad (14c)$$

defined on the domain $(z, t) \in [0, 1] \times \mathbb{R}_0^+$. The following lemma clarifies the solvability of (14).

Lemma 6 (Decoupling Equations). The decoupling Eqs. (14) have a unique piecewise C -solution $\mu(z, t) \in \mathbb{R}^n$ on the domain $(z, t) \in [0, 1] \times \mathbb{R}_0^+$ for any piecewise continuous IC $\mu_+(z, 0) = \mu_{+,0}(z)$.

Proof. The solution of the Cauchy problem (14) can be directly determined using the method of characteristics for each component μ_i of μ . With $H = \text{col}_i^+(h_i^+)$ and $Q_0 = \text{col}_i^+(q_{0,i}^+)$, one obtains

$$\begin{aligned} \mu_{-,i}(z, t) &= k_i(w(t + \phi_i^-(z))) \\ &- \int_0^z \frac{h_i^+(\zeta) c(w(t + \phi_i^-(z) - \phi_i^-(\zeta)), p(v(t + \phi_i^-(z) - \phi_i^-(\zeta))))}{\lambda_i^-(\zeta)} d\zeta \\ &- \int_0^z \sum_{j=1}^{i-1} \frac{a_{ij}^-(\zeta) k_j(w(t + \phi_i^-(z) - \phi_i^-(\zeta)))}{\lambda_i^-(\zeta)} d\zeta \end{aligned} \quad (15)$$

for $i = 1, \dots, n_-$. Similarly, for $i = 1, \dots, n_+$,

$$\begin{aligned} \mu_{+,i}(z, t) &= \mu_{+,0,i}(\psi_i^+(\phi_i^+(z) - t)) \\ &+ \int_0^t h_{i+n_-}^+(\psi_i^+(\phi_i^+(z) - t + \tau)) c(w(\tau), p(v(\tau))) d\tau \\ &+ \int_0^t \sum_{j=1}^{n_-} a_{ij}^+(\psi_i^+(\phi_i^+(z) - t + \tau)) k_j(w(\tau)) d\tau \end{aligned} \quad (16a)$$

if $t \in [0, \phi_i^+(z))$ and

$$\begin{aligned} \mu_{+,i}(z, t) &= q_{0,i}^+ k(w(t - \phi_i^+(z))) \\ &+ c_i(w(t - \phi_i^+(z)), p(v(t - \phi_i^+(z)))) \\ &- \int_0^z \frac{h_{i+n_-}^+(\zeta) c(w(t - \phi_i^+(z) + \phi_i^+(\zeta)), p(v(t - \phi_i^+(z) + \phi_i^+(\zeta))))}{\lambda_i^+(\zeta)} d\zeta \\ &- \int_0^z \sum_{j=1}^{n_-} \frac{a_{ij}^+(\zeta) k_j(w(t - \phi_i^+(z) + \phi_i^+(\zeta)))}{\lambda_i^+(\zeta)} d\zeta \end{aligned} \quad (16b)$$

if $t \geq \phi_i^+(z)$. Hence, $\mu(z, t)$ is continuous w.r.t. space and time, where $(z, t) \in [0, 1] \times \mathbb{R}_0^+$. \square

In view of (15), the proof of Lemma 6 shows that the evaluation of $\mu_-(1, t)$ in (13c) requires an online prediction of the ODE states v and w (see (4) and (2d)). For this, online predictors will be derived in Section 3.4. Note that $\mu_+(z, t)$ is not needed to determine the regulator.

3.3. Regulator equations

For the design of the state feedback regulator, the PDE subsystem (13a)–(13c) is decoupled from the signal model (4). To this end, the transformation

$$\tilde{\varepsilon}(z, t) = \varepsilon(z, t) - \pi(z, v(t)) \quad (17)$$

and a mapping $\gamma : v \mapsto \gamma(v) \in \mathbb{R}^{n_w}$, defined in an open neighborhood of the origin in \mathbb{R}^{n_v} , are utilized. The function $\pi(z, v(t)) \in \mathbb{R}^n$

is chosen such that (13) with the output tracking error e_y defined in (7) takes the form

$$\partial_t \tilde{\varepsilon}(z) = \Lambda(z) \partial_z \tilde{\varepsilon}(z) + A_0(z) \tilde{\varepsilon}_-(0) \quad (18a)$$

$$\tilde{\varepsilon}_+(0) = Q_0 \tilde{\varepsilon}_-(0) \quad (18b)$$

$$\tilde{\varepsilon}_-(1) = 0 \quad (18c)$$

$$\dot{w} = f(w, k(w) + \tilde{\varepsilon}_-(0) + \tilde{q}(v), p(v)) \quad (18d)$$

$$e_y = G(\tilde{\varepsilon}_-(0) + \tilde{q}(v) + k(w)) + g(w, p(v)) - q(v), \quad (18e)$$

where $\tilde{q}(v)$ is defined later (by (22)) and

$$\tilde{u} = \mu_-(1) + \pi_-(1, v). \quad (19)$$

From (18a)–(18c) it is apparent that $\tilde{\varepsilon}(z, t) = 0$ for $t \geq t_c = \sum_{i=1}^{n_-} \Delta_i^- + \Delta_+^+$.

Differentiating (17) w.r.t. time as well as inserting (4) and (13) shows that (17) maps (13) into (18) if $\pi(z, v)$ is the solution of

$$\partial_v \pi(z, v) s(v) - \Lambda(z) \partial_z \pi(z, v) = A_0(z) \tilde{q}(v) \quad (20a)$$

$$\pi_+(0, v) = Q_0 \tilde{q}(v) \quad (20b)$$

$$\pi_-(0, v) = \tilde{q}(v) \quad (20c)$$

for $(z, v) \in [0, 1] \times \mathbb{R}^{n_v}$ and $\gamma(v)$ satisfies the PDE

$$\partial_v \gamma(v) s(v) = f(\gamma(v), k(\gamma(v)) + \tilde{q}(v), p(v)) \quad (21)$$

with $\gamma(0) = 0$ as well as

$$0 = G(\tilde{q}(v) + k(\gamma(v))) + g(\gamma(v), p(v)) - q(v). \quad (22)$$

Both (21) and (22) are obtained under the assumption $\tilde{\varepsilon}(z, t) = 0$, which is valid for $t \geq t_c$, and by requiring that $w = \gamma(v)$ is an invariant manifold (see, e.g., Isidori (1995)). Note that (22) implies the definition of $\tilde{q}(v)$ because $\det G \neq 0$, by assumption. Consequently, (20) and (21) are the regulator equations.

The PDE (21) is well-known from the center manifold theory. Hence, there exists a (local) C^k -solution $\gamma(v)$ of (21) for any $k \in \mathbb{N}_0$ (see Isidori (1995, B.1)) allowing for a power series ansatz (see Huang (2004, Ch. 4) for details).

Remark 7. If $\det G = 0$, (21) and (22) constitute a classical output regulation problem. Results for its solution $\gamma(v)$, $\tilde{q}(v)$ can be found in Isidori (1995, Ch. 8).

The next lemma clarifies the solvability of (20).

Lemma 8 (Cauchy Problem). The Cauchy problem (20) has a C -solution $\pi(z, v) \in \mathbb{R}^m$.

Proof. Defining $\theta(z, v) = A_0(z) \tilde{q}(v)$, the PDE

$$\partial_v \pi_{-,i}(z, v) s(v) - \lambda_{-,i}(z) \partial_z \pi_{-,i}(z, v) = \theta_{-,i}(z, v) \quad (23)$$

follows from (20a) for the components $\pi_{-,i}$ of π_- . Its solution depends on the flow $\varphi_s : \mathbb{R} \times \mathbb{R}^{n_v} \rightarrow \mathbb{R}^{n_v}$ of the smooth vector field $s(v)$ with $v(t + \sigma) = \varphi_s(\sigma, v(t))$. Then, solving the PDE (23) with the BC (20c) by the method of characteristics yields

$$\begin{aligned} \pi_{-,i}(z, v) &= \tilde{q}_i(\varphi_s(\phi_i^-(z), v)) \\ &+ \int_0^{-\phi_i^-(z)} \theta_{-,i}(\psi_i^-(\sigma), \varphi_s(\sigma + \phi_i^-(z), v)) d\sigma \end{aligned} \quad (24)$$

for $i = 1, \dots, n_-$. In a similar fashion, one obtains

$$\begin{aligned} \pi_{+,i}(z, v) &= \tilde{q}_{0,i}^+ \tilde{q}(\varphi_s(-\phi_i^+(z), v)) \\ &+ \int_0^{\phi_i^+(z)} \theta_{+,i}(\psi_i^+(\sigma), \varphi_s(\sigma - \phi_i^+(z), v)) d\sigma \end{aligned} \quad (25)$$

for $i = 1, \dots, n_+$. Hence, the solution $\pi(z, v)$ of the Cauchy problem (20) is continuous w.r.t. both its arguments z and v . \square

Remark 9. The state feedback regulator (19) consists of a stabilizing part $\mu_-(1, t)$ and a part $\pi_-(1, v(t))$ responsible for output regulation in the presence of disturbance and reference signals originating from the signal model (4). This interpretation motivates the use of two separate transformations (12) and (17) instead of a combined one. In particular, in the absence of any disturbance or reference, i.e., when $n_v = 0$, the second transformation (17) is not required to ensure asymptotic stability. This is apparent from (13) with $\tilde{u}(t) = \mu_-(1, t)$.

In view of (15) and (24), the implementation of the state feedback regulator (19) (and (10)) requires an online prediction of both ODE states $v(t + \tau)$ and $w(t + \tau)$ for $\tau \in (0, \Delta_{n_-}^-]$. To better highlight that, introduce $\mu(z, t) = \mathcal{M}[w, v](z, t)$ and $\pi(z, v(t)) = \mathcal{P}[v](z, t)$ for the solutions of (14) and (20), respectively. With a slight abuse, this notation illustrates the functional dependence of μ and π on w and v . Specifically, the state feedback regulator (19) uses the components

$$\begin{aligned} \mu_{-,i}(\psi_i^-(\tau), t) &= \mathcal{M}_{-,i}[w, v](\psi_i^-(\tau), t) = k_i(w(t + \tau)) \\ &- \int_0^\tau \sum_{j=1}^{i-1} a_{ij}^-(\psi_i^-(\tau - \sigma)) k_j(w(t + \sigma)) d\sigma \\ &- \int_0^\tau h_i^-(\psi_i^-(\tau - \sigma)) c(w(t + \sigma), p(v(t + \sigma))) d\sigma, \end{aligned} \quad (26a)$$

$\tau \in (0, \Delta_i^-]$, $i = 1, \dots, n_-$, which essentially follow from (15) by substituting the integration variable, and

$$\begin{aligned} \pi_{-,i}(z, v(t)) &= \mathcal{P}_{-,i}[v](z, t) = \tilde{q}_i(v(t + \phi_i^-(z))) \\ &- \int_0^{\phi_i^-(z)} \theta_{-,i}(\psi_i^-(\phi_i^-(z) - \sigma), v(t + \sigma)) d\sigma \end{aligned} \quad (26b)$$

for $i = 1, \dots, n_-$, as obtained from (24) by using $v(t + \sigma) = \varphi_s(\sigma, v(t))$ and a substitution of the integration variable.

3.4. Prediction of the ODE states

To determine the ODE states on the interval $(t, t + \Delta_{n_-}^-]$, the prediction problem

$$d_\tau v_p(\tau; t) = s(v_p(\tau; t)) \quad (27a)$$

$$d_\tau w_p(\tau; t) = f(w_p(\tau; t), x_-(0, t + \tau), p(v_p(\tau; t))) \quad (27b)$$

with the ICs $v_p(0; t) = v(t)$ and $w_p(0; t) = w(t)$ is solved for $\tau \in (0, \Delta_{n_-}^-]$. It follows from (4a) and (2d) by substituting $v_p(\tau; t)$ for $v(t + \tau)$ and $w_p(\tau; t)$ for $w(t + \tau)$. Note that t plays the role of a parameter in (27).

The solution of the nonlinear ODE (27a) directly produces $v_p(\tau; t)$ for $\tau \in (0, \Delta_{n_-}^-]$ at each time t . It is thus considered to be known for the determination of $w_p(\tau; t)$. It is shown in the following that the required future values $x_-(0, t + \tau)$ can be written as

$$x_-(0, t + \tau) = S_\tau[w_p, v_p, x](\tau, t) \quad (28)$$

for $\tau \in (0, \Delta_{n_-}^-]$ and fixed t , i.e. a functional of $w_p(\tau; t)$, $v_p(\tau; t)$ and x . In particular, by evaluating the transformations (8), (12), and (17) at $z = 0$ and inserting (14c) and (20c) it follows that

$$x_-(0) = \tilde{\varepsilon}_-(0) + k(w) + \tilde{q}(v) \quad (29)$$

on $\tau \in (0, \Delta_{n_-}^-]$. Note that (12) and (17) imply $\tilde{\varepsilon}_{-,i}(\psi_i^-(\tau), t) = \tilde{x}_{-,i}(\psi_i^-(\tau), t) - \mu_{-,i}(\psi_i^-(\tau), t) - \pi_{-,i}(\psi_i^-(\tau), v(t))$, $i = 1, \dots, n_-$.

A. Irscheid, J. Deutscher, N. Gehring et al.

Automatica 148 (2023) 110748

Hence, $\tilde{e}_-(0)$ in (29) can be expressed as

$$\begin{aligned} \tilde{e}_{-,i}(0, t + \tau) &= e_i^T \mathcal{T}[x(t)](\psi_i^-(\tau)) \\ &\quad - \mathcal{M}_{-,i}[w, v](\psi_i^-(\tau), t) - \mathcal{P}_{-,i}[v](\psi_i^-(\tau), t) \\ &\quad + \int_0^\tau \sum_{j=1}^{i-1} a_{ij}^-(\psi_i^-(\tau - \sigma)) \tilde{e}_{-,j}(0, t + \sigma) d\sigma \end{aligned} \quad (30a)$$

for $\tau \in (0, \Delta_i^-]$, which follows from the solution of the PDE (18a) and taking the backstepping transformation (8) as well as (26) into account. For $\tau \in (\Delta_i^-, \sum_{k=1}^i \Delta_k^-]$ the solution

$$\tilde{e}_{-,i}(0, t + \tau) = \int_0^{\Delta_i^-} \sum_{j=1}^{i-1} a_{ij}^-(\psi_i^-(\sigma)) \tilde{e}_{-,j}(0, t + \tau - \sigma) d\sigma \quad (30b)$$

is obtained from (18a) and (18c), with

$$\tilde{e}_{-,i}(0, t + \tau) = 0 \quad (30c)$$

for $\tau \geq \sum_{k=1}^i \Delta_k^-$. Inserting the solution branches of $\tilde{e}_{-,i}(0, t + \tau)$, piecewise defined in (30), into (29) and using $v_p(\tau; t)$ and $w_p(\tau; t)$ instead of $v(t + \tau)$ and $w(t + \tau)$ defines \mathcal{S}_c in (28). Together with (27b), this results in a general nonlinear Volterra integro-differential equation (GNVIDE) for $w_p(\tau; t)$. This is clarified in the next lemma and proven in Appendix A.

Lemma 10 (Prediction). *There exists a unique solution $w_p(\tau; t)$ for $\tau \in (0, \Delta_n^-]$ of the GNVIDE resulting from (27b), (29), (30) and using $v_p(\tau; t)$ and $w_p(\tau; t)$ instead of $v(t + \tau)$ and $w(t + \tau)$, respectively, with the IC $w_p(0; t) = w(t)$.*

The prediction problem can be solved online using a time discretization. Details on the analysis of the corresponding implementation can be found in Feldstein and Sopka (1974). The various approximation schemes that are used in Karafyllis and Krstic (2017, Ch. 4) for prediction problems without an integral term can be applied in a similar fashion. Note that in the case of linear ODEs (2d) and (4), their analytical solution replaces the necessity of an online prediction (see, e.g., Irscheid et al. (2022)).

Corollary 11. *The solution $w_p(\tau; t)$ of the GNVIDE in Lemma 10 satisfies $w(t + \tau) = w_p(\tau; t)$, for $\tau \in [0, \Delta_n^-]$, and $v(t + \tau) = v_p(\tau; t)$ holds for $v_p(\tau; t)$ in (27a) with the IC $v_p(0; t) = v(t)$.*

Proof. As both $v(t + \tau)$ and $v_p(\tau; t)$ satisfy the same ODE w.r.t. τ (cf. (4a) and (27a)) and share the same IC, $v(t + \tau) = v_p(\tau; t)$ holds in view of the smoothness of the vector field s . Based on that, the GNVIDE for $w_p(\tau; t)$ in Lemma 10 and the one for $w(t + \tau)$ (resulting from (27b) with $w(t + \tau)$ instead of $w_p(\tau; t)$, (29) and (30)) are identical. Therefore, the equality $w(t + \tau) = w_p(\tau; t)$ is a consequence of the shared IC and the uniqueness of the solution of the GNVIDE (see Lemma 10). \square

3.5. Stability of the tracking error dynamics

The next theorem presents the solution of the state feedback regulation problem. It depends on the results derived in Sections 3.1–3.4, as illustrated in Fig. 2. Define $\mathcal{X}[w, v](z) = \mathcal{T}^{-1}[\mathcal{P}[v] + \mathcal{M}[w, v]](z)$ and introduce $x_{\text{ref}}(z) = \mathcal{X}[\gamma(v), v](z)$ and $w_{\text{ref}} = \gamma(v)$.

Theorem 12 (State Feedback Regulator). *Under the Assumptions 1 and 2, the state feedback regulator*

$$\begin{aligned} u(t) &= \mathcal{U}[w_p, v_p, x](t) = \mathcal{M}_{-,i}[w_p, v_p](1, t) + \mathcal{P}_{-,i}[v_p](1, t) \\ &\quad + \int_0^1 -K(1, \zeta)x(\zeta, t) d\zeta - Q_1 x_+(1, t) \end{aligned} \quad (31)$$

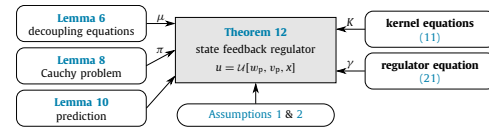


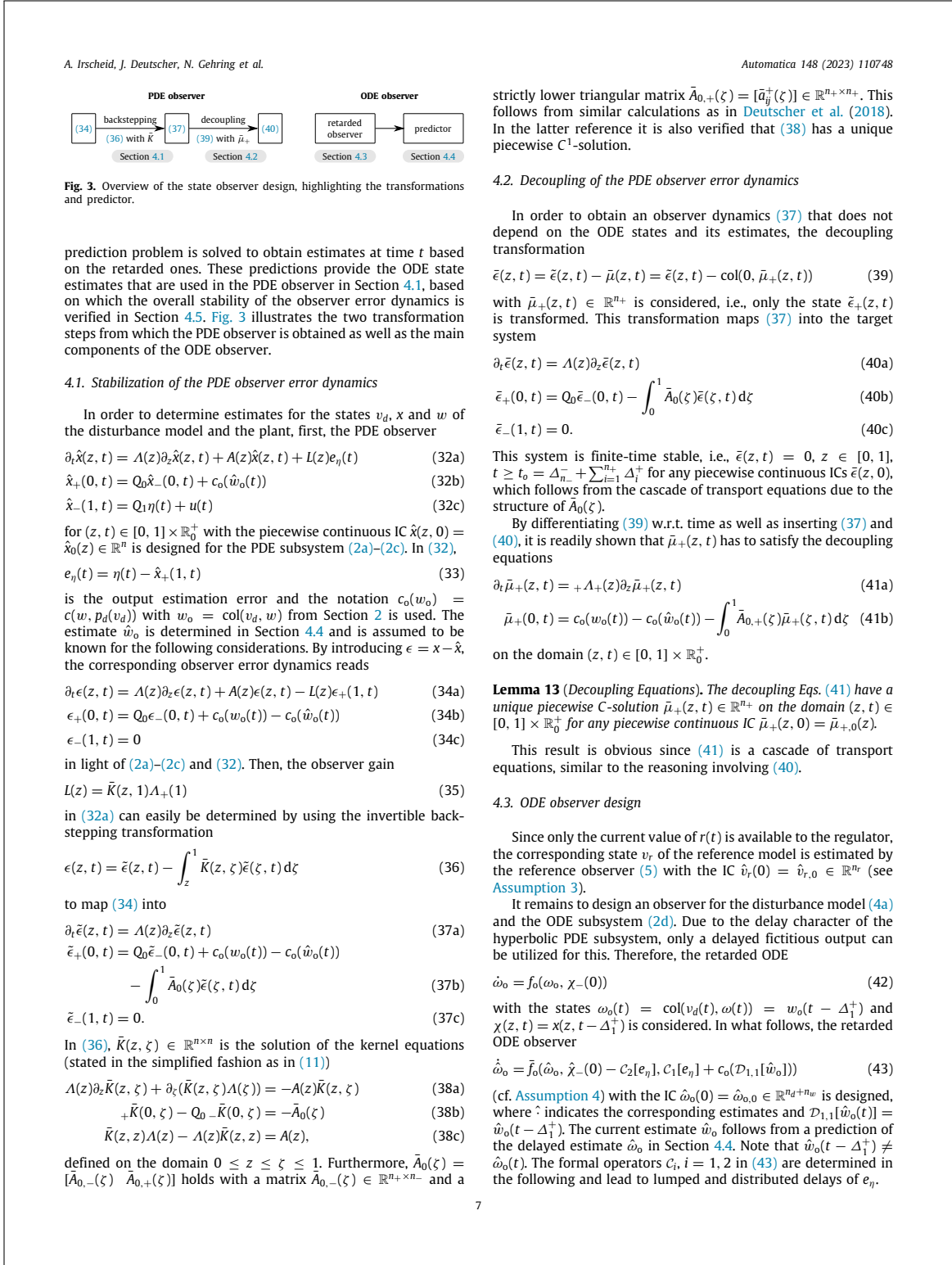
Fig. 2. Dependencies of the state feedback regulator design.

achieves output regulation (7) for all piecewise continuous ICs of the plant (2) and the signal model (4a) in open neighborhoods of the respective origins. Furthermore, the dynamics of the tracking errors $x(z, t) - x_{\text{ref}}(z, t)$ and $w(t) - w_{\text{ref}}(t)$ are asymptotically stable pointwise in space.

Proof. In view of Corollary 11, $\mathcal{U}[w_p, v_p, x](t) = \mathcal{U}[w, v, x](t)$ and the regulator (31) is equivalent to (10) and (19), in which the future values $w(t + \tau)$, $v(t + \tau)$, $\tau \in [0, \Delta_n^-]$ are substituted by the predictions $w_p(\tau; t)$, $v_p(\tau; t)$. Using the method of characteristics it is straightforward to verify that the solution $\tilde{e}_-(z, t)$ of the cascaded transport equations in (18a) and (18c) vanishes pointwise in space for $t \geq \tilde{t}_c$ with $\tilde{t}_c = \sum_{i=1}^n \Delta_i^-$ for the piecewise continuous IC $\tilde{e}_-(z, 0)$ following from the ICs of (2) and (4a), and the continuity of μ and π (see Lemmas 6 and 8). Since (18d) is forward complete and input-to-state stable w.r.t. $\varpi = \text{col}(\tilde{q}(v), p(v))$ by Assumption 1, the inequality $\|w(t)\| \leq \beta(\|\varpi(\tilde{t}_c)\|, t - \tilde{t}_c) + \vartheta(\sup_{z \geq \tilde{t}_c} \|\varpi(t)\|)$ holds for $t \geq \tilde{t}_c$, with a class $\mathcal{K}\mathcal{L}$ function β and a class \mathcal{K} function ϑ (see, e.g., Huang (2004, Def. 2.13)). As the equilibrium $v = 0$ of (4a) is stable in the sense of Lyapunov (cf. Assumption 2), the contribution of ϑ to the bound of $\|w(t)\|$ is arbitrarily small for $v(0)$ sufficiently small as $\tilde{q}(v)$ and $p(v)$ are continuous. Then, the solution of the composite system (4a) and (18d) remains in any arbitrarily small neighborhood of the origin in $\mathbb{R}^{n_w} \times \mathbb{R}^{n_v}$ for $t \geq t_0$ and t_0 sufficiently large, because β is a class $\mathcal{K}\mathcal{L}$ function. Since the equilibrium $w = 0$ of $\dot{w} = f(w, k(w), 0)$ is asymptotically stable in the linear approximation and the Jacobian of the signal model (4a) at $v = 0$ has only eigenvalues on the imaginary axis (see Assumptions 1 and 2), there exists an exponentially attractive center manifold $\{(w, v) \in \mathbb{R}^{n_w} \times \mathbb{R}^{n_v} | w = \gamma(v)\}$ for the composite system (4a) and (18d) (see Huang (2004, Th. 2.28)), in which γ is the solution of (21). In particular, this implies $\lim_{t \rightarrow \infty} (w(t) - w_{\text{ref}}(t)) = 0$. Consequently, (7) holds in view of (18e), the continuity of \tilde{q} and $\tilde{e}_-(z, t) = 0$ for $t \geq \tilde{t}_c$. Furthermore, (18a)–(18c) for $t \geq t_c = \tilde{t}_c + \Delta_1^+$ imply $\tilde{e}(z, t) = 0$, by which $x(z) = \mathcal{X}[w, v](z)$ follows from the chain of the bounded inverse transformations (cf. (8), (12), (17)). By that, the asymptotic stability of the tracking error $x - x_{\text{ref}}$ results from the linearity of (8) and the smoothness of the functions c and k in (15). \square

4. State observer

Based on the measurement η in (2f), state observers are designed for the different subsystems of (2) and (4). Essentially, the design is considered independently for the ODE and the PDE part of the system, with both observers combined only at the very end. To better structure the multi-step design, first, the observer for the PDE subsystem assumes knowledge of the ODE state estimates. The PDE observer is derived using a classical backstepping transformation. Then, similar to Section 3.2, another transformation of the PDE state is chosen such that the PDE observer error dynamics is decoupled from the ODE subsystem, in order to simplify the system representation. Next, Section 4.3 presents a novel retarded observer for the nonlinear boundary dynamics and the disturbance model. In the final design step, a



The computation of the output injection $C_1[e_\eta]$ is based on the decoupling Eqs. (41). By solving (41a) as well as using (33) and (39), the result

$$\bar{\mu}_{+,i}(0, t - \Delta_1^+) = \bar{\mu}_{+,i}(1, t) = e_{\eta,i}(t) - \bar{e}_{+,i}(1, t) \quad (44)$$

is obtained for $i = 1, \dots, n_+$. Similarly, representing the solution of (41a) in terms of the BC at $z = 1$ yields

$$\bar{\mu}_{+,i}(z, t) = \bar{\mu}_{+,i}(1, t - \phi_i^+(z) + \Delta_1^+), \quad i = 1, \dots, n_+. \quad (45)$$

In order to simplify the notation, the delay operators

$$\mathcal{D}_z[h(t)] = \text{col}_1^{n_+}(h_i(t - \phi_i^+(z))) \quad (46a)$$

$$\mathcal{D}_{z,k}[h(t)] = \text{col}_1^{n_+}(h_i(t - \phi_k^+(z))), \quad k = 1, \dots, n_+ \quad (46b)$$

are introduced for $h(t) = \text{col}_1^{n_+}(h_i(t))$. They are commutative and satisfy $\mathcal{D}_z^{-1}\mathcal{D}_z[h] = h$, with the same properties for $\mathcal{D}_{z,k}$. By that, (44) and (45) can be written more compactly in the form

$$e_\eta(t) - \bar{e}_+(1, t) = \bar{\mu}_+(1, t) = \mathcal{D}_1[\bar{\mu}_+(0, t)] \quad (47a)$$

$$\bar{\mu}_+(z, t) = \mathcal{D}_z\mathcal{D}_1^{-1}[\bar{\mu}_+(1, t)]. \quad (47b)$$

Applying \mathcal{D}_1 to (41b) and inserting (47) to eliminate all occurrences of $\bar{\mu}_+$ gives

$$\begin{aligned} e_\eta(t) + \int_0^1 \mathcal{D}_1[\bar{A}_{0,+}(\zeta)\mathcal{D}_\zeta\mathcal{D}_1^{-1}[e_\eta(t)]] d\zeta \\ = \bar{e}_+(1, t) + \int_0^1 \mathcal{D}_1[\bar{A}_{0,+}(\zeta)\mathcal{D}_\zeta\mathcal{D}_1^{-1}[\bar{e}_+(1, t)]] d\zeta \\ + \mathcal{D}_1[c_0(w_0(t)) - c_0(\hat{w}_0(t))], \end{aligned} \quad (48)$$

after a simple rearrangement. Note that the nested application of the delay operators \mathcal{D}_1 and $\mathcal{D}_\zeta\mathcal{D}_1^{-1}$ cannot be simplified due to $\bar{A}_{0,+}(\zeta)$, and that $\mathcal{D}_1[c_0(w_0)] \neq c_0(\mathcal{D}_1[w_0])$ (see (46a)). To design (43), apply $\mathcal{D}_{1,1}\mathcal{D}_1^{-1}$ to (48). Using $\mathcal{D}_{1,1}\bar{A}_{0,+}(\zeta)\mathcal{D}_\zeta = \bar{A}_{0,+}(\zeta)\mathcal{D}_\zeta\mathcal{D}_{1,1}$ and $\mathcal{D}_{1,1}[c_0(w_0)] = c_0(\mathcal{D}_{1,1}[w_0]) = c_0(w_0)$, this yields

$$C_1[e_\eta] = c_0(w_0) - c_0(\mathcal{D}_{1,1}\hat{w}_0) + \bar{\delta}_1, \quad (49)$$

wherein $\bar{\delta}_1 = C_1[\bar{e}_+(1)]$ and

$$C_1[h](t) = \mathcal{D}_{1,1}\mathcal{D}_1^{-1}[h(t)] + \int_0^1 \bar{A}_{0,+}(\zeta)\mathcal{D}_\zeta\mathcal{D}_{1,1}\mathcal{D}_1^{-1}[h(t)] d\zeta \quad (50)$$

depends on the values of each component h_i of $h = \text{col}_1^{n_+}(h_i)$ on the respective interval $[t - \Delta_1^+, t + \Delta_1^+ - \Delta_1^+]$. Recall that $\Delta_1^+ - \Delta_1^+ \leq 0$ for $i = 1, \dots, n_+$, and thus, $C_1[e_\eta](t)$ is known.

The expression $C_1[\bar{e}_+(1)]$ can be written in terms of \bar{e}_- to show that $\bar{\delta}_1(t) = 0$ for $t \geq \Delta_{n,-} + \Delta_1^+$. Since $\bar{e}_+(z, t)$ and $\bar{\mu}_+(z, t)$ share the same type of transport equation (cf. (40a) and (41a)), note that $\bar{e}_+(1, t) = \mathcal{D}_1[\bar{e}_+(0, t)]$ and $\bar{e}_+(z, t) = \mathcal{D}_z\mathcal{D}_1^{-1}[\bar{e}_+(1, t)]$ (see (47)). Inserting this into (50) produces

$$\bar{\delta}_1(t) = \mathcal{D}_{1,1} \left[Q_0\bar{e}_-(0, t) - \int_0^1 \bar{A}_{0,-}(\zeta)\bar{e}_-(\zeta, t) d\zeta \right] \quad (51)$$

in view of (40b) and $\bar{A}_{0,0}(\zeta) = [\bar{A}_{0,-}(\zeta) \quad \bar{A}_{0,+}(\zeta)]$. Since $\bar{e}_-(z, t) = 0$ for $t \geq \Delta_{n,-}$ pointwise in space (cf. (40)), (51) implies $\bar{\delta}_1(t) = 0$ for $t \geq \Delta_{n,-} + \Delta_1^+$.

In order to define the output injection $C_2[e_\eta]$, recall that $\chi = \mathcal{D}_{1,1}[x]$ as well as $\epsilon = x - \hat{x}$ and consider

$$\begin{aligned} \chi_-(0, t) = \hat{\chi}_-(0, t) + \mathcal{D}_{1,1}[\epsilon_-(0, t)] \\ = \hat{\chi}_-(0, t) + \mathcal{D}_{1,1} \left[- \int_0^1 \bar{K}(0, \zeta)\bar{\epsilon}_-(\zeta, t) d\zeta \right. \\ \left. + \bar{e}_-(0, t) - \int_0^1 \bar{K}_+(0, \zeta)\bar{\mu}_+(\zeta, t) d\zeta \right] \\ = \hat{\chi}_-(0, t) - C_2[e_\eta](t) + \bar{\delta}_2(t). \end{aligned} \quad (52)$$

This follows from inserting (36), (39), and (47), and splitting the right-hand side into $\hat{\chi}_-(0, t)$, the part

$$C_2[e_\eta](t) = \int_0^1 \bar{K}_+(0, \zeta)\mathcal{D}_\zeta\mathcal{D}_{1,1}\mathcal{D}_1^{-1}[e_\eta(t)] d\zeta, \quad (53)$$

that depends on values of the output estimation error components $e_{\eta,i}$ on the respective intervals $[t - \Delta_1^+, t + \Delta_1^+ - \Delta_1^+]$, and the part

$$\bar{\delta}_2(t) = \mathcal{D}_{1,1} \left[\bar{e}_-(0, t) - \int_0^1 \bar{K}_-(0, \zeta)\bar{e}_-(\zeta, t) d\zeta \right], \quad (54)$$

that vanishes for $t \geq \Delta_{n,-} + \Delta_1^+$.

In view of the second and third argument of \bar{f}_0 and based on (52) and (49), the retarded ODE observer (43) is of the form (6) (cf. Assumption 4 and recall that $\bar{\delta}_1(t) = \bar{\delta}_2(t) = 0$ for $t \geq \Delta_{n,-} + \Delta_1^+$). As such, the estimate \hat{w}_0 globally converges to the state w_0 of the retarded ODE (42).

Since the observers (32) and (43) require an estimate \hat{w}_0 of the current ODE state, a prediction based on the retarded ODE observer state $\hat{w}_0 = \text{col}(\hat{v}_d, \hat{w})$ is necessary.

4.4. Prediction of the retarded ODE observer states

Similar to Section 3.4, a prediction of the retarded ODE observer state $\hat{w}_0(t)$ yields the current estimate

$$\hat{w}_0(t) = \text{col}(\hat{v}_d(t), \hat{w}(t)) = \hat{w}_{0,p}(\Delta_1^+; t), \quad (55)$$

where $\hat{w}_{0,p} = \text{col}(\hat{v}_{d,p}, \hat{w}_p)$ is the solution of

$$d_t \hat{v}_{d,p}(\tau; t) = S_d(\hat{v}_{d,p}(\tau; t)) \quad (56a)$$

$$d_\tau \hat{w}_p(\tau; t) = f(\hat{w}_p(\tau; t), S_o[\hat{w}_{0,p}, \hat{w}_0, \hat{x}_-(0), e_\eta](\tau, t), p_d(\hat{v}_{d,p}(\tau; t))) \quad (56b)$$

for $\tau \in (0, \Delta_1^+)$, with the ICs $\hat{v}_{d,p}(0; t) = \hat{v}_d(t)$ and $\hat{w}_p(0; t) = \hat{w}(t)$ stemming from the retarded ODE observer (43). In the prediction problem (56), t is treated as a parameter and S_o is yet to be defined. The nonlinear ODE (56a) can be solved directly to produce $\hat{v}_{d,p}$, which is thus considered to be known in the following.

In particular, one would want $S_o[\hat{w}_{0,p}, \hat{w}_0, \hat{x}_-(0), e_\eta](\tau, t)$ in (56b) to be equal to $\chi_-(0, t + \tau)$, but the latter is unknown, and thus, not available for the online prediction. In view of (52),

$$\chi_-(0, t + \tau) = \hat{\chi}_-(0, t + \tau - \Delta_1^+) - C_2[e_\eta](t + \tau) + \bar{\delta}_2(t + \tau), \quad (57)$$

$\tau \in (0, \Delta_1^+)$, where $\hat{\chi}_-(0)$ is known and $\bar{\delta}_2(t)$ can be neglected as it vanishes for $t \geq \Delta_{n,-} + \Delta_1^+$. The evaluation of $C_2[e_\eta](t + \tau)$ requires past and future values of each component $e_{\eta,i}$ on the interval $[t - \Delta_1^+, t + \Delta_1^+]$ (cf. (53)). However, the unknown future values can be obtained from (49). For that, essentially, apply $\mathcal{D}_{1,1}\mathcal{D}_1^{-1}$ to (49), neglect $\bar{\delta}_1$ (by the same reasoning as for $\bar{\delta}_2$) and replace the unknown ODE state w_0 by its predicted estimate $\hat{w}_{0,p}$. This defines S_o as detailed in Appendix B. In fact, S_o involves only (known) past and present values of $\hat{w}_{0,p}$, $\hat{x}_-(0)$ and e_η . Its integral dependence on $\hat{w}_{0,p}$ is of Volterra type. Therefore, together with (56b), this results in a GNVIDE for $\hat{w}_p(\tau; t)$, $\tau \in (0, \Delta_1^+)$.

The prediction, similar to the one in Section 3.4, is clarified in the next lemma. The proof and further details can be found in Appendix B.

Lemma 14 (Prediction). *There exists a unique solution $\hat{w}_p(\tau; t)$ for $\tau \in (0, \Delta_1^+)$ of the GNVIDE (56b) with S_o defined in (B.7) and the IC $\hat{w}_p(0; t) = \hat{w}(t)$.*

A. Irscheid, J. Deutscher, N. Gehring et al.

Automatica 148 (2023) 110748

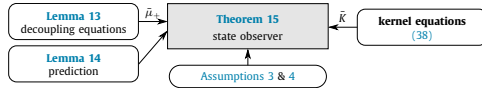


Fig. 4. Dependencies of the state observer design.

4.5. Stability of the observer error dynamics

The state observer for the system (2) and the signal model (4) follows from combining the results of Sections 4.1–4.4 (cf. Fig. 4). The next theorem clarifies the stability of the resulting observer error dynamics by taking the online prediction of the ODE states into account.

Theorem 15 (State Observer). *Let Assumptions 3 and 4 be satisfied and consider the PDE observer (32) with (35), the reference observer (5) and the retarded ODE observer (43) with the predictor (56) and (55). For all piecewise continuous ICs $x(z, 0), \hat{x}(z, 0) \in \mathbb{R}^n$, $v_r(0), \hat{v}_r(0) \in \mathbb{R}^{n_r}$ and $\omega_o(0), \hat{\omega}_o(0) \in \mathbb{R}^{n_d+n_w}$, the dynamics of the observer errors $\epsilon(z, t) = x(z, t) - \hat{x}(z, t)$, $v_r(t) - \hat{v}_r(t)$ and $e_{w_o}(t) = w_o(t) - \hat{w}_o(t)$ are globally convergent pointwise in space.*

Proof. The global convergence of the reference observer error $v_r(t) - \hat{v}_r(t)$ is ensured by Assumption 3. Furthermore, inserting (49) and (52) in (43) yields

$$\dot{\hat{\omega}}_o = \bar{f}_o(\hat{\omega}_o, \chi_-(0) - \bar{\delta}_2, c_o(\omega_o) + \bar{\delta}_1). \quad (58)$$

By Assumption 4, the error $e_{w_o} = \omega_o - \hat{\omega}_o$ is input-to-state stable w.r.t. $\bar{\delta} = \text{col}(\bar{\delta}_1, \bar{\delta}_2)$. As (40) implies $\bar{\epsilon}_-(z, t) = 0$ for $t \geq \Delta_-^-$ pointwise in space, $\bar{\delta} = 0$ for $t \geq \Delta_{n_-}^- + \Delta_1^+$ (see (51) and (54)). Thus, the error $e_{w_o} = 0$ is globally attractive (cf. Assumption 4). Moreover, $\bar{\delta} = 0$ means that the GNVIDE for $\hat{\omega}_p$ (cf. (56b) with (B.7)) coincides with the one for ω , which follows from using (57), (B.5) and (B.3) in (42). Additionally, v_d and $\hat{v}_{d,p}$ satisfy the same ODE (cf. (42) and (56a)). Then, the smoothness of f_o implies continuous dependence of these initial value problems on their ICs, by which there exists a constant $\mathcal{E} > 0$ in the domain of interest such that the prediction error $e_{o,p}(\tau; t) = \omega_o(t + \tau) - \hat{\omega}_{o,p}(\tau; t)$, $\tau \in [0, \Delta_1^+]$ satisfies $\|e_{o,p}(\tau; t)\| \leq \mathcal{E} \|e_{o,p}(0; t)\|$ for $t \geq \Delta_{n_-}^- + \Delta_1^+$. As $e_{w_o}(t) = e_{o,p}(0; t)$ is globally convergent, so is $e_{w_o}(t) = e_{o,p}(\Delta_1^+; t)$ (cf. (55)) and thus $\lim_{t \rightarrow \infty} \|e_{w_o}(t)\| = 0$. This in turn implies that $\lim_{t \rightarrow \infty} \sup_{z \in [0, 1]} \|\bar{\epsilon}(z, t)\| = 0$ since $\|c_o(\hat{\omega}_o(t)) - c_o(\hat{\omega}_o(0))\| \leq \mathcal{E}_c \|e_{w_o}(t)\|$ with the Lipschitz constant \mathcal{E}_c of c_o in the domain of interest (cf. (37) and (39)). Finally, the global convergence of $\bar{\epsilon}(z, t)$ pointwise in space follows from the same being true for $\bar{\epsilon}(z, t)$ and $e_{w_o}(t)$, and the bounded invertibility of the transformation (36). \square

5. Output feedback regulator

The output feedback regulator is sketched in Fig. 5 and consists of the reference observer (5), the PDE observer (32), the retarded ODE observer (43) and the associated predictor (56) with (55), as well as the output feedback regulator

$$u(t) = \mathcal{U}[\hat{w}_p, \hat{v}_p, \hat{x}](t), \quad (59)$$

in which \hat{w}_p, \hat{v}_p are the solution of the prediction problem

$$d_\tau \hat{v}_p(\tau; t) = s(\hat{v}_p(\tau; t)) \quad (60a)$$

$$d_\tau \hat{w}_p(\tau; t) = f(\hat{w}_p(\tau; t), S_c[\hat{w}_p, \hat{v}_p, \hat{x}](\tau, t), p(\hat{v}_p(\tau; t))), \quad (60b)$$

$\tau \in (0, \Delta_{n_-}^-]$, with ICs $\hat{v}_p(0; t) = \hat{v}(t) = \text{col}(\hat{v}_r(t), \hat{v}_d(t))$ and $\hat{w}_p(0; t) = \hat{w}(t)$. In contrast to the prediction problem (27) with

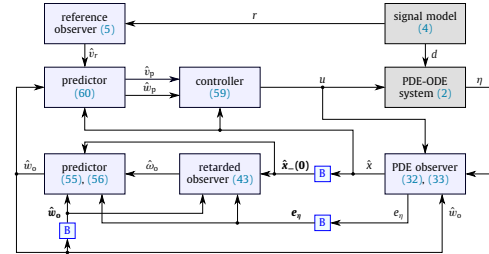


Fig. 5. Schematic overview of the output feedback regulator in the closed loop. Buffers (B) store values on the interval $[t - \Delta_1^+, t]$. Thus their outputs, highlighted in bold, are available on the same interval.

(28), which is based on the state of the plant (2) and the signal model (4), only the corresponding observer states are available for the solution of (60). By that, the output feedback regulator (59) follows from the state feedback regulator (31) by substituting the predictions $w_p(\tau; t), v_p(\tau; t)$, $\tau \in [0, \Delta_{n_-}^-]$ and $x(z, t)$ with their respective estimates $\hat{w}_p(\tau; t), \hat{v}_p(\tau; t)$ and $\hat{x}(z, t)$. The next theorem states the main result.

Theorem 16 (Output Feedback Regulator). *Let Assumptions 1–4 hold and consider the compensator consisting of the reference observer (5), the PDE observer (32), the retarded ODE observer (43) with the predictor (56) and (55), and the output feedback regulator (59) with the predictor (60). Then, the dynamics of the tracking errors $x(z, t) - x_{\text{ref}}(z, t)$ and $w(t) - w_{\text{ref}}(t)$ are asymptotically convergent pointwise in space for all piecewise continuous ICs $x(z, 0), \hat{x}(z, 0) \in \mathbb{R}^n$, $v_r(0), \hat{v}_r(0) \in \mathbb{R}^{n_r}$ and $\omega_o(0), \hat{\omega}_o(0) \in \mathbb{R}^{n_d+n_w}$ in open neighborhoods of the corresponding origins. This implies output regulation (7) for the closed-loop system.*

Proof. Define the prediction errors $e_{w_p}(\tau; t) = w(t + \tau) - \hat{w}_p(\tau; t)$ and $e_{v_p}(\tau; t) = v(t + \tau) - \hat{v}_p(\tau; t)$ for $\tau \in [0, \Delta_{n_-}^-]$, and recall that $w(t + \tau) = w_p(\tau; t)$ and $v(t + \tau) = v_p(\tau; t)$ by Corollary 11. As the assumptions of Theorem 15 are satisfied, the dynamics of the observer errors $\epsilon(z, t) = x(z, t) - \hat{x}(z, t)$, $v_r(t) - \hat{v}_r(t)$ and $e_{w_o}(t) = w_o(t) - \hat{w}_o(t)$ are globally convergent pointwise in space. Furthermore, there exist constants $\mathcal{E}_{f,i} > 0$, $i = 1, 2, 3$ and $\mathcal{E}_3 > 0$ such that the continuous dependence of the solutions $\hat{w}_p, \hat{v}_p, w_p$ and v_p on their respective ICs implies $\|e_{w_p}(\tau; t)\| \leq \mathcal{E}_{f,1} \|w(t) - \hat{w}(t)\| + \mathcal{E}_{f,2} \|v(t) - \hat{v}(t)\| + \mathcal{E}_{f,3} \sup_{z \in [0, 1]} \|x(z, t) - \hat{x}(z, t)\|$ and $\|e_{v_p}(\tau; t)\| \leq \mathcal{E}_3 \|v(t) - \hat{v}(t)\|$ (similar to the proof of Theorem 15). Thereby, the prediction error is bounded by the observer error, and, consequently, $\lim_{t \rightarrow \infty} e_{w_p}(\tau; t) = 0$ and $\lim_{t \rightarrow \infty} e_{v_p}(\tau; t) = 0$ pointwise in τ . Then, by applying the transformations (8), (12) and (17) to (2) and using the output feedback regulator (59), the boundary condition (18c) in the error dynamics (18) is replaced by

$$\begin{aligned} \bar{\epsilon}_-(1) = & Q_1 \epsilon_+(1) - \int_0^1 -K(1, \zeta) \epsilon(\zeta) d\zeta \\ & + \mathcal{M}_- [w - e_{w_p}, v - e_{v_p}](1) - \mathcal{M}_- [w, v](1) \\ & + \mathcal{P}_- [v - e_{v_p}](1) - \mathcal{P}_- [v](1). \end{aligned} \quad (61)$$

Following several steps of calculation, the Lipschitz continuity of the functions k, c, p in \mathcal{M}_- and \bar{q}, γ in \mathcal{P}_- (cf. (26)), as well as the asymptotic convergence of $\epsilon, e_{w_p}, e_{v_p}$ imply $\lim_{t \rightarrow \infty} \bar{\epsilon}_-(1, t) = 0$. From that and in view of (18a), (18b) and (61), similar to Theorem 12, it is straightforward to verify that the solution $\bar{\epsilon}(z, t)$ also converges to zero asymptotically pointwise in space. In particular,

9

A. Irscheid, J. Deutscher, N. Gehring et al.

Automatica 148 (2023) 110748

$\tilde{\varepsilon}_-(0, t)$ in (18d) and (18e) vanishes for $t \rightarrow \infty$, by which the remaining proof directly follows from the one of Theorem 12. This means that $x(t) \rightarrow x_{\text{ref}}(t)$, $w(t) \rightarrow w_{\text{ref}}(t)$, $y(t) \rightarrow r(t)$ for $t \rightarrow \infty$, and output regulation (7) is achieved. \square

6. Example

The theoretical results presented in this paper are illustrated for a numerical example in this section.

6.1. System equations

Consider the plant (2) with the transport velocities $\Lambda(z) = \text{diag}(3 + \frac{z}{2}, \frac{5}{2} + \frac{z}{4}, -\frac{5}{2} - \frac{z}{4}, -3 - \frac{z}{2})$, in-domain and boundary coupling

$$A(z) = \begin{bmatrix} 0 & \frac{3}{10} e^{z/3} & 0 & -\frac{1}{6} - \frac{z}{5} \\ -\frac{3}{10} e^{z/3} & 0 & -\frac{1}{4} - \frac{z}{2} & 0 \\ 0 & \frac{1}{4} + \frac{z}{2} & 0 & \frac{2}{10} e^{-z/2} \\ \frac{1}{6} + \frac{z}{5} & 0 & -\frac{2}{10} e^{-z/2} & 0 \end{bmatrix} \quad (62)$$

and $Q_0 = Q_1 = -I_2$, respectively, as well as $G = I_2$ and

$$c(w, d) = \begin{bmatrix} e^{w_1} - 1 \\ 2w_2 + w_3 \end{bmatrix}, \quad g(w, d) = \begin{bmatrix} 0 \\ 0 \end{bmatrix}. \quad (63)$$

The nonlinear boundary ODE (2d) is

$$\dot{w} = f(w, x_-(0), d) = \begin{bmatrix} 2x_{-,2}(0) - w_1 \\ (1 + w_1^2)x_{-,1}(0) - w_2 + d \\ (1 + w_1^2)x_{-,1}(0) - 2w_3 + d \end{bmatrix} \quad (64)$$

and the signal model (4) reads

$$\dot{v} = s(v) = \begin{bmatrix} 0 & 5 & 0 \\ -5 & 0 & 0 \\ 0 & 0 & 0 \end{bmatrix} v \quad (65)$$

with the states $v_r = q(v) = (v_1, v_2)^\top$ and $v_d = p(v) = v_3$ that model a harmonic reference and a (piecewise) constant disturbance, respectively. Therefore, Assumption 2 is met. Note that the linear model (65) is chosen since solving (21) for general nonlinear signal models (4) is not trivial and not the scope of this work.

6.2. Output feedback design

The state feedback

$$k(w) = \begin{bmatrix} (1 + w_1^2)^{-1} & 0 \\ 0 & 1 \end{bmatrix} \begin{bmatrix} 0 & -6 & 2 \\ -7 & 0 & 0 \end{bmatrix} w \quad (66)$$

is designed to compensate the nonlinearities in (64) and to stabilize $w = 0$ for $d = 0$, by which Assumption 1 is satisfied. A standard linear Luenberger observer is chosen for the reference model observer (5) in Assumption 3, with eigenvalues $-20, -20$ for the linear error dynamics of $v_r - \hat{v}_r$. The nonlinear observer

$$\begin{aligned} \dot{\hat{w}}_0 &= \bar{f}_0(\hat{w}_0, x_-(0), c_0(w_0)) \\ &= f_0(\hat{w}_0, x_-(0)) + \begin{bmatrix} 0 \\ 0 \\ (\ln(1 + c_{0,1}(w_0)))^2 - \hat{w}_{0,2}^2 \\ (\ln(1 + c_{0,1}(w_0)))^2 - \hat{w}_{0,2}^2 \end{bmatrix} x_{-,1}(0) \\ &\quad + L_0 \begin{bmatrix} \hat{w}_{0,2} - \ln(1 + c_{0,1}(w_0)) \\ c_{0,2}(\hat{w}_0) - c_{0,2}(w_0) \end{bmatrix} \end{aligned} \quad (67)$$

(cf. (6) in Assumption 4) results in a linear ODE for the estimation error $w_0 - \hat{w}_0$, with $w_0 = \text{col}(v_d, w)$ and L_0 such that $-\frac{7}{2}, -4, -\frac{9}{2}, -19$ are the eigenvalues of the error dynamics.

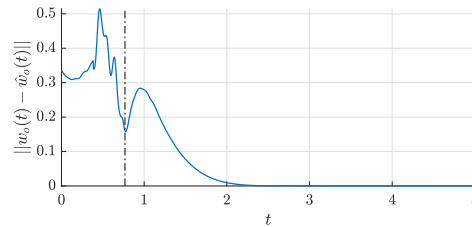


Fig. 6. Norm of the ODE observer error $e_{w_0} = w_0 - \hat{w}_0$ with dash-dotted vertical line at $t \approx 0.76$, after which $\delta_1 = \delta_2 = 0$.

6.3. Implementation

The overall implementation of the output feedback regulator (59) is illustrated in Fig. 5. It not only highlights the various elements of the regulator and the most important signals, including the predictor states and the different observer estimates, but it also implies the sequence of implementation.

The kernel Eqs. (11) and (38) are solved (offline) using several functions of the *con1* MATLAB library (Fischer, Gabriel, & Kerschbaum, 2021), with all artificial BCs chosen constant (see Hu et al. (2019) for those BCs). The explicit Euler method is used to implement the reference observer (5), the retarded ODE observer (42) with \bar{f}_0 defined in (67) and the PDE observer (32), which is also spatially discretized by characteristic projection. The integrals appearing in the predictors (56) and (60) as well as the ones involved in $\mathcal{M}_-, \mathcal{P}_-, C_1$ and C_2 (cf. (26), (50) and (53)) are discretized either by the explicit Euler or the trapezoidal method. This discretization scheme allows the explicit numerical solution of the GNVIDEs (cf. Lemmas 10 and 14).

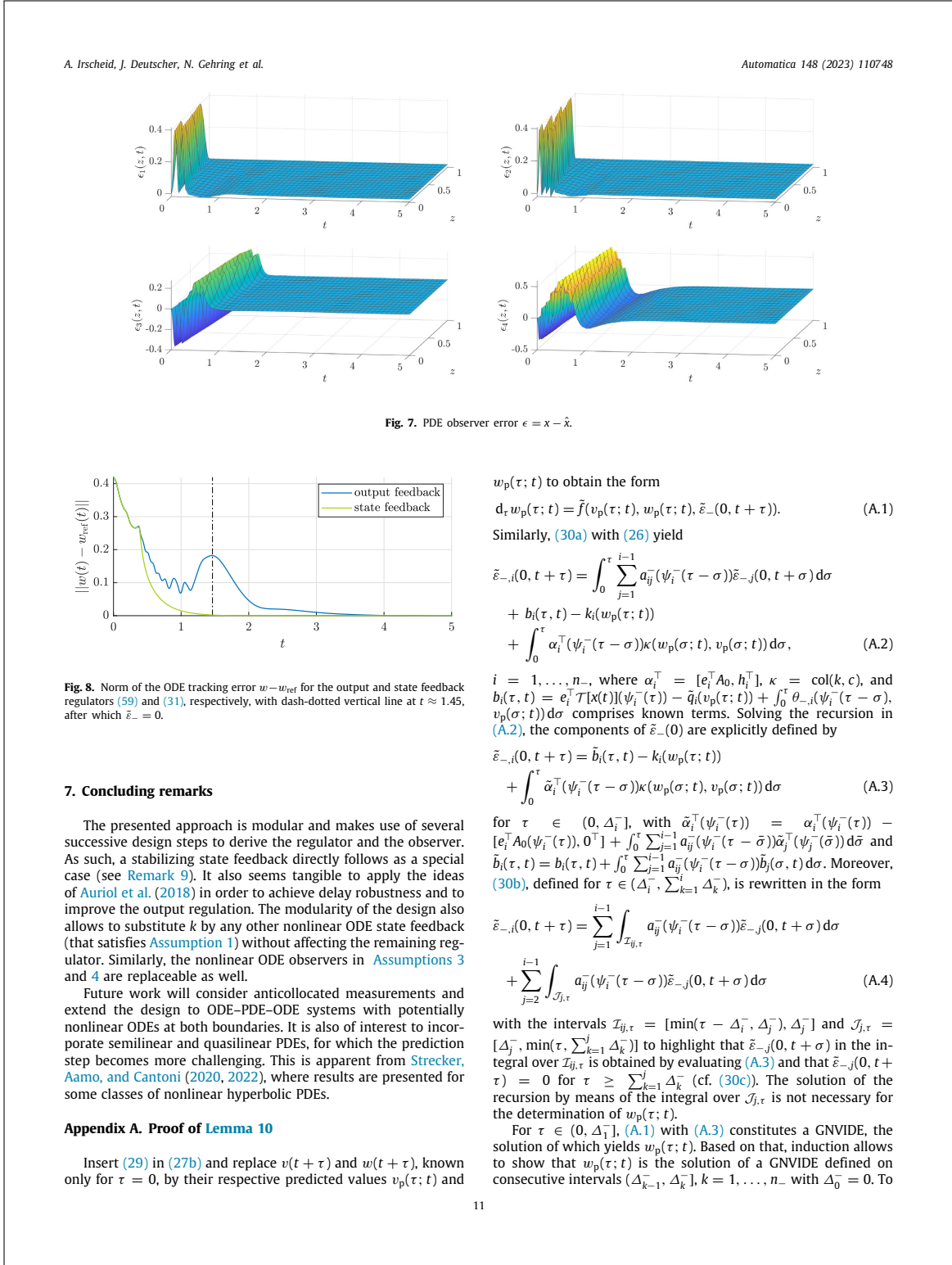
6.4. Simulation results

The following results are obtained for a simulation on an equidistant temporal grid with the step size $2 \cdot 10^{-3}$ and the initial conditions

$$x_{\mp,i}(z, 0) = \pm \frac{2}{5} \sin^2(2\pi iz), \quad i = 1, 2 \quad (68a)$$

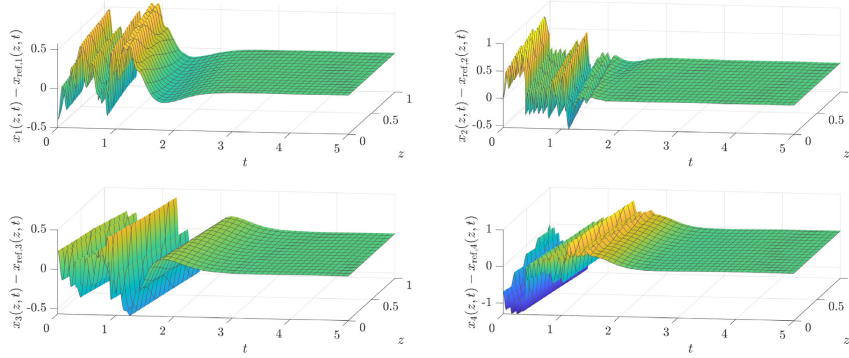
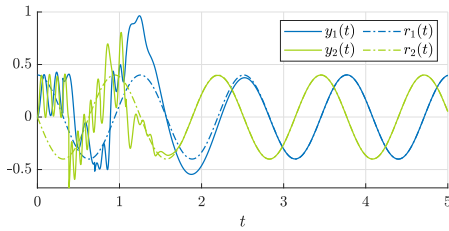
$$w(0) = (0, \frac{1}{10}, -\frac{1}{5})^\top, \quad v(0) = (\frac{2}{5}, 0, \frac{1}{4})^\top \quad (68b)$$

for the plant. All observer states are initialized with zero. Furthermore, the retarded ODE observer and the predictor (56) are only activated for $t > \Delta_1^+$ (see buffers in Fig. 5), resulting in $\hat{w}_0(t) = 0$ for $t \leq \Delta_1^+$. The convergence of the ODE and PDE observer errors e_{w_0} and ϵ in Figs. 6 and 7 validates Theorem 15. For the retarded ODE observer (58) to converge, $\delta_1(t) = \delta_2(t) = 0$ is required, which is the case after the dash-dotted vertical line in Fig. 6 at $t = \Delta_{n-}^- + \Delta_1^+ \approx 0.76$. Furthermore, Figs. 8 and 9 confirm the asymptotic stability of the ODE and PDE tracking errors $w - w_{\text{ref}}$ and $x - x_{\text{ref}}$ (see Theorem 16), with the references inferred from the state v of the signal model. The dash-dotted line in Fig. 8 at $t \approx 1.45$ corresponds to the one in Fig. 6 with an additional delay of $\tilde{t}_c \approx 0.69$, i.e. the time after which $\tilde{\varepsilon}_-(z, t) = 0$ (cf. (18)). Fig. 8 also illustrates the behavior of the ODE tracking error using the state feedback regulator (31), where the exponential decay of the tracking error is clearly visible for $t \geq \Delta_{n-}^- \approx 0.38$, which is smaller than the theoretical time instant \tilde{t}_c (see proof of Theorem 12). In the end, the control output y tracks the reference r as shown in Fig. 10, i.e. output regulation is achieved for this (zero-input) unstable plant in the presence of disturbances and nonlinearities.



A. Irscheid, J. Deutscher, N. Gehring et al.

Automatica 148 (2023) 110748

Fig. 9. PDE tracking error $x - x_{ref}$ in closed loop using the output feedback regulator (59).Fig. 10. The control output y tracks the reference r .

this end, assume that $w_p(\tau; t)$ is known for $\tau \in (0, \Delta_k^-]$, which in turn provides $\tilde{e}_-(0, t + \tau)$ on the same interval by means of (A.3) and (A.4), and consider $\tau \in (\Delta_k^-, \Delta_{k+1}^-]$. Then, recalling that $\Delta_1^- < \dots < \Delta_{n_-}^-$, the components $\tilde{e}_{-i}(0, t + \tau)$, $i = 1, \dots, k$ are also known as they follow from the recursion in (A.4), where the integral over $\mathcal{I}_{ij, \tau}$ depends only on $\tilde{e}_-(0, t + \tau)$, $\tau \in (0, \Delta_k^-]$. The remaining components $\tilde{e}_{-i}(0, t + \tau)$, $i = k+1, \dots, n_-$ are given by (A.3), which results in a GNVIDE for $w_p(\tau; t)$ for $\tau \in (\Delta_k^-, \Delta_{k+1}^-]$.

Solvability conditions for GNVIDEs can be found in Feldstein and Sopka (1974). In particular, the smoothness of the functions involved ensures a unique solution $w_p(\tau; t)$ for $\tau \in (0, \Delta_{n_-}^-]$ based on the IC $w_p(0; t) = w(t)$.

Appendix B. Proof of Lemma 14

Based on (53), substituting the integration variable and introducing $\alpha_i(\tau) = \lambda_i^+(\psi_i^+(\tau - \Delta_{ii}^+)) - \tilde{K}_+(0, \psi_i^+(\tau - \Delta_{ii}^+))e_i$ with the notation $\Delta_{ij}^+ = \Delta_i^+ - \Delta_j^+ \geq 0$, $i = 1, \dots, n_+$, $j \geq i$ allow to rewrite $C_2[e_\eta]$ as

$$C_2[e_\eta](t + \tau) = \sum_{i=1}^{n_+} \int_{\tau - \Delta_{ii}^+}^{\min(0, \tau - \Delta_{ii}^+)} \alpha_i(\tau - \sigma) e_{\eta, i}(t + \sigma) d\sigma + \sum_{i=1}^{n_+} \int_{\min(0, \tau - \Delta_{ii}^+)}^{\tau - \Delta_{ii}^+} \alpha_i(\tau - \sigma) e_{\eta, i}(t + \sigma) d\sigma, \quad (\text{B.1})$$

where the integral is split into a part depending only on (known) past values of the measurement error e_η and one involving future values. Although the latter are unknown, they can be obtained from a careful inspection of (48). For that, observe that the i th component $e_{\eta, i}(t + \sigma)$, $\sigma \in (0, \Delta_{ii}^+]$, of e_η can be expressed as

$$e_{\eta, i}(t + \sigma) = b_i(\sigma, t) + \sum_{j=1}^{i-1} \int_0^{\sigma + \Delta_{ij}^+} \bar{\alpha}_{ij}(\sigma - \bar{\sigma}) e_{\eta, j}(t + \bar{\sigma}) d\bar{\sigma}, \quad (\text{B.2})$$

with $\bar{\alpha}_{ij}(\tau) = -\lambda_j^+(\psi_j^+(\tau + \Delta_{ji}^+)) \bar{\alpha}_j^+(\psi_j^+(\tau + \Delta_{ji}^+))$ and

$$b_i(\sigma, t) = c_{o, i}(w_o(t + \sigma - \Delta_i^+)) - c_{o, i}(\hat{w}_o(t + \sigma - \Delta_i^+)) + \sum_{j=1}^{i-1} \int_{\sigma - \Delta_{ij}^+}^0 \bar{\alpha}_{ij}(\sigma - \bar{\sigma}) e_{\eta, j}(t + \bar{\sigma}) d\bar{\sigma} + \bar{\delta}_{1, i}(t + \sigma). \quad (\text{B.3})$$

Note that the integral over e_η is split into a known and an unknown part. The explicit solution

$$e_{\eta, i}(t + \sigma) = b_i(\sigma, t) + \sum_{j=1}^{i-1} \int_0^{\sigma + \Delta_{ij}^+} \check{\alpha}_{ij}(\sigma, \bar{\sigma}) b_j(\bar{\sigma}, t) d\bar{\sigma} \quad (\text{B.4})$$

with $\check{\alpha}_{ij}(\sigma, \bar{\sigma}) = \sum_{k=j+1}^{i-1} \int_{\max(0, \bar{\sigma} - \Delta_{jk}^+)}^{\sigma + \Delta_{ji}^+} \bar{\alpha}_{ik}(\sigma - \bar{\sigma}) \check{\alpha}_{kj}(\bar{\sigma}, \bar{\sigma}) d\bar{\sigma} + \bar{\alpha}_{ij}(\sigma - \bar{\sigma})$ of the recursion (B.2) can then be used to replace the future values of e_η in (B.1) by

$$C_2[e_\eta](t + \tau) = \sum_{i=1}^{n_+} \int_{\tau - \Delta_{ii}^+}^{\min(0, \tau - \Delta_{ii}^+)} \alpha_i(\tau - \sigma) e_{\eta, i}(t + \sigma) d\sigma + \sum_{i=1}^{n_+} \int_{\min(0, \tau - \Delta_{ii}^+)}^{\tau - \Delta_{ii}^+} \tilde{\alpha}_i(\tau, \sigma) b_i(\sigma, t) d\sigma, \quad (\text{B.5})$$

$\tilde{\alpha}_i(\tau, \sigma) = \sum_{j=i+1}^{n_+} \int_{\max(0, \sigma - \Delta_{ij}^+)}^{\max(\tau - \Delta_{ij}^+, \max(0, \sigma - \Delta_{ij}^+))} \alpha_j(\tau - \bar{\sigma}) \check{\alpha}_{ji}(\bar{\sigma}, \sigma) d\bar{\sigma} + \alpha_i(\tau - \sigma)$. This explicit expression for $C_2[e_\eta](t + \tau)$ is inserted into (57).

As $\bar{\delta}_1$ and $\bar{\delta}_2$ vanish in finite time, they can be neglected. Additionally, b_i in (B.5) is replaced by

$$\tilde{b}_i(\sigma, t) = c_{o, i}(\hat{\omega}_{o, p}(\sigma + \Delta_{ii}^+; t)) - c_{o, i}(\hat{w}_o(t + \sigma - \Delta_i^+)) + \sum_{j=1}^{i-1} \int_{\sigma - \Delta_{ij}^+}^0 \bar{\alpha}_{ij}(\sigma - \bar{\sigma}) e_{\eta, j}(t + \bar{\sigma}) d\bar{\sigma} \quad (\text{B.6})$$

(see (B.3)), which depends on known quantities only, because $\hat{w}_{o,p}(\sigma + \Delta_{1i}^+; t)$ is used instead of $w_o(t + \sigma - \Delta_{1i}^+)$. These previous modifications of the explicit expression of $\chi_-(0)$ in (57) yield the operator

$$S_o[\hat{w}_{o,p}, \hat{w}_o, \hat{x}_-(0), e_\eta](\tau, t) = \hat{x}_-(0, t + \tau - \Delta_1^+) + \sum_{i=1}^{n_+} \int_{\tau - \Delta_{1i}^+}^{\min(0, \tau - \Delta_{1i}^+)} \alpha_i(\tau - \sigma) e_{\eta,i}(t + \sigma) d\sigma + \sum_{i=1}^{n_+} \int_{\min(0, \tau - \Delta_{1i}^+)}^{\tau - \Delta_{1i}^+} \tilde{\alpha}_i(\tau, \sigma) \tilde{b}_i(\sigma, t) d\sigma \quad (B.7)$$

for $\tau \in (0, \Delta_1^+]$, which is used in (56b). Consequently, (56b) with (B.7) is a nonlinear integro-differential equation for \hat{w}_p (as $\hat{v}_{d,p}$ is known) due to the integral dependence on $c_{o,i}(\hat{w}_{o,p}(\sigma; t))$ for $\sigma \in [\min(\Delta_{1i}^+, \tau), \tau]$.

For $\tau \in (0, \Delta_{12}^+]$, (56b) with (B.7) constitute a GNVIDE, the solution $\hat{w}_p(\tau; t)$ of which exists and is unique (see Feldstein and Sopka (1974)). Based on that, for each $k = 1, \dots, n_+$, assume that $\hat{w}_p(\tau; t)$ is known for $\tau \in (0, \Delta_{1k}^+]$ and consider (B.7) for $\tau \in (\Delta_{1k}^+, \Delta_{1(k+1)}^+]$, $\Delta_{1(n_+)}^+ = 0$. Careful inspection of the integral dependence on $\hat{w}_{o,p}$ over the interval $[\min(\Delta_{1i}^+, \tau), \tau]$ and recalling that $\Delta_{11}^+ < \dots < \Delta_{1n_+}^+$ reveals that \hat{w}_p satisfies a GNVIDE for each successive interval $\tau \in (\Delta_{1k}^+, \Delta_{1(k+1)}^+]$. Thus, by induction and the smoothness of the functions involved, the existence of a unique solution $\hat{w}_p(\tau; t)$ for $\tau \in (0, \Delta_1^+]$ is ensured based on the IC $\hat{w}_p(0; t) = \hat{w}(t)$.

References

Aamo, O. (2013). Disturbance rejection in 2×2 linear hyperbolic systems. *IEEE Transactions on Automatic Control*, 58, 1095–1106.

Anfinson, H., & Aamo, O. (2017). Disturbance rejection in general heterodirectional 1-D linear hyperbolic systems using collocated sensing and control. *Automatica*, 76, 230–242.

Aulisa, E., & Gilliam, D. (2016). *A practical guide to geometric regulation for distributed parameter systems*. Boca Raton: CRC Press.

Auriol, J., Bribiesca-Argomedo, F., Bou Saba, D., Di Loreto, M., & Di Meglio, F. (2018). Delay-robust stabilization of a hyperbolic PDE-ODE system. *Automatica*, 95, 494–502.

Auriol, J., Bribiesca-Argomedo, F., Niculescu, S.-I., & Redaud, J. (2021). Stabilization of a hyperbolic PDEs-ODE network using a recursive dynamics interconnection framework. In *2021 European control conference (ECC)* (pp. 2485–2491).

Bekiaris-Liberis, N., & Krstic, M. (2013). *Nonlinear control under nonconstant delays*. Philadelphia: SIAM.

Bekiaris-Liberis, N., & Krstic, M. (2014). Compensation of wave actuator dynamics for nonlinear systems. *IEEE Transactions on Automatic Control*, 59, 1555–1570.

Bernard, P. (2019). *Observer design for nonlinear systems*. Cham: Springer.

Birk, J., & Zeitz, M. (1988). Extended luenberger observer for non-linear multivariable systems. *International Journal of Control*, 47, 1823–1836.

Cai, X., & Diagne, M. (2021). Boundary control of nonlinear ODE/Wave PDE systems with a spatially varying propagation speed. *IEEE Transactions on Automatic Control*, 66, 4401–4408.

Deutscher, J. (2017). Output regulation for general linear heterodirectional hyperbolic systems with spatially-varying coefficients. *Automatica*, 85, 34–42.

Deutscher, J., & Gabriel, J. (2021). A backstepping approach to output regulation for coupled linear wave-ODE systems. *Automatica*, 123, Article 109338.

Deutscher, J., Gehring, N., & Kern, R. (2018). Output feedback control of general linear heterodirectional hyperbolic ODE-PDE-ODE systems. *Automatica*, 95, 472–480.

Deutscher, J., Gehring, N., & Kern, R. (2019). Output feedback control of general linear heterodirectional hyperbolic PDE-ODE systems with spatially-varying coefficients. *International Journal of Control*, 92, 2274–2290.

Di Meglio, F., Argomedo, F. B., Hu, L., & Krstic, M. (2018). Stabilization of coupled linear heterodirectional hyperbolic PDE-ODE systems. *Automatica*, 87, 281–289.

Feldstein, A., & Sopka, J. (1974). Numerical methods for nonlinear Volterra integro-differential equations. *SIAM Journal of the Numerical Analysis*, 11, 826–846.

Fischer, F., Gabriel, J., & Kerschbaum, S. (2021). conl - a Matlab toolbox facilitating the solution of control problems. Available at zenodo.org.

Gehring, N., & Woittennek, F. (2022). Flatness-based output feedback tracking control of a hyperbolic distributed-parameter system. *IEEE Control Systems Letters*, 6, 992–997.

Gu, J.-J., Wang, J.-M., & Guo, Y.-P. (2018). Output regulation of anti-stable coupled wave equations via the backstepping technique. *IET Control Theory and Applications*, 12, 431–445.

Hu, L., Di Meglio, F., Vazquez, R., & Krstic, M. (2016). Control of homodirectional and general heterodirectional linear coupled hyperbolic PDEs. *IEEE Transactions on Automatic Control*, 61, 3301–3314.

Hu, L., Vazquez, R., Di Meglio, F., & Krstic, M. (2019). Boundary exponential stabilization of 1-dimensional inhomogeneous quasi-linear hyperbolic systems. *SIAM Journal on Control and Optimization*, 57, 963–998.

Huang, J. (2004). *Nonlinear output regulation*. Philadelphia: SIAM.

Irscheid, A., Gehring, N., Deutscher, J., & Rudolph, J. (2021). Observer design for 2×2 linear hyperbolic PDEs that are bidirectionally coupled with nonlinear ODEs. In *2021 European control conference (ECC)* (pp. 2506–2511).

Irscheid, A., Gehring, N., Deutscher, J., & Rudolph, J. (2022). Tracking control for 2×2 linear heterodirectional hyperbolic PDEs that are bidirectionally coupled with nonlinear ODEs. In J. Auriol, J. Deutscher, G. Mazanti, & G. Valmorbidia (Eds.), *Advances in distributed parameter systems* (pp. 117–142). Springer.

Irscheid, A., Gehring, N., & Rudolph, J. (2021). Trajectory tracking control for a class of 2×2 hyperbolic PDE-ODE systems. *IFAC-PapersOnLine*, 54, 416–421.

Isidori, A. (1995). *Nonlinear control systems*. London: Springer-Verlag.

Karafyllis, I., & Krstic, M. (2017). *Predictor feedback for delay systems: implementations and approximations*. Cham: Birkhäuser.

Knüppel, T., Woittennek, F., Boussaada, I., Mounier, H., & Niculescu, S.-I. (2014). Flatness-based control for a non-linear spatially distributed model of a drilling system. In A. Seuret, H. Ozbay, C. Bonnet, & H. Mounier (Eds.), *Low-complexity controllers for time-delay systems* (pp. 205–218). Cham: Springer.

Krstic, M. (2010). Input delay compensation for forward complete and strict-feedforward nonlinear systems. *IEEE Transactions on Automatic Control*, 55, 287–303.

Krstic, M., & Smyshlyayev, A. (2008). *Boundary control of PDEs – a course on backstepping designs*. Philadelphia: SIAM.

Liu, J.-J., & Wang, J.-M. (2017). Boundary stabilization of a cascade of ODE-wave systems subject to boundary control matched disturbance. *International Journal of the Robotics Nonlinear Control*, 27, 252–280.

Natarajan, V., Gilliam, D., & Weiss, G. (2014). The state feedback regulator problem for regular linear systems. *IEEE Transactions on Automatic Control*, 59, 2708–2723.

Paunonen, L., & Pohjolainen, S. (2014). The internal model principle for systems with unbounded control and observation. *SIAM Journal on Control and Optimization*, 52, 3967–4000.

Redaud, J., Auriol, J., & Niculescu, S.-I. (2021). Output-feedback control of an underactuated network of interconnected hyperbolic PDE-ODE systems. *Systems & Control Letters*, 154, Article 104984.

Röbenack, K., & Lynch, A. (2007). High-gain nonlinear observer design using the observer canonical form. *IET Control Theory & Applications*, 1, 1574–1579.

Sagert, C., Di Meglio, F., Krstic, M., & Rouchon, P. (2013). Backstepping and flatness approaches for stabilization of the stick-slip phenomenon for drilling. *IFAC Proceedings Volumes*, 46, 779–784.

Saldívar, B., Knüppel, T., Woittennek, F., Boussaada, I., Mounier, H., & Niculescu, S. (2014). Flatness-based control of torsional-axial coupled drilling vibrations. *IFAC Proceedings Volumes*, 47, 7324–7329.

Strecker, T., & Aamo, O. (2017). Output feedback boundary control of 2×2 semilinear hyperbolic systems. *Automatica*, 83, 290–302.

Strecker, T., Aamo, O., & Cantoni, M. (2020). Output feedback boundary control of heterodirectional semilinear hyperbolic systems. *Automatica*, 117, Article 108990.

Strecker, T., Aamo, O., & Cantoni, M. (2022). Predictive feedback boundary control of semilinear and quasilinear 2×2 hyperbolic PDE-ODE systems. *Automatica*, 140, Article 110272.

Woittennek, F. (2013). Flatness based feedback design for hyperbolic distributed parameter systems with spatially varying coefficients. *IFAC Proceedings of Volumes*, 46, 37–42.

Zhou, H.-C., Guo, B.-Z., & Wu, Z.-H. (2016). Output feedback stabilisation for a cascaded wave PDE-ODE system subject to boundary control matched disturbance. *International Journal of Control*, 89, 2396–2405.

A. Irscheid, J. Deutscher, N. Gehring et al.

Automatica 148 (2023) 110748



Abdurrahman Irscheid received the B.Sc. degree in Mechatronics and the M.Sc. degree with honors in Computational Engineering of Technical Systems from Saarland University, Germany, in 2015 and 2017, respectively. He is currently working towards his Dr.-Ing. degree at the Chair of Systems Theory and Control Engineering at Saarland University. His main research topics concern the controller and observer design for nonlinear distributed-parameter systems as well as control theoretic methods for convergence in prescribed finite time.



Joachim Deutscher received the Dipl.-Ing. (FH) degree in electrical engineering from the University of Applied Sciences Würzburg-Schweinfurt-Aschaffenburg, Germany, in 1996, the Dipl.-Ing. Univ. degree in electrical engineering, the Dr.-Ing. and the Dr.-Ing. habil. degrees both in automatic control from Friedrich-Alexander-Universität Erlangen-Nürnberg (FAU), Germany, in 1999, 2003 and 2010, respectively. From 2003–2010 he was a Senior Researcher at the Chair of Automatic Control (FAU), in 2011 he was appointed Associate Professor and in 2017 he became a Professor at the same university. Since April 2020 he is a Full Professor at the Institute of Measurement, Control and Microtechnology at Ulm University. His research interests include control of distributed-parameter and multi-agent systems with applications in mechatronics. He has co-authored a book on state feedback control for linear lumped-parameter systems: Design of Observer-Based

Compensators (Springer, 2009) and is author of the book: State Feedback Control of Distributed-Parameter Systems (in German) (Springer, 2012). At present he serves as Associate Editor for *Automatica*.



Nicole Gehring received the Dipl.-Ing. degree in electrical engineering from Dresden University of Technology, Germany, in 2007. Following a two-year stint of industrial work in the control of power plants and motor vehicles, in 2015, she finished her doctoral thesis at Saarland University, Germany, and received the Dr.-Ing. degree. As a Postdoc, she stayed with Technical University of Munich, Germany, for two years. Currently, she is with Johannes Kepler University Linz, Austria.

Her research mainly focuses on linear distributed-parameter systems and linear time-delay systems, especially in the context of control and observer design, as well as parameter identification.



Joachim Rudolph received the doctorate degree from Université Paris XI, Orsay, France, in 1991, and the Dr.-Ing. habil. degree from Technische Universität Dresden, Germany, in 2003. Since 2009, he has been the Head of the Chair of Systems Theory and Control Engineering at Saarland University, Saarbrücken, Germany. His current research interests include controller and observer design for nonlinear and infinite dimensional systems, algebraic systems theory, and the solution of demanding practical control problems.

5.2 Stabilizing nonlinear ODEs with diffusive actuator dynamics

The contributions of each author are listed in what follows.

Abdurrahman Irscheid (55 %)

Conceptualization, Methodology, Writing of Original Draft, Software, Review & Editing, Visualization

Nicole Gehring (25 %)

Methodology, Writing of Original Draft, Validation, Review & Editing

Joachim Deutscher (15 %)

Methodology, Validation, Review & Editing

Joachim Rudolph (5 %)

Review & Editing, Supervision

This article has been accepted for publication in IEEE Control Systems Letters. This is the author's version which has not been fully edited and content may change prior to final publication. Citation information: DOI 10.1109/LCSYS.2024.3406924

Stabilizing nonlinear ODEs with diffusive actuator dynamics

Abdurrahman Irscheid, Nicole Gehring, Joachim Deutscher, *Member, IEEE*, and Joachim Rudolph

Abstract—This paper presents a design of stabilizing controllers for a cascaded system consisting of a boundary actuated parabolic PDE and nonlinear dynamics at the unactuated boundary. Although the considered PDE is linear, the nonlinearity of the ODE constitutes a significant challenge. In order to solve this problem, it is shown that the classical backstepping transformation of Volterra type directly results from the solution of a Cauchy problem. This new perspective enables the derivation of a controller for the nonlinear setup, where a Volterra integral representation does not exist. Specifically, the solution of an appropriate linear Cauchy problem yields a novel state transformation facilitating the design of a stabilizing state feedback. This control law is shown to ensure asymptotic closed-loop stability of the origin. An efficient implementation of the controller is proposed and demonstrated for an example.

Index Terms—parabolic systems, nonlinear PDE-ODE systems, state feedback, backstepping, Cauchy problem

I. INTRODUCTION

THE stabilization of linear ODEs with infinite-dimensional actuator dynamics has been successfully addressed in recent years [1], [10], [13]. Typically, they describe time delays or diffusion phenomena in the actuation channel, which are modeled by linear hyperbolic or parabolic PDEs, respectively. Such settings lead to problems of boundary control for distributed parameter systems that are coupled with ODEs at the unactuated boundary, i.e., so-called PDE-ODE systems. In the linear case, the backstepping method [13] solves this task systematically (see [3], [4] for hyperbolic systems and [2], [20] for parabolic systems). This paper is concerned with the stabilization of nonlinear ODEs with linear parabolic actuator dynamics. While nonlinear ODEs are regularly addressed in the hyperbolic setting, e.g., where input delays occur (see [1]), to the best knowledge of the authors, a combination with

diffusive actuator dynamics has not been considered in the literature before.

This paper offers a new perspective for stabilizing parabolic PDE-ODE cascades on the basis of previous works on hyperbolic systems (see, e.g., [7], [8]). To overcome the challenges associated with nonlinearities, [7] uses predictions in the control and observer designs that follow from the solution of associated Cauchy problems, which are closely linked to a flatness-based parameterization of solutions. For parabolic systems, such parameterizations are well-known in the context of flatness-based open-loop control (see, e.g., [5], [14], [16]). Inspired by that and by classical backstepping controllers for linear parabolic PDE-ODE cascades (see, e.g., [10]), a novel nonlinear state transformation is derived. This generalizes classical backstepping transformations in the sense that their equivalence can be shown in the linear case. The transformation is determined from the solution of a suitable (linear) Cauchy problem that depends on the system state. The structure of the transformed system significantly facilitates the solution of the related stabilization problem. The latter only requires the existence of a (globally) stabilizing feedback for the ODE subsystem. Ultimately, applying the proposed controller to the nonlinear PDE-ODE cascade ensures asymptotic stability of the origin in closed loop.

The paper is organized as follows. Section II introduces the nonlinear PDE-ODE cascade as well as the control objective. As the main result, in Section III, a controller is derived on the basis of a novel nonlinear state transformation. It follows from the solution of a Cauchy problem, which is shown to admit a unique solution, analytic in the spatial variable and of Gevrey class two in time. In the special case of a linear system, the proposed approach coincides with classical backstepping, as clarified in Section IV. Finally, Section V illustrates the immense potential of the design and the overall control performance for a non-trivial example. For that, an efficient implementation of the controller is presented.

Notation: The k -th derivative $\frac{d^k h}{dt^k}(t) = \frac{d}{dt} h^{(k)}(t)$, $k \in \mathbb{N}_0$, of a smooth function h is written in terms of the operator $\frac{d}{dt}$. Introduce the class \mathcal{C}^ω of analytic functions. A function h is called Gevrey of order $\alpha > 0$, in short $h \in \mathcal{G}_\alpha$, if $\exists M, R > 0$ such that $\sup_{t \geq 0} \left| \frac{d^k h}{dt^k}(t) \right| \leq M \frac{(k!)^\alpha}{R^k}$ for all $k \in \mathbb{N}_0$ (see, e.g., [18, Def. 1.4.1]). Note that $\mathcal{C}^\omega = \mathcal{G}_1$, and that $h \in \mathcal{G}_{\alpha_1}$ implies $h \in \mathcal{G}_{\alpha_2}$ for all $\alpha_1 \leq \alpha_2$. For any distributed variable $x(z, t) \in \mathbb{R}$, $(z, t) \in [0, 1] \times \mathbb{R}_0^+$, denote by $\|x(t)\|_\infty$ the supremum norm $\sup_{z \in [0, 1]} |x(z, t)|$. If x is analytic in z and of Gevrey class two w.r.t. t , then $x \in \mathcal{C}^\omega \mathcal{G}_2$.

This research was funded in part by the Deutsche Forschungsgemeinschaft (DFG, German Research Foundation) under project no. 517291864 and the Austrian Science Fund (FWF) under project no. I 6519-N. For the purpose of Open Access, the author has applied a CC BY public copyright licence to any Author Accepted Manuscript (AAM) version arising from this submission.

Abdurrahman Irscheid and Joachim Rudolph are with the Chair of Systems Theory and Control Engineering, Saarland University, Germany (email: {a.irscheid, j.rudolph}@lsc.uni-saarland.de).

Nicole Gehring is with the Institute of Automatic Control and Control Systems Technology, Johannes Kepler University Linz, Austria (e-mail: nicole.gehring@jku.at).

Joachim Deutscher is with the Institute for Measurement, Control and Microtechnology, Ulm University, Germany (e-mail: joachim.deutscher@uni-ulm.de).

© 2024 IEEE. Personal use is permitted, but republication/redistribution requires IEEE permission. See <https://www.ieee.org/publications/rights/index.html> for more information.

This article has been accepted for publication in IEEE Control Systems Letters. This is the author's version which has not been fully edited and content may change prior to final publication. Citation information: DOI 10.1109/LCSYS.2024.3406924

II. PROBLEM FORMULATION

The boundary-actuated PDE-ODE system

$$\dot{\mathbf{w}}(t) = \mathbf{f}(\mathbf{w}(t), \partial_z x(0, t)) \quad (1a)$$

$$x(0, t) = 0 \quad (1b)$$

$$\partial_t x(z, t) = \partial_z^2 x(z, t) + rx(z, t) \quad (1c)$$

$$x(1, t) = u(t) \quad (1d)$$

consists of the nonlinear ODE subsystem (1a) with the lumped state $\mathbf{w}(t) \in \mathbb{R}^n$ and the parabolic PDE subsystem (1b)–(1d) with the distributed state $x(z, t) \in \mathbb{R}$ defined for $(z, t) \in [0, 1] \times \mathbb{R}_0^+$. The PDE (1c) is a linear reaction-diffusion equation with constant reaction coefficient $r \in \mathbb{R}$. The boundary conditions (1b) and (1d) at $z = 0$ and $z = 1$ are of Dirichlet type¹. Since the input $u(t) \in \mathbb{R}$ acts at $z = 1$, the boundary at $z = 0$ is referred to as the unactuated boundary. System (1) is completed with initial conditions $\mathbf{w}(0) = \mathbf{w}_0 \in \mathbb{R}^n$ and $x(z, 0) = x_0(z) \in \mathbb{R}$. Note that (1) is a cascade since the boundary value $\partial_z x(0, t)$ of the PDE subsystem (1b)–(1d) acts on the ODE subsystem (1a) through the vector field \mathbf{f} .

Remark 1. Any constant diffusion coefficient in (1c) could always be normalized by scaling the spatial variable. Moreover, advection terms of the form $a\partial_z x(z, t)$, $a \in \mathbb{R}$, could be eliminated by a scaling transformation of the distributed variable. See, e.g., [17] for details. The case of coefficients depending on space and time is left out here for simplicity.

The objective is to design a state feedback that asymptotically stabilizes the origin of the PDE-ODE cascade (1). A novel approach is presented to overcome the challenge that arises from the nonlinearity of the ODE subsystem (1a). It is inspired by the solution-based design proposed in [7] for hyperbolic systems. The design is modular in the sense that the controller for the PDE-ODE system (1) is based on the existence of a stabilizing controller for the ODE subsystem (1a), wherein $\partial_z x(0, t)$ plays the role of an input. This is guaranteed by the following assumption.

Assumption 1. There exists an analytic function $\kappa(\mathbf{w}(t))$ such that

$$\dot{\mathbf{w}}(t) = \mathbf{f}(\mathbf{w}(t), \kappa(\mathbf{w}(t)) + \varpi(t)) \quad (2)$$

implies input-to-state stability of the origin w.r.t. $\varpi(t) \in \mathbb{R}$.

Input-to-state stability is a typical prerequisite for various system classes of both finite and infinite dimension that involve nonlinear ODEs [7], [12]. Since designing a specific controller $\kappa(\mathbf{w}(t))$ is not the focus here, any well-known method for stabilizing nonlinear ODEs could be used. Note that input-to-state stability implies that the state feedback $\kappa(\mathbf{w}(t))$ globally asymptotically stabilizes the origin for $\varpi(t) = 0$.

Furthermore, the control design requires the solution of (1) to exhibit properties that are sufficient for the well-posedness of the Cauchy problem in Section III. For that, the following technical assumption is imposed.

Assumption 2. The ODE subsystem (1a) is forward complete, the nonlinear function \mathbf{f} is analytic, and the initial condition x_0 is analytic on $[0, 1]$.

¹The design approach presented in this work is easily modified to account for Neumann or Robin boundary conditions.

Forward completeness (see, e.g., [11]) means that the solution of (1a) exists for all initial conditions $\mathbf{w}(0)$ and locally bounded input signals $\partial_z x(0, t)$ for $t \in \mathbb{R}_0^+$. This implies that the nonlinear ODE subsystem (1a) does not exhibit a finite escape time. Additionally, solutions of parabolic PDEs need not be analytic functions of time. This is particularly true for the excitation of (1a) through the boundary value $\partial_z x(0, t)$. Therefore, it does not suffice to restrict solutions $\mathbf{w}(t)$ of (1a) to be analytic in time. The following lemma addresses these properties.

Lemma 1. Let Assumption 2 hold and $u \in \mathcal{G}_2$. Then, the solution of (1) is analytic in z and of Gevrey class two in t , i.e., $\mathbf{w} \in \mathcal{G}_2$ and $x \in C^\omega \mathcal{G}_2$ for $(z, t) \in [0, 1] \times \mathbb{R}_0^+$.

As a detailed proof is very extensive, only a sketch is provided here. It follows the lines of [9], where it is shown that $x \in C^\omega \mathcal{G}_2$ if the boundary values in (1b) and (1d) are of Gevrey class two in t . This is true for $u \in \mathcal{G}_2$. Furthermore, $\mathbf{w} \in \mathcal{G}_2$ follows from $x \in C^\omega \mathcal{G}_2$ and \mathbf{f} being analytic since the compositions in (1a) of analytic functions and elements of \mathcal{G}_2 are also in \mathcal{G}_2 (see, e.g., [18, Prop. 1.4.6]). Notice that the forward completeness of the ODE subsystem (1a) guarantees global existence of the solution $\mathbf{w}(t)$.

III. CONTROL DESIGN

In this section it is shown that the origin of the PDE-ODE system (1) can be stabilized with the controller

$$u(t) = \chi(1, t) + \int_0^1 k(1, \zeta)x(\zeta, t) d\zeta, \quad (3)$$

where the kernel $k(z, \zeta) \in \mathbb{R}$ satisfies the kernel equations

$$\partial_z^2 k(z, \zeta) - \partial_\zeta^2 k(z, \zeta) = rk(z, \zeta) \quad (4a)$$

$$2k(z, z) = -rz \quad (4b)$$

$$k(z, 0) = 0 \quad (4c)$$

for $0 \leq \zeta \leq z \leq 1$ and $\chi(z, t) \in \mathbb{R}$ is the unique solution of the Cauchy problem²

$$\partial_z^2 \chi(z, t) = \partial_t \chi(z, t) \quad (5a)$$

$$\chi(0, t) = 0 \quad (5b)$$

$$\partial_z \chi(0, t) = \kappa(\mathbf{w}(t)) \quad (5c)$$

w.r.t. z for $(z, t) \in [0, 1] \times \mathbb{R}_0^+$. The kernel equations (4) admit an explicit solution [13, Ch. 4.4]. The solvability of the Cauchy problem (5) is discussed in what follows.

In order to better highlight the main idea of the paper, the design is split into multiple elementary steps. First, a preliminary backstepping transformation is used to simplify the representation of the PDE subsystem by compensating the reaction term in (1c). Then, based on the solution $\chi(z, t)$ of the Cauchy problem (5), a novel nonlinear transformation of the infinite-dimensional state is derived. As a result, the nonlinear ODE (1a) is input-to-state stable w.r.t. the transformed coordinates and, thus, the choice of a stabilizing state feedback for the PDE-ODE system is straightforward. By applying the controller (3), the origin of the PDE-ODE system (1) is shown to be asymptotically stable.

²Recall that $\kappa(\mathbf{w}(t))$ is the stabilizing controller from Assumption 1.

This article has been accepted for publication in IEEE Control Systems Letters. This is the author's version which has not been fully edited and content may change prior to final publication. Citation information: DOI 10.1109/LCSYS.2024.3406924

A. Preliminary Backstepping Transformation

The possibly destabilizing reaction term $rx(z, t)$ in the linear PDE (1c) is eliminated by utilizing PDE backstepping (cf. [13]). For that, and in light of the kernel equations (4), the invertible backstepping transformation

$$\bar{x}(z, t) = x(z, t) - \int_0^z k(z, \zeta)x(\zeta, t) d\zeta \quad (6)$$

maps the PDE-ODE system (1) into the intermediate system

$$\begin{aligned} \dot{\mathbf{w}}(t) &= \mathbf{f}(\mathbf{w}(t), \partial_z \bar{x}(0, t)) & (7a) \\ \bar{x}(0, t) &= 0 & (7b) \\ \partial_t \bar{x}(z, t) &= \partial_z^2 \bar{x}(z, t) & (7c) \\ \bar{x}(1, t) &= \bar{u}(t) & (7d) \end{aligned}$$

after introducing the new input

$$\bar{u}(t) = u(t) - \int_0^1 k(1, \zeta)x(\zeta, t) d\zeta. \quad (8)$$

An alternative method to derive (6) is to use the general coordinate transformation

$$\bar{x}(z, t) = x(z, t) - \beta(z, t), \quad (9)$$

where $\beta(z, t) \in \mathbb{R}$ uniquely solves the Cauchy problem

$$\partial_z^2 \beta(z, t) = \partial_t \beta(z, t) - rx(z, t) \quad (10a)$$

$$\beta(0, t) = 0 \quad (10b)$$

$$\partial_z \beta(0, t) = 0 \quad (10c)$$

for $(z, t) \in [0, 1] \times \mathbb{R}_0^+$. It is easy to verify that

$$\beta(z, t) = \int_0^z k(z, \zeta)x(\zeta, t) d\zeta \quad (11)$$

solves the Cauchy problem (10) after a simple calculation in light of the kernel equations (4). Hence, (6) and (9) are equivalent, which also implies that

$$\bar{u}(t) = u(t) - \beta(1, t) \quad (12)$$

is equivalent to (8).

It is worth emphasizing that the Volterra integral transformation (6) can be directly deduced from the solution of the Cauchy problem (10). In this sense, the latter can be seen as the underlying transformation equations. In what follows, this observation enables a more general, nonlinear state transformation without an a priori defined form.

B. A Novel Nonlinear State Transformation

For the considered setup, a backstepping controller no longer exists in form of a simple Volterra integral. In what follows, the latter is replaced by a general expression $\chi(z, t)$ (cf. $\beta(z, t)$ in (9)). This leads to the change of coordinates

$$\bar{x}(z, t) = \bar{x}(z, t) - \chi(z, t) \quad (13)$$

that maps the intermediate PDE-ODE system (7) into the final target system

$$\dot{\mathbf{w}}(t) = \mathbf{f}(\mathbf{w}(t), \kappa(\mathbf{w}(t))) + \partial_z \bar{x}(0, t) \quad (14a)$$

$$\bar{x}(0, t) = 0 \quad (14b)$$

$$\partial_t \bar{x}(z, t) = \partial_z^2 \bar{x}(z, t) \quad (14c)$$

$$\bar{x}(1, t) = \bar{u}(t) - \chi(1, t) \quad (14d)$$

if the auxiliary transformation variable $\chi(z, t)$ satisfies the Cauchy problem (5). The following lemma clarifies its solvability.

Lemma 2. *Let Assumption 1 hold and $\mathbf{w} \in \mathcal{G}_2$. The Cauchy problem (5) admits a unique $C^\omega \mathcal{G}_2$ -solution $\chi(z, t)$ for $(z, t) \in [0, 1] \times \mathbb{R}_0^+$.*

Proof. It follows from [6, Par. 52] (or [18, Prop. 1.4.6]) that the function $\kappa(\mathbf{w}(t))$ is of Gevrey class two w.r.t. t , since it is a composition of the analytic function κ (see Assumption 1) and $\mathbf{w} \in \mathcal{G}_2$. In light of this, it is shown in [6, Par. 55] that the (linear) Cauchy problem (5) admits a unique solution $\chi \in C^\omega \mathcal{G}_2$. In particular, the series

$$\chi(z, t) = \sum_{k=0}^{\infty} \frac{z^{2k+1}}{(2k+1)!} \frac{d^k}{dt^k} \kappa(\mathbf{w}(t)) \quad (15)$$

can be easily verified to solve (5). The convergence of the series is guaranteed by the Gevrey property of $\kappa(\mathbf{w}(t))$. \square

Remark 2. *Note that (5) is a Cauchy problem w.r.t. z , whereas t plays the role of a parameter. Hence, it does not require an initial condition $\chi(z, 0)$ w.r.t. t .*

Using (7) to replace the time derivatives in (15), it can be shown that the auxiliary transformation variable $\chi(z, t)$ depends nonlinearly on $\mathbf{w}(t)$ and $\bar{x}(z, t)$, which implies that (13) is a nonlinear state transformation. For that, an alternative representation of the intermediate system (7) is considered. It makes use of the fact that $y_0(t) = \partial_z \bar{x}(0, t)$ is a flat output of the PDE subsystem (7b)–(7d) (see, e.g., [5], [14]). Introducing the flat coordinates $y_k(t) = \frac{d^k}{dt^k} \partial_z \bar{x}(0, t)$, $k \in \mathbb{N}_0$ and inserting the power series

$$\bar{x}(z, t) = \sum_{k=0}^{\infty} \frac{z^{2k+1}}{(2k+1)!} y_k(t) \quad (16)$$

into the intermediate system (7) yields

$$\frac{d}{dt} \underbrace{\begin{bmatrix} \mathbf{w}(t) \\ y_0(t) \\ y_1(t) \\ \vdots \end{bmatrix}}_{\bar{\mathbf{w}}(t)} = \underbrace{\begin{bmatrix} \mathbf{f}(\mathbf{w}(t), y_0(t)) \\ y_1(t) \\ y_2(t) \\ \vdots \end{bmatrix}}_{\mathbf{g}(\bar{\mathbf{w}}(t))} \quad (17a)$$

$$\sum_{k=0}^{\infty} \frac{1}{(2k+1)!} y_k(t) = \bar{u}(t) \quad (17b)$$

with the (infinite-dimensional) state $\bar{\mathbf{w}}(t)$. The system representation (17) is equivalent to (7) for $\bar{x} \in C^\omega \mathcal{G}_2$. In fact, since the set of monomials of odd degree is linearly independent and dense in $\mathcal{L}_2([0, 1])$, (16) can be viewed as a transformation between the PDE state $\bar{x}(z, t)$ of (7) and the flat coordinates

© 2024 IEEE. Personal use is permitted, but republication/redistribution requires IEEE permission. See <https://www.ieee.org/publications/rights/index.html> for more information.

This article has been accepted for publication in IEEE Control Systems Letters. This is the author's version which has not been fully edited and content may change prior to final publication. Citation information: DOI 10.1109/LCSYS.2024.3406924

$y_k(t)$ in (17). Defining $\mathbf{y}^{[k]} = (y_0, \dots, y_k)$ for $k \in \mathbb{N}_0$, the k -th derivative of $\kappa(\mathbf{w}(t))$ in (15) can be written in terms of the state $\bar{\mathbf{w}}(t)$ as

$$\frac{d}{dt}{}^k \kappa(\mathbf{w}(t)) = \phi_k(\mathbf{w}(t), \mathbf{y}^{[k-1]}(t)), \quad (18)$$

where $\phi_k = \mathbf{L}_{\mathbf{g}}^k \eta$ denotes the k -th Lie-derivative of $\eta(\bar{\mathbf{w}}) := \kappa(\mathbf{w})$ along \mathbf{g} and $\mathbf{y}^{[k-1]}$ is empty. With that, the auxiliary transformation variable in (15) takes the form

$$\chi(z, t) = \sum_{k=0}^{\infty} \frac{z^{2k+1}}{(2k+1)!} \phi_k(\mathbf{w}(t), \mathbf{y}^{[k-1]}(t)) \quad (19)$$

and, in view of (16), the coordinate change (13) reads

$$\bar{x}(z, t) = \sum_{k=0}^{\infty} \frac{z^{2k+1}}{(2k+1)!} (y_k(t) - \phi_k(\mathbf{w}(t), \mathbf{y}^{[k-1]}(t))). \quad (20)$$

Due to the equivalence between the flat coordinates $y_k(t)$ and the PDE state $\bar{x}(z, t)$ (recall the state transformation (16)), $\bar{x}(z, t)$ can be expressed in terms of the ODE state $\mathbf{w}(t)$ and the PDE state $\bar{x}(z, t)$ of the intermediate system (7). As a consequence, the coordinate change in (13) (and (20)) is a nonlinear state transformation of the PDE state $\bar{x}(z, t)$, mapping (7) into (14). It is worth noting that this nonlinear state transformation results from the solution of the linear Cauchy problem (5). This new perspective allows a generalization of the classical backstepping transformation of Volterra type to nonlinear settings. In fact, it is shown in Section IV that this general result also yields the well-known backstepping transformation in the special case of linear systems.

Remark 3. For the (nonlinear) inverse transformation $\bar{x}(z, t) = \bar{x}(z, t) + \chi(z, t)$, in order to express the auxiliary transformation variable $\chi(z, t)$ in terms of $\mathbf{w}(t)$ and $\bar{x}(z, t)$, the time derivatives in (15) are replaced using (14). By introducing flat coordinates $\tilde{y}_k(t) = \frac{d}{dt}{}^k \bar{x}(0, t)$, $k \in \mathbb{N}_0$, such an expression for $\chi(z, t)$ is obtained in analogy to (19).

The nonlinear state transformation (13) represents the main result of the control design. It maps (7) into a convenient form where the ODE subsystem (14a) is input-to-state stable w.r.t. $\partial_z \bar{x}(0, t)$ by Assumption 1. Therefore, next, the PDE subsystem (14b)–(14d) is stabilized by choice of $\bar{u}(t)$.

C. State Feedback Controller and Closed-Loop Stability

Inserting the control law

$$\bar{u}(t) = \chi(1, t) \quad (21)$$

into the input transformation (8) yields the proposed controller (3). The latter is a (static) state feedback of the ODE state $\mathbf{w}(t)$ and the PDE state $x(z, t)$, in view of (19) evaluated at $z = 1$, (16) relating $\bar{x}(z, t)$ and $\bar{\mathbf{w}}(t)$ as well as the backstepping transformation (6).

As a consequence of (14) and (21), the closed loop reads

$$\dot{\mathbf{w}}(t) = \mathbf{f}(\mathbf{w}(t), \kappa(\mathbf{w}(t)) + \partial_z \bar{x}(0, t)) \quad (22a)$$

$$\bar{x}(0, t) = 0 \quad (22b)$$

$$\partial_t \bar{x}(z, t) = \partial_z^2 \bar{x}(z, t) \quad (22c)$$

$$\bar{x}(1, t) = 0. \quad (22d)$$

The origin of (22) can be shown to be stable (in an appropriate sense). However, it is necessary to verify that this infers the same for the closed-loop system that results from applying the controller (3) to the PDE-ODE system (1). The following theorem addresses this issue.

Theorem 1. Let Assumptions 1 and 2 hold. Apply the controller (3), wherein $k(z, \zeta)$ solves the kernel equations (4) and $\chi(z, t)$ solves the Cauchy problem (5), to the PDE-ODE cascade (1). Then, $\lim_{t \rightarrow \infty} \|x(t)\|_{\infty} = 0$ and $\lim_{t \rightarrow \infty} \|\mathbf{w}(t)\| = 0$ for all initial conditions $\mathbf{w}(0) = \mathbf{w}_0 \in \mathbb{R}^n$ and $x(z, 0) = x_0(z) \in \mathbb{R}$ satisfying (1b).

Proof. Similar to [15], set $u(t) = 0$, $t \in [0, \varepsilon]$ with $\varepsilon > 0$ infinitesimally small. The forward completeness of the ODE subsystem (1a) prevents finite-time blow up on $[0, \varepsilon]$. Thus, at least for $t > \varepsilon$, the Cauchy problem (5) is solvable in closed loop with $x, \chi \in C^{\omega} \mathcal{G}_2$ and $\mathbf{w}, u \in \mathcal{G}_2$ by Lemmas 1 and 2. Applying the state transformations (6) and (13) together with the controller (3) to the plant (1) yields the closed-loop system (22), where the PDE subsystem (22b)–(22d) is exponentially stable in $\mathcal{L}_2([0, 1])$ (see, e.g., [17, Lem. 6]). In fact, [17, Lem. 7] allows to verify that both the \mathcal{H}^1 -norm and the supremum norm of \bar{x} decay exponentially. By that, the transformed PDE state $\bar{x}(z, t)$ of the closed-loop system (22) converges to zero exponentially and pointwise in space (see, e.g., [13, Ch. 2.3]). This also implies $\partial_z \bar{x}(0, t) \rightarrow 0$ as $t \rightarrow \infty$. Consequently, in view of Assumption 1, the asymptotic stabilization of the origin of the ODE subsystem (22a) is achieved. By the invertibility of (13) (see Remark 3), (22) infers that the origin of (7) with $\bar{u}(t) = \chi(1, t)$ is asymptotically stable pointwise in space. Consequently, the bounded invertibility of the backstepping transformation (6) (see, e.g., [13, Ch. 4.5]) ensures the same in the original coordinates. \square

IV. THE LINEAR CASE

In order to give insight into the structure of the state transformation (13) (or equivalently (20)) and to compare it to the results in [10] for linear systems, consider

$$\dot{\mathbf{w}}(t) = F\mathbf{w}(t) + \mathbf{b}\partial_z \bar{x}(0, t) \quad (23a)$$

$$\bar{x}(0, t) = 0 \quad (23b)$$

$$\partial_t \bar{x}(z, t) = \partial_z^2 \bar{x}(z, t) \quad (23c)$$

$$\bar{x}(1, t) = \bar{u}(t) \quad (23d)$$

as a special case of (7). Verifying Assumptions 1 and 2 is straightforward if the pair (F, \mathbf{b}) is stabilizable, i.e., there exists a feedback $\kappa(\mathbf{w}(t)) = \mathbf{k}^T \mathbf{w}(t)$ such that $F + \mathbf{b}\mathbf{k}^T$ is Hurwitz. In this linear case, the analytic solution of the Cauchy problem (5) can be expressed explicitly in terms of $\mathbf{w}(t)$ and $\bar{x}(z, t)$. This follows from the Lie-derivatives in (18), which can be written in the form

$$\frac{d}{dt}{}^k \mathbf{k}^T \mathbf{w}(t) = \mathbf{k}^T F^k \mathbf{w}(t) + \mathbf{k}^T \sum_{i=0}^{k-1} F^{k-1-i} \mathbf{b} y_i(t). \quad (24)$$

Inserting (24) in (15) yields the series (19) for $\chi(z, t)$ that is linear in the ODE state $\mathbf{w}(t)$ and the flat coordinates $y_k(t)$, $k \in$

© 2024 IEEE. Personal use is permitted, but republication/redistribution requires IEEE permission. See <https://www.ieee.org/publications/rights/index.html> for more information.

This article has been accepted for publication in IEEE Control Systems Letters. This is the author's version which has not been fully edited and content may change prior to final publication. Citation information: DOI 10.1109/LCSYS.2024.3406924

\mathbb{N}_0 . After lengthy calculations (see Remark 4), it is possible to write the auxiliary transformation variable

$$\chi(z, t) = \mathbf{n}^T(z) \mathbf{w}(t) + \int_0^z \mathbf{n}^T(z - \zeta) \mathbf{b} \bar{x}(\zeta, t) d\zeta \quad (25)$$

explicitly in terms of the state $\mathbf{w}(t)$ and $\bar{x}(z, t)$ of (23), where $\mathbf{n}^T(z)$ is the unique solution of the initial value problem

$$d_z^2 \mathbf{n}^T(z) = \mathbf{n}^T(z) F, \quad z \in (0, 1] \quad (26a)$$

$$\mathbf{n}^T(0) = \mathbf{0}^T \quad (26b)$$

$$d_z \mathbf{n}^T(0) = \mathbf{k}^T. \quad (26c)$$

This can easily be verified by inserting (25) into (5). Substituting the explicit expression (25) of the auxiliary transformation variable $\chi(z, t)$ into (13) yields the linear state transformation

$$\bar{x}(z, t) = \bar{x}(z, t) - \mathbf{n}^T(z) \mathbf{w}(t) - \int_0^z \mathbf{n}^T(z - \zeta) \mathbf{b} \bar{x}(\zeta, t) d\zeta. \quad (27)$$

Note that the same transformation is obtained by applying the backstepping design in [10] to the linear PDE-ODE system³ (23). Consequently, the backstepping controller and the one in (21) are identical in the linear case.

Remark 4. In order to obtain (25), first, insert (24) in (15). Then, for the double sum therein, shift the summation index of the outer sum and use the relation

$$\frac{z^{2k+3}}{(2k+3)!} = \int_0^z \frac{(z-\zeta)^{2(k-i)+1}}{(2(k-i)+1)!} \frac{\zeta^{2i+1}}{(2i+1)!} d\zeta, \quad (28)$$

which can be shown to hold for $k \in \mathbb{N}_0$ and $i \in \{0, 1, \dots, k\}$ using integration by parts. Afterwards, interchange the order of summation and integration and apply the Cauchy product formula to recover (16). In the end, define $\mathbf{n}^T(z) = \mathbf{k}^T \sum_{k=0}^{\infty} \frac{z^{2k+1}}{(2k+1)!} F^k$, which solves (26).

V. EXAMPLE

The theoretical results presented in this paper are illustrated for the nonlinear PDE-ODE system (1) with

$$\mathbf{f}(\mathbf{w}, \partial_z x(0)) = \begin{bmatrix} w_1 \sin(2w_1) + w_2 \\ \partial_z x(0) - \ln(1 + w_1^2) + 2 \sin(3w_2) \end{bmatrix} \quad (29)$$

where $\mathbf{w} = [w_1, w_2]^T$, a reaction coefficient $r = 20$ and initial conditions

$$\mathbf{w}(0) = [2, -2]^T, \quad x(z, 0) = \sin^3(2\pi z) \quad (30)$$

for $z \in [0, 1]$. It can be verified that Assumption 2 holds. The zero equilibrium of the plant is unstable for $u(t) = 0$ since there exist positive eigenvalues of the PDE subsystem for $r > \pi^2$ (see, e.g., [13, Ch. 3]) and, additionally, the eigenvalues of the linearization of the ODE subsystem about the origin are 0 and 6.

³The system in [10] involves a Neumann boundary condition (instead of (23b)), with $x(0, t)$ (instead of $\partial_z x(0, t)$) driving the ODE (23a).

A. Control Design

Using the exactly and globally linearizing controller

$$\kappa(\mathbf{w}) = \ln(1 + w_1^2) - 2 \sin(3w_2) - k_0 w_1 - (\sin(2w_1) + 2w_1 \cos(2w_1) + k_1)(w_1 \sin(2w_1) + w_2) \quad (31)$$

with $k_0, k_1 > 0$, (2) can equivalently be written as⁴

$$\ddot{w}_1(t) + k_1 \dot{w}_1(t) + k_0 w_1(t) = \varpi(t). \quad (32)$$

With that, Assumption 1 is fulfilled. Hence, all assumptions of Theorem 1 hold. For the assignment of the eigenvalues -2 and -3 in (32), the control parameters $k_0 = 6$ and $k_1 = 5$ are chosen. The following numerical scheme allows for an efficient implementation of the controller (3).

B. Numerical Implementation

The Volterra integral in (3) is implemented with the trapezoidal rule. Therein, the explicit solution $k(z, \zeta)$ of the kernel equations (4) is taken from [13, Ch. 4.4]. To obtain $\chi(1, t)$, the following scheme can be used.

On an equidistant spatial grid with $N+1$ distinct grid points $z_j = j/N$, $j \in \{0, \dots, N\}$, the convergence of (19) allows for its approximation by

$$\chi(z, t) \approx \sum_{k=0}^N \frac{z^{2k+1}}{(2k+1)!} \phi_k(\mathbf{w}(t), \mathbf{y}^{[k-1]}(t)) \quad (33)$$

to any desired level of accuracy. This truncation depends on both the ODE state $\mathbf{w}(t)$ and the state components $y_k(t)$ for $k \in \{0, \dots, N-1\}$. The latter is determined from the PDE state $\bar{x}(z, t)$ by approximating the convergent series (16) on the same spatial grid with the approximation order $N-1$, i.e.,

$$\bar{x}(z, t) \approx \sum_{k=0}^{N-1} \frac{z^{2k+1}}{(2k+1)!} y_k(t). \quad (34)$$

Evaluating the latter on N grid points z_j , $j \in \{1, \dots, N\}$, yields the system of equations

$$\begin{bmatrix} \bar{x}(z_1, t) \\ \bar{x}(z_2, t) \\ \vdots \\ \bar{x}(z_N, t) \end{bmatrix} = V_N \begin{bmatrix} y_0(t) \\ \frac{1}{3!} y_1(t) \\ \vdots \\ \frac{1}{(2N-1)!} y_{N-1}(t) \end{bmatrix}, \quad (35)$$

where

$$V_N = \begin{bmatrix} z_1 & z_1^3 & \dots & z_1^{2N-1} \\ z_2 & z_2^3 & \dots & z_2^{2N-1} \\ \vdots & \vdots & \ddots & \vdots \\ z_N & z_N^3 & \dots & z_N^{2N-1} \end{bmatrix} \in \mathbb{R}^{N \times N} \quad (36)$$

denotes an invertible (Vandermonde-like) matrix. Although V_N can be ill-conditioned for large N , there exist several numerical methods to obtain its inverse accurately (see, e.g., [21]). Moreover, closed-form expressions are well known for the entries of V_N^{-1} . For a fixed grid, V_N^{-1} is computed offline. Thus, (35) can be inverted to obtain the flat coordinates in $\mathbf{y}^{[N-1]}$. Finally, the latter is inserted into the truncated series (33), where the Lie-derivatives ϕ_k can be obtained through symbolic computation or evaluated numerically.

⁴Note that $w_1(t)$ is a flat output of the ODE subsystem (1a) (see [19]).

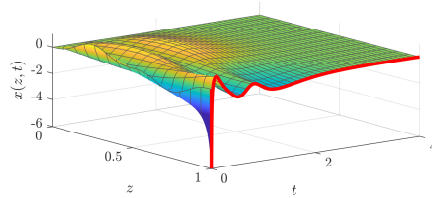


Fig. 1. Evolution of the PDE state $x(z, t)$, where the input $u(t)$ is highlighted in red, and the ODE state $w(t)$ in closed loop.

C. Simulation Results

The following results are obtained for a finite-differences simulation of the plant with initial conditions (30) on an equidistant spatial grid $z_j = j/N$, $j \in \{0, \dots, N\}$ with $N = 30$ and an equidistant temporal grid resulting from a CFL condition number of 1/6. The simulation results in Figure 1 illustrate the control input $u(t)$ and demonstrate that the ODE state $w(t)$ and the PDE state $x(z, t)$ vanish asymptotically and pointwise in space. Specifically, as $\varpi(t) = \partial_z \bar{x}(0, t) \approx 0$ for $t > 1$ (see Figure 2), the controlled ODE (32) is essentially undisturbed by the PDE.

VI. CONCLUDING REMARKS

The new control strategy introduced in this paper has huge potential for the boundary control of a large class of nonlinear PDE-ODE systems, both of parabolic and hyperbolic type (see, e.g., [7] for the latter). The approach can be interpreted as an extension of the well-known backstepping design for PDEs in the sense that the nonlinear state transformation in Section III-B generalizes the Volterra integral transformation and that the Cauchy problem (5) yields the kernel equations in the linear case. Based on this new perspective, it is essentially straightforward to generalize the results of this paper to stabilize a reference trajectory as well as to account for bidirectional coupling between the ODE and PDE in (1). Future research is also concerned with an observer design for nonlinear ODEs with diffusive sensor dynamics using boundary measurement.

REFERENCES

- [1] N. Bekiaris-Liberis and M. Krstic. *Nonlinear Control Under Nonconstant Delays*. SIAM, 2013.
- [2] J. Deutscher and N. Gehring. Output feedback control of coupled linear parabolic ODE-PDE-ODE systems. *IEEE Trans. Autom. Control*, 66(10):4668–4683, 2021.
- [3] J. Deutscher, N. Gehring, and R. Kern. Output feedback control of general linear heterodirectional hyperbolic ODE-PDE-ODE systems. *Automatica*, 95(9):472–480, 2018.
- [4] F. Di Meglio, F. Bribiesca Argomedo, L. Hu, and M. Krstic. Stabilization of coupled linear heterodirectional hyperbolic PDE-ODE systems. *Automatica*, 87:281–289, 2018.
- [5] M. Fliess, H. Mounier, P. Rouchon, and J. Rudolph. A distributed parameter approach to the control of a tubular reactor: a multivariable case. In *Proceedings of the 37th IEEE Conference on Decision and Control*, volume 1, pages 439–442, 1998.
- [6] M. Gevrey. Sur les équations aux dérivées partielles du type parabolique. *J. Math. Pures Appl.*, 9:305–471, 1913.
- [7] A. Irscheid, J. Deutscher, N. Gehring, and J. Rudolph. Output regulation for general heterodirectional linear hyperbolic PDEs coupled with nonlinear ODEs. *Automatica*, 148:110748, 2023.
- [8] A. Irscheid, N. Gehring, J. Deutscher, and J. Rudolph. Tracking control for 2×2 linear heterodirectional hyperbolic PDEs that are bidirectionally coupled with nonlinear ODEs. In J. Auriol, J. Deutscher, G. Mazanti, and G. Valmorbidia, editors, *Advances in Distributed Parameter Systems*, pages 117–142. Springer, 2022.
- [9] D. Kinderlehrer and L. Nirenberg. Analyticity at the boundary of solutions of nonlinear second-order parabolic equations. *Comm. Pure Appl. Math.*, 31(3):283–338, 1978.
- [10] M. Krstic. Compensating actuator and sensor dynamics governed by diffusion PDEs. *Syst. Control Lett.*, 58(5):372–377, 2009.
- [11] M. Krstic. Input delay compensation for forward complete and strict-feedforward nonlinear systems. *IEEE Trans. Autom. Control*, 55(2):287–303, 2010.
- [12] M. Krstic, I. Kanellakopoulos, and P.V. Kokotovic. *Nonlinear and Adaptive Control Design*. John Wiley & Sons, Inc., 1995.
- [13] M. Krstic and A. Smyshlyayev. *Boundary Control of PDEs: A Course on Backstepping Designs*. SIAM, 2008.
- [14] B. Laroche, P. Martin, and P. Rouchon. Motion planning for the heat equation. *Int. J. Robust Nonlinear Control*, 10(8):629–643, 2000.
- [15] P. Martin, L. Rosier, and P. Rouchon. Null controllability of the heat equation using flatness. *Automatica*, 50(12):3067–3076, 2014.
- [16] T. Meurer. *Control of Higher-Dimensional PDEs: Flatness and Backstepping Designs*. Springer, 2013.
- [17] T. Meurer and A. Kugi. Tracking control for boundary controlled parabolic PDEs with varying parameters: Combining backstepping and differential flatness. *Automatica*, 45(5):1182–1194, 2009.
- [18] L. Rodino. *Linear Partial Differential Operators in Gevrey Spaces*. World Scientific, 1993.
- [19] J. Rudolph. *Flatness-Based Control: An Introduction*. Shaker Verlag, 2021.
- [20] J. Wang and M. Krstic. Output feedback boundary control of a heat PDE sandwiched between two ODEs. *IEEE Trans. Autom. Control*, 64(11):4653–4660, 2019.
- [21] H. Wertz. On the numerical inversion of a recurrent problem: The Vandermonde matrix. *IEEE Trans. Autom. Control*, 10(4):492–492, 1965.

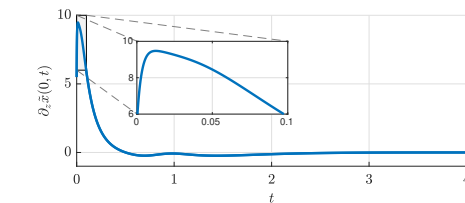
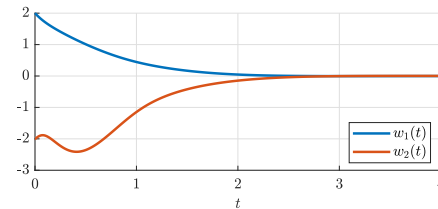


Fig. 2. Evolution of $\varpi(t) = \partial_z \bar{x}(0, t)$ in closed loop (cf. (22a) and (32)). As indicated in the magnified plot, the initial transient is not discontinuous.

Appendix A

Detailed calculations

A.1 Solving the Cauchy problem for a linear reaction-diffusion equation

This section is devoted to the solution of the Cauchy problem (3.7) to obtain an analytical expression with functional dependence on the PDE state $x(z, t)$ of a linear reaction-diffusion equation. More specifically, in Section A.1.1, $x(z, t)$ satisfies (3.1) with unactuated Neumann boundary, whereas the case of unactuated Dirichlet boundary is considered in Section A.1.2 for the sake of completeness.

A.1.1 Unactuated Neumann boundary

The formal solution (3.10) of (3.7) (with $y_r(t) = 0$) contains infinitely many applications of the operator $\frac{d}{dt} - r$ on $y(t)$, as in the parameterization of $x(z, t)$ in (3.3), but also infinitely many applications of the operator $\frac{d}{dt}$. Since the latter operator does not appear in the solution (3.3) of the original problem (3.1), express $\left(\frac{d}{dt}\right)^k$ as

$$\left(\frac{d}{dt}\right)^k = \left(\frac{d}{dt} - r + r\right)^k = \sum_{l=0}^k \binom{k}{l} r^{k-l} \left(\frac{d}{dt} - r\right)^l \quad (\text{A.1})$$

using the binomial formula. Substituting this into (3.10) yields

$$\chi(z, t) = \sum_{k=0}^{\infty} \sum_{l=0}^k \frac{-z^{2k+2} (k+1)! r^{k+1-l}}{(2k+2)! l! (k+1-l)!} \left(\frac{d}{dt} - r\right)^l y(t) \quad (\text{A.2})$$

after a shift of the summation index, with $\frac{d}{dt} - r$ being the only operator applied to $y(t)$. The following lemma provides the necessary tools to further simplify (A.2).

Lemma A.1. *The equation*

$$\frac{z^{2k+1}(k+1)!}{(2k+2)!l!} = \frac{1}{(2l)!2^{k+1-l}} \int_0^z \frac{\left(\frac{z^2-\zeta^2}{2}\right)^{k-l}}{(k-l)!} \zeta^{2l} d\zeta \quad (\text{A.3})$$

holds for $k \in \mathbb{N}_0$, $l \in \{0, 1, 2, \dots, k\}$ and $z \in [0, 1]$.

Proof. For any natural number $q \in \mathbb{N}_0$, it is easy to verify that

$$(2q)! = q! 2^q \prod_{m=0}^{q-1} (2m+1). \quad (\text{A.4})$$

Use that for $q = l$ and $q = k+1$ to verify

$$\frac{(2k+2)!l!}{(k+1)!} \prod_{m=l}^k (2m+1)^{-1} = (2l)! 2^{k+1-l} \quad (\text{A.5})$$

in light of $l \leq k$. Furthermore, integration by parts yields

$$z^{2k+1} \prod_{m=l}^k (2m+1)^{-1} = \int_0^z \frac{\left(\frac{z^2-\zeta^2}{2}\right)^{k-l}}{(k-l)!} \zeta^{2l} d\zeta. \quad (\text{A.6})$$

By division, (A.3) results from (A.6) and (A.5). \square

After inserting (A.3) into (A.2), the formal solution of (3.7) can be expressed as

$$\chi(z, t) = \int_0^z \sum_{k=0}^{\infty} \sum_{l=0}^k a_{k-l}(z, \zeta) b_l(\zeta, t) d\zeta \quad (\text{A.7})$$

with

$$a_k(z, \zeta) = -\frac{rz}{2^{2k+1}} \frac{(r(z^2 - \zeta^2))^k}{k!(k+1)!} \quad (\text{A.8a})$$

$$b_k(\zeta, t) = \frac{\zeta^{2k}}{(2k)!} \left(\frac{d}{dt} - r\right)^k y(t), \quad (\text{A.8b})$$

after interchanging the order of summation and integration. Rearranging the Cauchy product in (A.7) yields (3.11), wherein the integral kernel (3.11b) follows from

$$k(z, \zeta) = \sum_{k=0}^{\infty} a_k(z, \zeta) \quad (\text{A.9})$$

in light of (A.8a) and the series representation of the modified Bessel function I_1 of first kind and first order (cf. Abramowitz and Stegun (1964)). The herewith obtained formal solution (3.11) is easily verified to satisfy (3.7).

Remark A.1. *Interchanging the order of summation and integration to obtain (A.7) requires uniform convergence of the involved series. Similarly, rearranging the Cauchy product requires absolute convergence. As the final result (3.11) of these formal manipulations solves the Cauchy problem (3.7), such convergence requirements are justified here and in the remainder of this chapter.*

A.1.2 Unactuated Dirichlet boundary

In order to demonstrate the solution-based controller for other types of boundary conditions, consider the exemplary case of a reaction-diffusion equation with Dirichlet boundaries, i.e.,

$$\bar{x}(0, t) = 0 \quad (\text{A.10a})$$

$$\partial_t \bar{x}(z, t) = \partial_z^2 \bar{x}(z, t) + r \bar{x}(z, t) \quad (\text{A.10b})$$

$$\bar{x}(1, t) = u(t) \quad (\text{A.10c})$$

(cf. (3.1)). With the flat output $\bar{y}(t) = \partial_z \bar{x}(0, t)$, the flatness-based parameterization of the PDE state $\bar{x}(z, t)$ reads

$$\bar{x}(z, t) = \sum_{k=0}^{\infty} \frac{z^{2k+1}}{(2k+1)!} \left(\frac{d}{dt} - r \right)^k \bar{y}(t). \quad (\text{A.11})$$

Compared to (3.3) with even powers of z , it comprises the odd powers only. Analogously to Section 3.1.1, (A.10) is asymptotically stabilized by the solution-based controller $u(t) = \bar{\chi}(1, t)$, where $\bar{\chi}(z, t)$ satisfies the Cauchy problem

$$\partial_z^2 \bar{\chi}(z, t) = \partial_t \bar{\chi}(z, t) - r \bar{\chi}(z, t) \quad (\text{A.12a})$$

$$\bar{\chi}(0, t) = 0 \quad (\text{A.12b})$$

$$\partial_z \bar{\chi}(0, t) = 0 \quad (\text{A.12c})$$

(cf. (3.7) with $y_r(t) = 0$). Taking into account (A.11), it is straightforward to obtain the formal power-series

$$\bar{\chi}(z, t) = \sum_{k=0}^{\infty} \frac{z^{2k+1}}{(2k+1)!} \left(\left(\frac{d}{dt} - r \right)^k - \left(\frac{d}{dt} \right)^k \right) \bar{y}(t). \quad (\text{A.13})$$

Similar to the calculations in Section A.1.1, the formal solution (A.13) can be manipulated in such a way that it is expressed in terms of the operator $\frac{d}{dt} - r$ only. For that, insert the binomial formula (A.1) into (A.13) to obtain

$$\bar{\chi}(z, t) = \sum_{k=0}^{\infty} \sum_{l=0}^k \frac{-z^{2k+3} (k+1)! r^{k+1-l}}{(2k+3)! l! (k+1-l)!} \left(\frac{d}{dt} - r \right)^l \bar{y}(t) \quad (\text{A.14})$$

after a shift of the summation index. Note that its structure differs from (A.2) in the sense that terms with $2k+2$ are replaced by $2k+3$. Therefore, for further simplification, Lemma A.1 cannot be used and is, thus, replaced with the following one.

Lemma A.2. *The equation*

$$\frac{z^{2k+3}(k+1)!}{(2k+3)!l!} = \frac{1}{(2l+1)!2^{k+1-l}} \int_0^z \zeta \frac{\left(\frac{z^2-\zeta^2}{2}\right)^{k-l}}{(k-l)!} \zeta^{2l+1} d\zeta \quad (\text{A.15})$$

holds for $k \in \mathbb{N}_0$, $l \in \{0, 1, 2, \dots, k\}$ and $z \in [0, 1]$.

Proof. Multiplying the left-hand side of (A.5) by the trivial expression $(2k+3)/(2k+3)$ gives

$$\frac{(2k+3)!l!}{(k+1)!} \prod_{m=l}^{k+1} (2m+1)^{-1} = (2l)!2^{k+1-l}. \quad (\text{A.16})$$

Furthermore, substituting k in (A.6) with $k+1$ results in

$$z^{2k+3} \prod_{m=l}^{k+1} (2m+1)^{-1} = \int_0^z \frac{\left(\frac{z^2-\zeta^2}{2}\right)^{k+1-l}}{(k+1-l)!} \zeta^{2l} d\zeta, \quad (\text{A.17})$$

which yields

$$z^{2k+3} \prod_{m=l}^{k+1} (2m+1)^{-1} = \int_0^z \zeta \frac{\left(\frac{z^2-\zeta^2}{2}\right)^{k-l}}{(k-l)!} \frac{\zeta^{2l+1}}{2l+1} d\zeta \quad (\text{A.18})$$

after integration by parts. By division, (A.15) results from (A.18) and (A.16). \square

After inserting (A.15) into (A.14), one obtains an expression of the form

$$\bar{\chi}(z, t) = \int_0^z \sum_{k=0}^{\infty} \sum_{l=0}^k \bar{a}_{k-l}(z, \zeta) \bar{b}_l(\zeta, t) d\zeta \quad (\text{A.19})$$

with

$$\bar{a}_k(z, \zeta) = -\frac{r\zeta}{2^{2k+1}} \frac{(r(z^2 - \zeta^2))^k}{k!(k+1)!} \quad (\text{A.20a})$$

$$\bar{b}_k(\zeta, t) = \frac{\zeta^{2k+1}}{(2k+1)!} \left(\frac{d}{dt} - r\right)^k \bar{y}(t), \quad (\text{A.20b})$$

after interchanging the order of summation and integration. Rearranging the Cauchy product in (A.19) yields

$$\bar{\chi}(z, t) = \int_0^z \bar{k}(z, \zeta) \bar{x}(\zeta, t) d\zeta \quad (\text{A.21a})$$

with the integral kernel

$$\bar{k}(z, \zeta) = -r\zeta \frac{\text{I}_1(\sqrt{r(z^2 - \zeta^2)})}{\sqrt{r(z^2 - \zeta^2)}} \quad (\text{A.21b})$$

that follows from

$$\bar{k}(z, \zeta) = \sum_{k=0}^{\infty} \bar{a}_k(z, \zeta) \quad (\text{A.22})$$

in light of (A.20a) and the series representation of the modified Bessel function I_1 of first kind and first order (cf. Abramowitz and Stegun (1964)). Note that the difference between (A.20a) and (A.8a) infers that the kernels in (A.21b) and (3.11b) only differ by the factor in front of the modified Bessel function I_1 . Finally, it is easy to verify that the solution (A.21) satisfies (A.12).

Remark A.2. *In analogy to Remark 3.1, by inserting the Volterra integral (A.21a) with an unknown kernel $\bar{k}(z, \zeta)$ into (A.12) and taking into account the plant (A.10), it can be shown that the kernel has to satisfy*

$$\partial_z^2 \bar{k}(z, \zeta) - \partial_\zeta^2 \bar{k}(z, \zeta) = r \bar{k}(z, \zeta) \quad (\text{A.23a})$$

$$2\bar{k}(z, z) = -rz \quad (\text{A.23b})$$

$$\bar{k}(z, 0) = 0 \quad (\text{A.23c})$$

for $0 \leq \zeta \leq z \leq 1$. These are in fact the kernel equations that arise in Krstic and Smyshlyaev (2008, Ch. 4) in order to derive the corresponding backstepping controller for (A.10). Note that they coincide with the kernel equations (3.13) except for the boundary condition at $\zeta = 0$.

A.2 Solving the Cauchy problem for a linear parabolic PDE-ODE system

Section A.2.1 is devoted to the solution of the Cauchy problem (3.17) to obtain an analytical expression with functional dependence on the state of the linear parabolic PDE-ODE system (3.16) with unactuated Neumann boundary at $z = 0$. For the sake of completeness, Section A.2.2 considers the case of an unactuated Dirichlet boundary instead of (3.16b).

A.2.1 Unactuated Neumann boundary

First, insert (3.23) into (3.22) to get rid of the time derivatives of the ODE state $\mathbf{w}(t)$. This gives

$$\chi(z, t) = \chi_1(z, t) + \chi_2(z, t) \quad (\text{A.24})$$

with

$$\chi_1(z, t) = \mathbf{k}^T \sum_{k=0}^{\infty} \frac{z^{2k}}{(2k)!} F^k \mathbf{w}(t) \quad (\text{A.25a})$$

$$\chi_2(z, t) = \mathbf{k}^T \sum_{k=0}^{\infty} \sum_{l=0}^k \frac{z^{2k+2}}{(2k+2)!} F^{k-l} \mathbf{b} \mathbf{y}^{(l)}(t) \quad (\text{A.25b})$$

after shifting the summation index. Note that $\chi_1(z, t)$ in (A.25a) can also be written as

$$\chi_1(z, t) = \mathbf{n}^T(z) \mathbf{w}(t), \quad (\text{A.26})$$

where

$$\mathbf{n}^T(z) = \mathbf{k}^T \sum_{k=0}^{\infty} \frac{z^{2k}}{(2k)!} F^k \quad (\text{A.27})$$

is the (unique) solution of the initial value problem (3.25). To simplify $\chi_2(z, t)$ in (A.25b), use the relation

$$\frac{z^{2k+2}}{(2k+2)!} = \int_0^z \frac{(z-\zeta)^{2(k-l)+1}}{(2(k-l)+1)!} \frac{\zeta^{2l}}{(2l)!} d\zeta, \quad (\text{A.28})$$

which can be shown to hold for $k \in \mathbb{N}_0$ and $l \in \{0, 1, 2, \dots, k\}$ after integration by parts. By substituting the latter in (A.25b), $\chi_2(z, t)$ can be expressed as

$$\chi_2(z, t) = \int_0^z \sum_{k=0}^{\infty} \sum_{l=0}^k a_{k-l}(z, \zeta) b_l(\zeta, t) d\zeta \quad (\text{A.29})$$

with

$$a_k(z, \zeta) = \mathbf{k}^T \frac{(z-\zeta)^{2k+1}}{(2k+1)!} F^k \mathbf{b} \quad (\text{A.30a})$$

$$b_k(\zeta, t) = \frac{\zeta^{2k}}{(2k)!} \left(\frac{d}{dt}\right)^k y(t), \quad (\text{A.30b})$$

after interchanging the order of summation and integration. Rearranging the Cauchy product in (A.29) yields

$$\chi_2(z, t) = \int_0^z \mathbf{m}^T(z-\zeta) \mathbf{b} x(\zeta, t) d\zeta \quad (\text{A.31})$$

in light of (3.26), (A.27) and (3.21). The herewith obtained formal solution (3.24), resulting from inserting (A.26) and (A.31) into (A.24), is easily verified to satisfy (3.17).

A.2.2 Unactuated Dirichlet boundary

As done for the reaction-diffusion equation in Section A.1.2, the solution-based controller for the PDE-ODE system (3.16) can easily be adapted to the case of Dirichlet boundaries. To demonstrate that, consider the linear parabolic PDE-ODE system

$$\dot{\mathbf{w}}(t) = F \mathbf{w}(t) + \mathbf{b} \partial_z \bar{x}(0, t) \quad (\text{A.32a})$$

$$\bar{x}(0, t) = 0 \quad (\text{A.32b})$$

$$\partial_t \bar{x}(z, t) = \partial_z^2 \bar{x}(z, t) \quad (\text{A.32c})$$

$$\bar{x}(1, t) = u(t) \quad (\text{A.32d})$$

instead of (3.16). Note that $\bar{y}(t) = \partial_z \bar{x}(0, t)$ is the flat output of the PDE subsystem (A.32b)–(A.32d). The latter subsystem coincides with the system (A.10) for $r = 0$ and, thus, one recovers the flatness-based parameterization

$$\bar{x}(z, t) = \sum_{k=0}^{\infty} \frac{z^{2k+1}}{(2k+1)!} \left(\frac{d}{dt}\right)^k \bar{y}(t) \quad (\text{A.33})$$

of the PDE state $\bar{x}(z, t)$ as a special case of (A.11). Furthermore, in analogy to Section 3.2.1, it is easy to verify that $u(t) = \bar{\chi}(1, t)$ is an asymptotically stabilizing control law, where $\bar{\chi}(z, t)$ satisfies the Cauchy problem

$$\partial_z^2 \bar{\chi}(z, t) = \partial_t \bar{\chi}(z, t) \quad (\text{A.34a})$$

$$\bar{\chi}(0, t) = 0 \quad (\text{A.34b})$$

$$\partial_z \bar{\chi}(0, t) = \mathbf{k}^T \mathbf{w}(t) \quad (\text{A.34c})$$

(cf. (3.17)). A power-series ansatz for the solution $\bar{\chi}(z, t)$ of the inverse problem (A.34) yields

$$\bar{\chi}(z, t) = \mathbf{k}^T \sum_{k=0}^{\infty} \frac{z^{2k+1}}{(2k+1)!} \left(\frac{d}{dt}\right)^k \mathbf{w}(t), \quad (\text{A.35})$$

which is similar to the result in (3.22) for the case of an unactuated Neumann boundary. Analogously to (3.23), the k -th derivative of $\mathbf{k}^T \mathbf{w}(t)$ in (A.35) can be expressed as

$$\left(\frac{d}{dt}\right)^k \mathbf{k}^T \mathbf{w}(t) = \mathbf{k}^T F^k \mathbf{w}(t) + \mathbf{k}^T \sum_{l=0}^{k-1} F^{k-1-l} \mathbf{b} \bar{y}^{(l)}(t) \quad (\text{A.36})$$

by successively inserting the ODE (A.32a) and recalling $\bar{y}(t) = \partial_z \bar{x}(0, t)$. Analogously to Section A.2.1, insert (A.36) into (A.35) to get rid of the time derivatives of the ODE state $\mathbf{w}(t)$. This results in

$$\bar{\chi}(z, t) = \bar{\chi}_1(z, t) + \bar{\chi}_2(z, t) \quad (\text{A.37})$$

with

$$\bar{\chi}_1(z, t) = \mathbf{k}^T \sum_{k=0}^{\infty} \frac{z^{2k+1}}{(2k+1)!} F^k \mathbf{w}(t) \quad (\text{A.38a})$$

$$\bar{\chi}_2(z, t) = \mathbf{k}^T \sum_{k=0}^{\infty} \sum_{l=0}^k \frac{z^{2k+3}}{(2k+3)!} F^{k-l} \mathbf{b} \bar{y}^{(l)}(t) \quad (\text{A.38b})$$

after shifting the summation index. Note that $\bar{\chi}_1(z, t)$ in (A.38a) can also be written as

$$\bar{\chi}_1(z, t) = \bar{\mathbf{n}}^T(z) \mathbf{w}(t), \quad (\text{A.39})$$

where

$$\bar{\mathbf{n}}^T(z) = \mathbf{k}^T \sum_{k=0}^{\infty} \frac{z^{2k+1}}{(2k+1)!} F^k \quad (\text{A.40})$$

is the (unique) solution of the initial value problem

$$\frac{d^2 \bar{\mathbf{n}}^T}{dz^2}(z) = \bar{\mathbf{n}}^T(z)F \quad (\text{A.41a})$$

$$\bar{\mathbf{n}}^T(0) = \mathbf{0}^T \quad (\text{A.41b})$$

$$\frac{d\bar{\mathbf{n}}^T}{dz}(0) = \mathbf{k}^T \quad (\text{A.41c})$$

on $z \in [0, 1]$. To simplify $\bar{\chi}_2(z, t)$ in (A.38b), use the relation

$$\frac{z^{2k+3}}{(2k+3)!} = \int_0^z \frac{(z-\zeta)^{2(k-l)+1}}{(2(k-l)+1)!} \frac{\zeta^{2l+1}}{(2l+1)!} d\zeta, \quad (\text{A.42})$$

which can be shown to hold for $k \in \mathbb{N}_0$ and $l \in \{0, 1, 2, \dots, k\}$ after integration by parts. By inserting the latter in (A.38b), $\bar{\chi}_2(z, t)$ can be expressed as

$$\bar{\chi}_2(z, t) = \int_0^z \sum_{k=0}^{\infty} \sum_{l=0}^k \bar{a}_{k-l}(z, \zeta) \bar{b}_l(\zeta, t) d\zeta \quad (\text{A.43})$$

with

$$\bar{a}_k(z, \zeta) = \mathbf{k}^T \frac{(z-\zeta)^{2k+1}}{(2k+1)!} F^k \mathbf{b} \quad (\text{A.44a})$$

$$\bar{b}_k(\zeta, t) = \frac{\zeta^{2k+1}}{(2k+1)!} \left(\frac{d}{dt}\right)^k \bar{\mathbf{y}}(t), \quad (\text{A.44b})$$

after interchanging the order of summation and integration. Rearranging the Cauchy product in (A.43) yields

$$\bar{\chi}_2(z, t) = \int_0^z \bar{\mathbf{n}}^T(z-\zeta) \mathbf{b} \bar{\mathbf{x}}(\zeta, t) d\zeta \quad (\text{A.45})$$

in light of (A.40) and (A.33). The herewith obtained formal solution

$$\bar{\chi}(z, t) = \bar{\mathbf{n}}^T(z) \mathbf{w}(t) + \int_0^z \bar{\mathbf{n}}^T(z-\zeta) \mathbf{b} \bar{\mathbf{x}}(\zeta, t) d\zeta, \quad (\text{A.46})$$

resulting from inserting (A.39) and (A.45) in (A.37), is easily verified to satisfy (A.34). This confirms the results in Irscheid et al. (2024). Similar to the case of the Neumann boundary condition at $z = 0$ in Section 3.2, the control law $u(t) = \bar{\chi}(1, t)$ is indeed a feedback of the ODE state $\mathbf{w}(t)$ and the PDE state $\bar{\mathbf{x}}(z, t)$ of (A.32).

References

- Abramowitz, M. and Stegun, I. A. (1964). *Handbook of Mathematical Functions with Formulas, Graphs, and Mathematical Tables*. U.S. Government Printing Office.
- Allen, L., O’Connell, A., and Kiermer, V. (2019). How can we ensure visibility and diversity in research contributions? How the Contributor Role Taxonomy (CRediT) is helping the shift from authorship to contributorship. *Learn. Publ.*, 32(1):71–74.
- Angeli, D. and Sontag, E. D. (1999). Forward completeness, unboundedness observability, and their Lyapunov characterizations. *Syst. Control Lett.*, 38(4–5):209–217.
- Aoustin, Y., Fliess, M., Mounier, H., Rouchon, P., and Rudolph, J. (1997). Theory and practice in the motion planning and control of a flexible robot arm using Mikusiński operators. *IFAC Proc. Vol.*, 30(20):267–273.
- Auriol, J., Bribiesca Argomedo, F., Bou Saba, D., Di Loreto, M., and Di Meglio, F. (2018). Delay-robust stabilization of a hyperbolic PDE-ODE system. *Automatica*, 95:494–502.
- Auriol, J. and Di Meglio, F. (2016). Minimum time control of heterodirectional linear coupled hyperbolic PDEs. *Automatica*, 71:300–307.
- Balas, M. J. (1978). Active control of flexible systems. *J. Optim. Theory Appl.*, 25(3):415–436.
- Bastin, G. and Dochain, D. (1990). *On-line Estimation and Adaptive Control of Bioreactors*. Elsevier.
- Bekiaris-Liberis, N. and Krstic, M. (2013). *Nonlinear Control Under Nonconstant Delays*. SIAM.
- Bekiaris-Liberis, N. and Krstic, M. (2014). Compensation of wave actuator dynamics for nonlinear systems. *IEEE Trans. Autom. Control*, 59(6):1555–1570.
- Bekiaris-Liberis, N. and Vazquez, R. (2019). Nonlinear bilateral output-feedback control for a class of viscous Hamilton–Jacobi PDEs. *Automatica*, 101:223–231.
- Christofides, P. D. (2001). *Nonlinear and Robust Control of PDE Systems: Methods and Applications to Transport-Reaction Processes*. Springer.

- de Halleux, J., Prieur, C., Coron, J.-M., d'Andréa Novel, B., and Bastin, G. (2003). Boundary feedback control in networks of open channels. *Automatica*, 39(8):1365–1376.
- Deutscher, J. (2015). A backstepping approach to the output regulation of boundary controlled parabolic PDEs. *Automatica*, 57:56–64.
- Deutscher, J. and Gehring, N. (2021). Output feedback control of coupled linear parabolic ODE-PDE-ODE systems. *IEEE Trans. Autom. Control*, 66(10):4668–4683.
- Deutscher, J., Gehring, N., and Kern, R. (2017). Backstepping Control of Linear 2×2 Hyperbolic Systems with Dynamic Boundary Conditions. *IFAC-PapersOnLine*, 50(1):4522–4527.
- Deutscher, J., Gehring, N., and Kern, R. (2018). Output feedback control of general linear heterodirectional hyperbolic ODE-PDE-ODE systems. *Automatica*, 95(9):472–480.
- Deutscher, J., Gehring, N., and Kern, R. (2019). Output feedback control of general linear heterodirectional hyperbolic PDE-ODE systems with spatially-varying coefficients. *Int. J. Contr.*, 92(10):2274–2290.
- Di Meglio, F., Bribiesca Argomedo, F., Hu, L., and Krstic, M. (2018). Stabilization of coupled linear heterodirectional hyperbolic PDE-ODE systems. *Automatica*, 87:281–289.
- Dochain, D. and Vanrolleghem, P. (2005). *Dynamical Modelling & Estimation in Wastewater Treatment Processes*. IWA Publishing.
- Espitia, N., Girard, A., Marchand, N., and Prieur, C. (2017). Dynamic boundary control synthesis of coupled PDE-ODEs for communication networks under fluid flow modeling. In *Proceedings of the 56th IEEE Conference on Decision and Control*, pages 1260–1265.
- Fischer, F. and Deutscher, J. (2022). Fault diagnosis for linear heterodirectional hyperbolic ODE-PDE systems using backstepping-based trajectory planning. *Automatica*, 135:109952.
- Fischer, F., Gabriel, J., and Kerschbaum, S. (2021). coni - a Matlab toolbox facilitating the solution of control problems.
- Fliess, M., Mounier, H., Rouchon, P., and Rudolph, J. (1998). A distributed parameter approach to the control of a tubular reactor: a multivariable case. In *Proceedings of the 37th IEEE Conference on Decision and Control*, volume 1, pages 439–442.
- Gehring, N., Irscheid, A., Deutscher, J., Woittennek, F., and Rudolph, J. (2023). Control of distributed-parameter systems using normal forms: an introduction. *at – Automatisierungstechnik*, 71(8):624–646.

- Gehring, N. and Woittennek, F. (2022). Flatness-based output feedback tracking control of a hyperbolic distributed-parameter system. *IEEE Control Syst. Lett.*, pages 992–997.
- Gschweng, M., Sawodny, O., Eisenbarth, C., Haase, W., and Böhm, M. (2024). One-dimensional distributed parameter modeling of evaporative cooling facades. In *2024 IEEE/SICE International Symposium on System Integration (SII)*, pages 906–911.
- Hu, L., Di Meglio, F., Vazquez, R., and Krstic, M. (2016). Control of homodirectional and general heterodirectional linear coupled hyperbolic PDEs. *IEEE Trans. Autom. Control*, 61(11):3301–3314.
- Hu, L., Vazquez, R., Di Meglio, F., and Krstic, M. (2019). Boundary exponential stabilization of 1-dimensional inhomogeneous quasi-linear hyperbolic systems. *SIAM J. Control Optim.*, 57(2):963–998.
- Irscheid, A., Bleyemehl, S., and Rudolph, J. (2021a). Prescribed finite-time stabilization for flat systems (in German). *at – Automatisierungstechnik*, 69(7):585–596.
- Irscheid, A., Deutscher, J., Gehring, N., and Rudolph, J. (2023). Output regulation for general heterodirectional linear hyperbolic PDEs coupled with nonlinear ODEs. *Automatica*, 148:110748.
- Irscheid, A., Espitia, N., Perruquetti, W., and Rudolph, J. (2022a). Prescribed-time control for a class of semilinear hyperbolic PDE-ODE systems. *IFAC-PapersOnLine*, 55(26):47–52.
- Irscheid, A., Gehring, N., Deutscher, J., and Rudolph, J. (2021b). Observer design for 2×2 linear hyperbolic PDEs that are bidirectionally coupled with nonlinear ODEs. In *2021 European Control Conference (ECC)*, pages 2506–2511.
- Irscheid, A., Gehring, N., Deutscher, J., and Rudolph, J. (2022b). Tracking control for 2×2 linear heterodirectional hyperbolic PDEs that are bidirectionally coupled with nonlinear ODEs. In Auriol, J., Deutscher, J., Mazanti, G., and Valmorbidia, G., editors, *Advances in Distributed Parameter Systems*, pages 117–142. Springer.
- Irscheid, A., Gehring, N., Deutscher, J., and Rudolph, J. (2024). Stabilizing nonlinear ODEs with diffusive actuator dynamics. *IEEE Control Syst. Lett.*, 8:1259–1264.
- Irscheid, A., Gehring, N., and Rudolph, J. (2021c). Trajectory tracking control for a class of 2×2 hyperbolic PDE-ODE systems. *IFAC-PapersOnLine*, 54(9):416–421.
- Irscheid, A., Konz, M., and Rudolph, J. (2019). A Flatness-Based Approach to the Control of Distributed Parameter Systems Applied to Load Transportation with Heavy Ropes. In Kondratenko, Y. P., Chikrii, A. A., Gubarev, V. F., and Kacprzyk, J., editors, *Advanced Control Techniques in Complex Engineering Systems: Theory*

- and Applications: Dedicated to Professor Vsevolod M. Kuntsevich*, pages 279–294. Springer.
- Knüppel, T., Woittennek, F., Boussada, I., Mounier, H., and Niculescu, S.-I. (2014). Flatness-based control for a non-linear spatially distributed model of a drilling system. In Seuret, A., Özbay, H., Bonnet, C., and Mounier, H., editors, *Low-Complexity Controllers for Time-Delay Systems*, pages 205–218. Springer.
- Krstic, M. (2009). Compensating actuator and sensor dynamics governed by diffusion PDEs. *Syst. Control Lett.*, 58(5):372–377.
- Krstic, M., Kanellakopoulos, I., and Kokotovic, P. V. (1995). *Nonlinear and Adaptive Control Design*. John Wiley & Sons, Inc.
- Krstic, M. and Smyshlyaev, A. (2008). *Boundary Control of PDEs: A Course on Backstepping Designs*. SIAM.
- Laroche, B., Martin, P., and Rouchon, P. (1998). Motion planning for a class of partial differential equations with boundary control. In *Proceedings of the 37th IEEE Conference on Decision and Control*, volume 3, pages 3494–3497.
- Laroche, B., Martin, P., and Rouchon, P. (2000). Motion planning for the heat equation. *Int. J. Robust Nonlinear Control*, 10(8):629–643.
- Lattanzio, C., Maurizi, A., and Piccoli, B. (2011). Moving bottlenecks in car traffic flow: A PDE-ODE coupled model. *SIAM J. Math. Anal.*, 43(1):50–67.
- Linz, P. (1985). *Analytical and Numerical Methods for Volterra Equations*. SIAM.
- Lynch, A. F. and Rudolph, J. (2002). Flatness-based boundary control of a class of quasilinear parabolic distributed parameter systems. *Int. J. Contr.*, 75(15):1219–1230.
- Meurer, T. (2013). *Control of Higher-Dimensional PDEs: Flatness and Backstepping Designs*. Springer.
- Meurer, T. and Kugi, A. (2009). Tracking control for boundary controlled parabolic PDEs with varying parameters: Combining backstepping and differential flatness. *Automatica*, 45(5):1182–1194.
- Meurer, T., Thull, D., and Kugi, A. (2008). Flatness-based tracking control of a piezoactuated Euler-Bernoulli beam with non-collocated output feedback: theory and experiments. *Int. J. Contr.*, 81(3):475–493.
- Meurer, T. and Zeitz, M. (2005). Feedforward and feedback tracking control of nonlinear diffusion-convection-reaction systems using summability methods. *Ind. Eng. Chem. Res.*, 44(8):2532–2548.

- Petit, N. and Rouchon, P. (2002). Flatness of heavy chain systems. In *Proceedings of the 41st IEEE Conference on Decision and Control*, volume 1, pages 362–367.
- Redaud, J., Auriol, J., and Niculescu, S.-I. (2021). Output-feedback control of an underactuated network of interconnected hyperbolic PDE-ODE systems. *Syst. Control Lett.*, 154:104984.
- Rodino, L. (1993). *Linear Partial Differential Operators in Gevrey Spaces*. World Scientific.
- Rudolph, J. (2003). *Flatness Based Control of Distributed Parameter Systems*. Shaker Verlag.
- Rudolph, J. (2021). *Flatness-Based Control: An Introduction*. Shaker Verlag.
- Rudolph, J., Winkler, J., and Woittennek, F. (2005). Flatness based approach to a heat conduction problem in a crystal growth process. In Meurer, T., Graichen, K., and Gilles, E. D., editors, *Control and Observer Design for Nonlinear Finite and Infinite Dimensional Systems*, pages 387–401. Springer.
- Rudolph, J. and Woittennek, F. (2008). Motion planning and open loop control design for linear distributed parameter systems with lumped controls. *Int. J. Contr.*, 81(3):457–474.
- Saldivar, B., Knüppel, T., Woittennek, F., Boussaada, I., Mounier, H., and Niculescu, S.-I. (2014). Flatness-based control of torsional-axial coupled drilling vibrations. *IFAC Proc. Vol.*, 47(3):7324–7329.
- Schörkhuber, B., Meurer, T., and Jüngel, A. (2012). Flatness-based trajectory planning for semilinear parabolic PDEs. In *Proceedings of the 51st IEEE Conference on Decision and Control*, pages 3538–3543.
- Schörkhuber, B., Meurer, T., and Jüngel, A. (2013). Flatness of semilinear parabolic PDEs—A generalized Cauchy–Kowalevski approach. *IEEE Trans. Autom. Control*, 58(9):2277–2291.
- Smyshlyaev, A. and Krstic, M. (2004). Closed-form boundary state feedbacks for a class of 1-D partial integro-differential equations. *IEEE Trans. Autom. Control*, 49(12):2185–2202.
- Song, Y., Wang, Y., Holloway, J., and Krstic, M. (2017). Time-varying feedback for regulation of normal-form nonlinear systems in prescribed finite time. *Automatica*, 83:243–251.
- Staudecker, M., Schlacher, K., and Hansl, R. (2008). Passivity based control and time optimal trajectory planning of a single mast stacker crane. *IFAC Proc. Vol.*, 41(2):875–880.

- Steeves, D., Krstic, M., and Vazquez, R. (2019). Prescribed-time stabilization of reaction-diffusion equation by output feedback. In *2019 American Control Conference (ACC)*, pages 2570–2575.
- Strecker, T. and Aamo, O. M. (2017). Output feedback boundary control of 2×2 semilinear hyperbolic systems. *Automatica*, 83:290–302.
- Strecker, T., Aamo, O. M., and Cantoni, M. (2022). Predictive feedback boundary control of semilinear and quasilinear 2×2 hyperbolic PDE-ODE systems. *Automatica*, 140:110272.
- Vazquez, R. and Krstic, M. (2008a). Control of 1-D parabolic PDEs with Volterra nonlinearities, Part I: Design. *Automatica*, 44(11):2778–2790.
- Vazquez, R. and Krstic, M. (2008b). Control of 1-D parabolic PDEs with Volterra nonlinearities, Part II: Analysis. *Automatica*, 44(11):2791–2803.
- Wang, J. and Krstic, M. (2019). Output feedback boundary control of a heat PDE sandwiched between two ODEs. *IEEE Trans. Autom. Control*, 64(11):4653–4660.
- Wang, J. and Krstic, M. (2022). *PDE Control of String-Actuated Motion*. Princeton University Press.
- Woittennek, F. (2013). Flatness based feedback design for hyperbolic distributed parameter systems with spatially varying coefficients. *IFAC Proc. Vol.*, 46(26):37–42.
- Woittennek, F., Irscheid, A., and Gehring, N. (2022). Flatness-based analysis and control design for 2×2 hyperbolic PDEs with nonlinear boundary dynamics. *IFAC-PapersOnLine*, 55(26):13–19.
- Zimmert, N., Pertsch, A., and Sawodny, O. (2011). 2-DOF control of a fire-rescue turntable ladder. *IEEE Trans. Control Syst. Technol.*, 20(2):438–452.